Aspects of Galactic science that may either be uncovered or significantly affected by HESS II observations

Diego F. Torres

With the support of

ICREA — Institució Catalana de Recerca i Estudis Avançats
IEEC — Institut d'Estudis Espacials de Catalunya
CSIC — Consejo Superior de Investigaciones Científicas
Alexander von Humboldt Stiftung/Foundation

Outline

- Diffuse emission and consequences
  - Correlation between gas, dust, and sources
  - Fermi bubbles?
- Supernovae remnants research
  - A few slides of intro to SNR observational status and problems.
- Pulsars and PWNe
  - Crab flares in action? Crab nebulae variability in general. Other nebulae?
  - Are there other hard energy pulsar tails?
  - Can pulsar wind zones provide DM-like signals? Are they needed?
  - Influence of magnetization in PWNe
- Stars, winds, and associations
  - Especial Binaries
  - Eta Car
  - Collective winds and CR modulation
- Microquasars, gamma, and X-ray binaries
  - Short timescale variability in X-ray binaries
  - Sub-orbital behavior of short-period gamma-ray binaries (like LS 5039)
  - Model testing, components of emission?
  - Long-term variability as a way of discovering new binaries?

Concluding remarks

Diffuse emission in the Galactic center and elsewhere

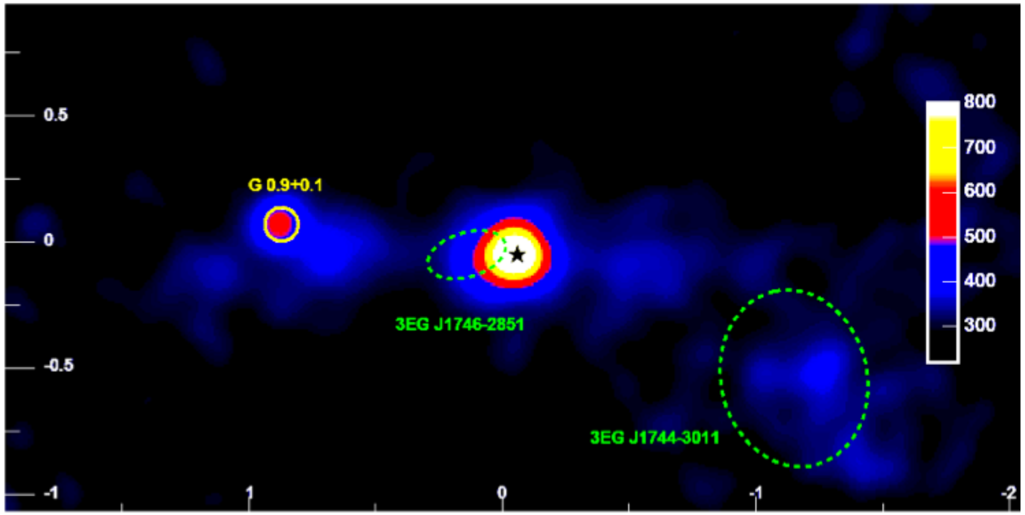

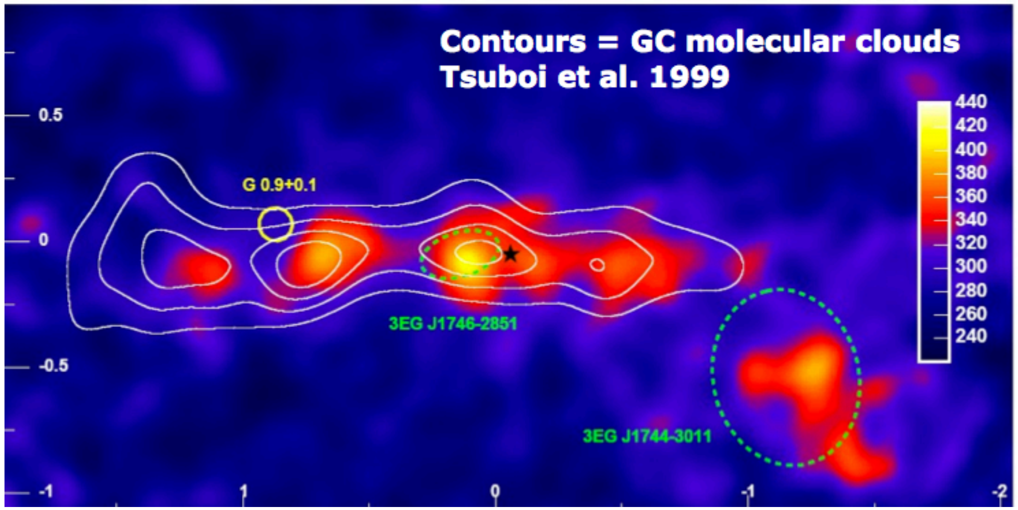

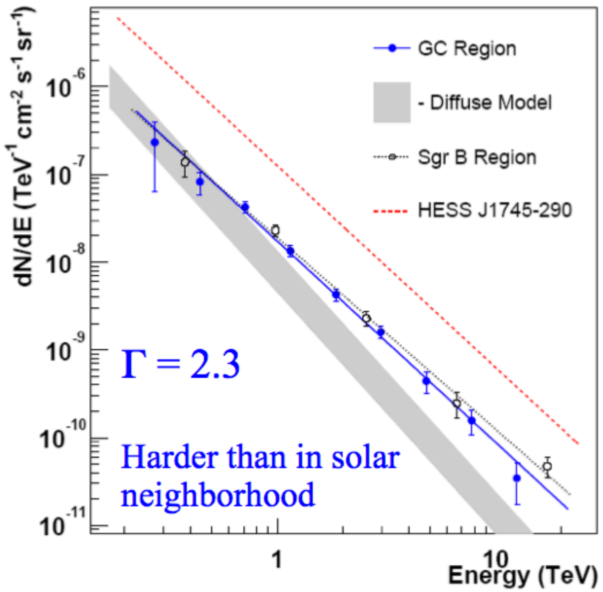

- Direct measurement of diffuse emission?
- Correlation of gas and sources?
- Difference in source localization / fluxes / population?
- Diffuse emission in other particularly strong star forming regions?

Kathrin's talk on Friday

Correlation of gas and dust with TeV sources

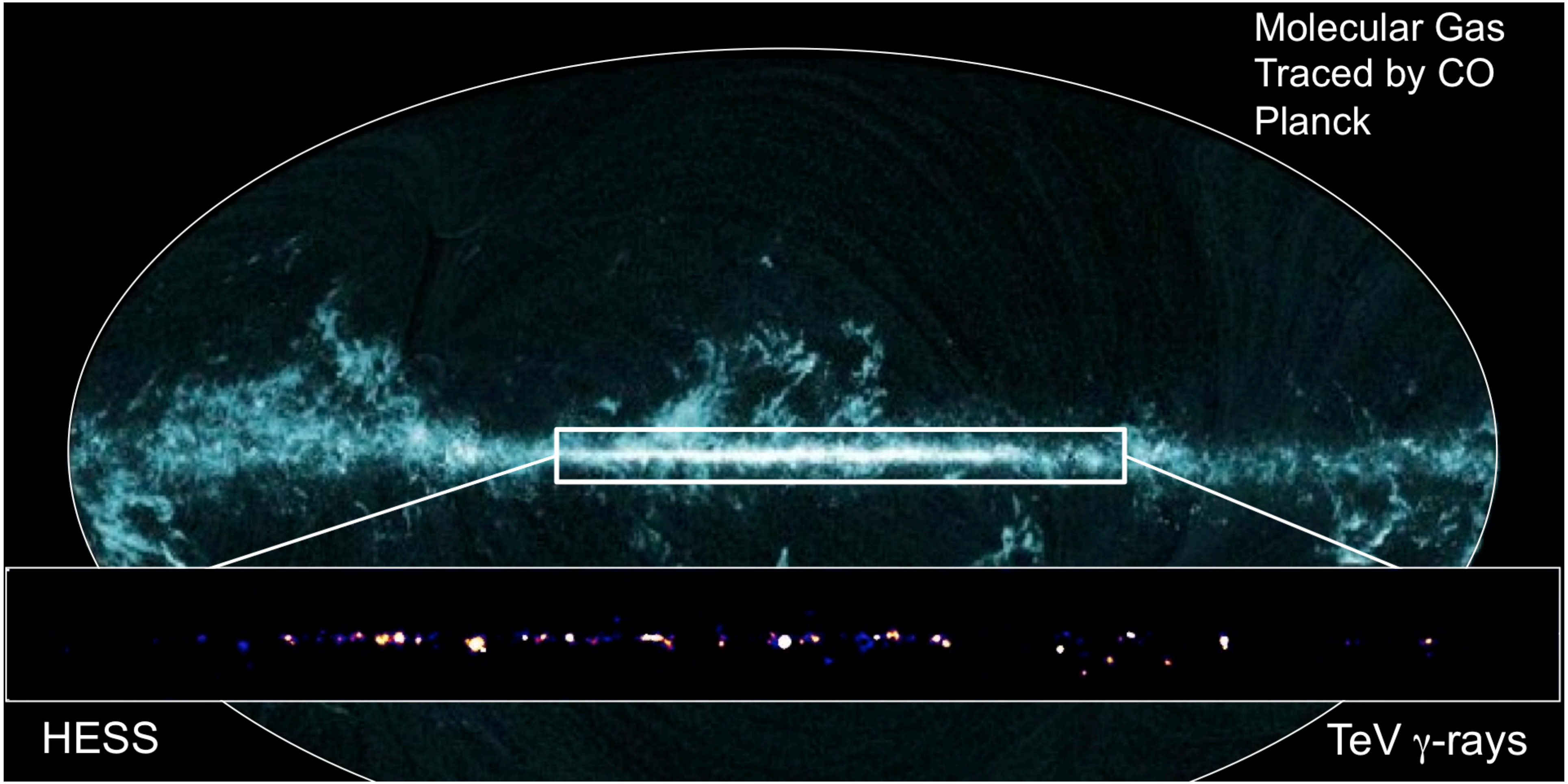

How well do TeV sources correlate with gas and dust enhancements?

Correlation of gas and dust (LOS integrated) with TeV sources

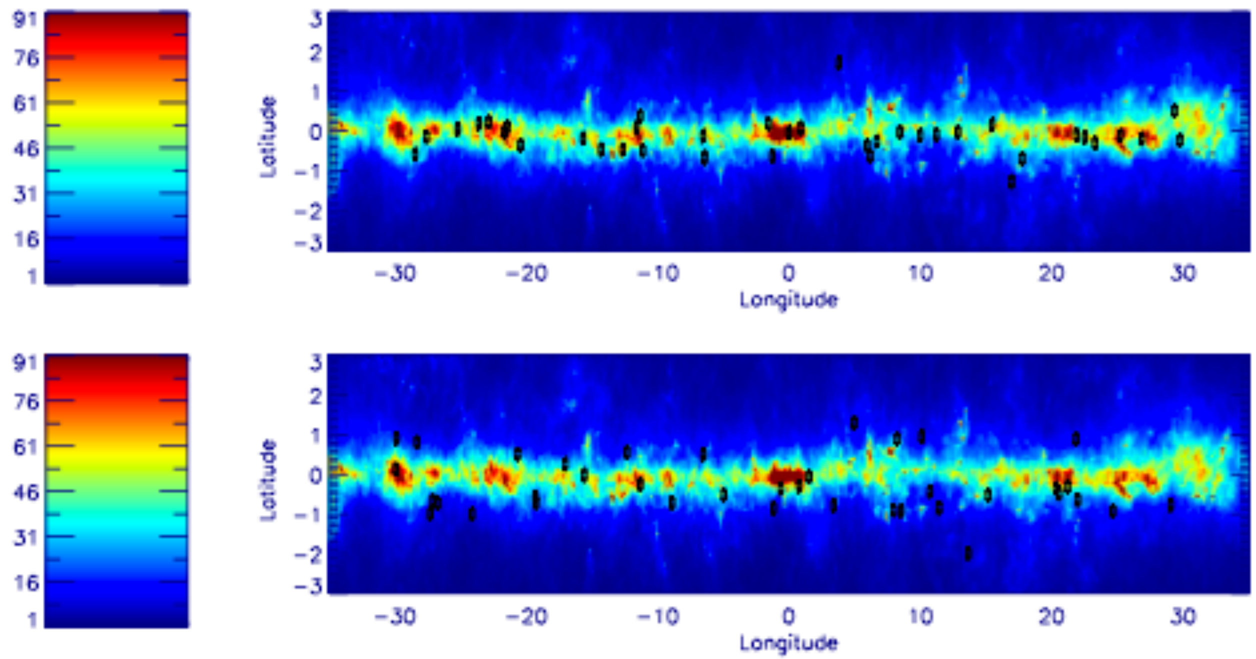

Real (top) and random realization (bottom) of the inner GPS TeV sources overlaid on Planck data at 353 GHz.

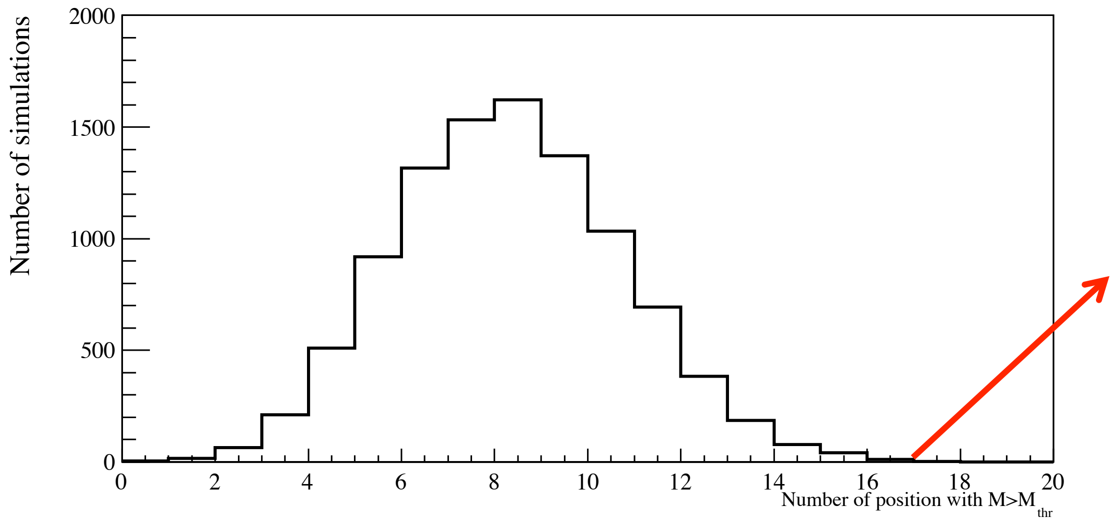

Occurences in randomized sample of positions relative to an integrated mass > 0.3M⊙. There are 17 in the real GPS, >3σ away from the mean of the distribution, which is at 8.3.

3σ in just one tracer!

Pedaletti, de Oña Wilhelmi, & DFT 2013, in preparation

Fermi Bubbles

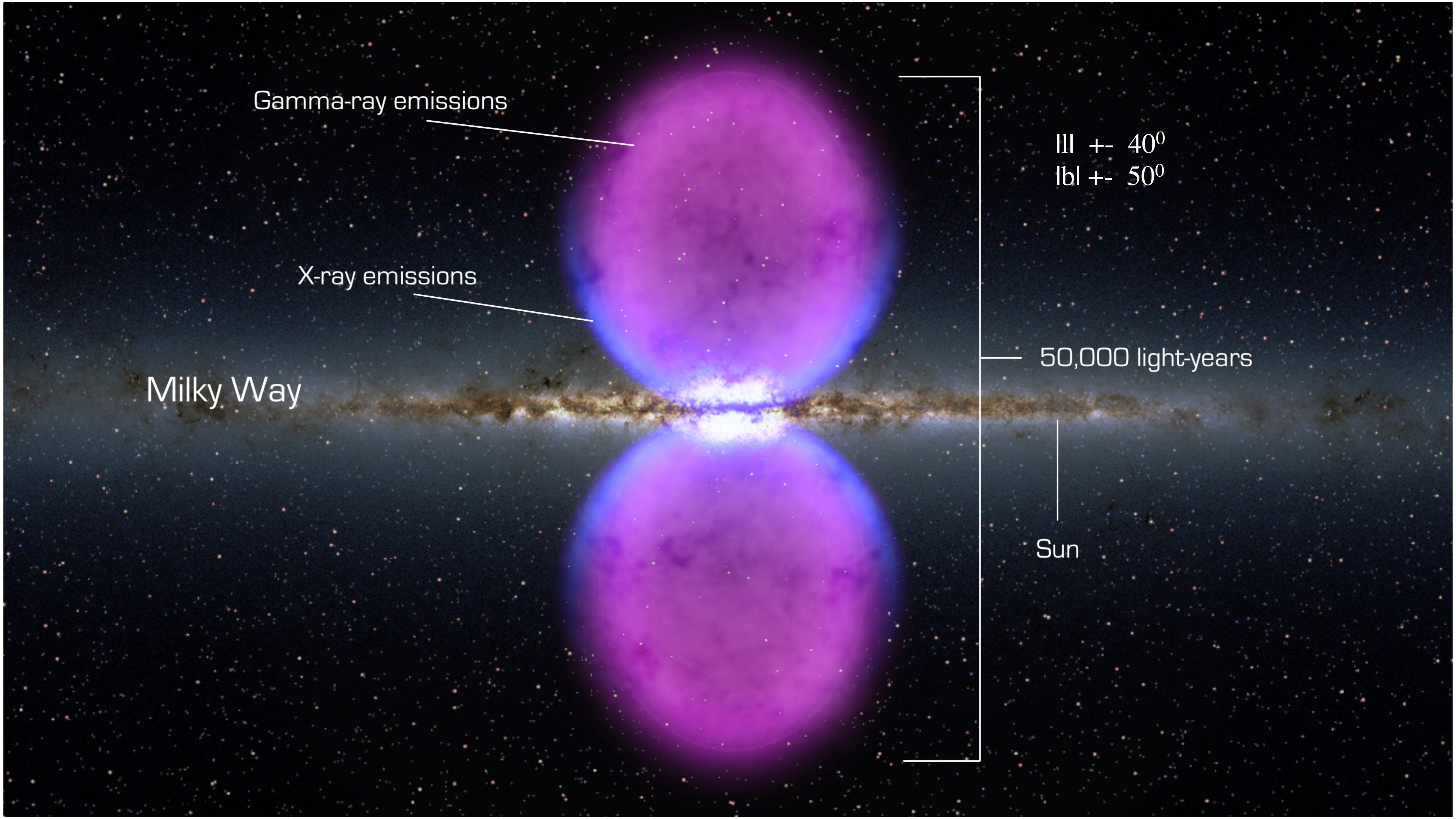

Fermi Bubbles

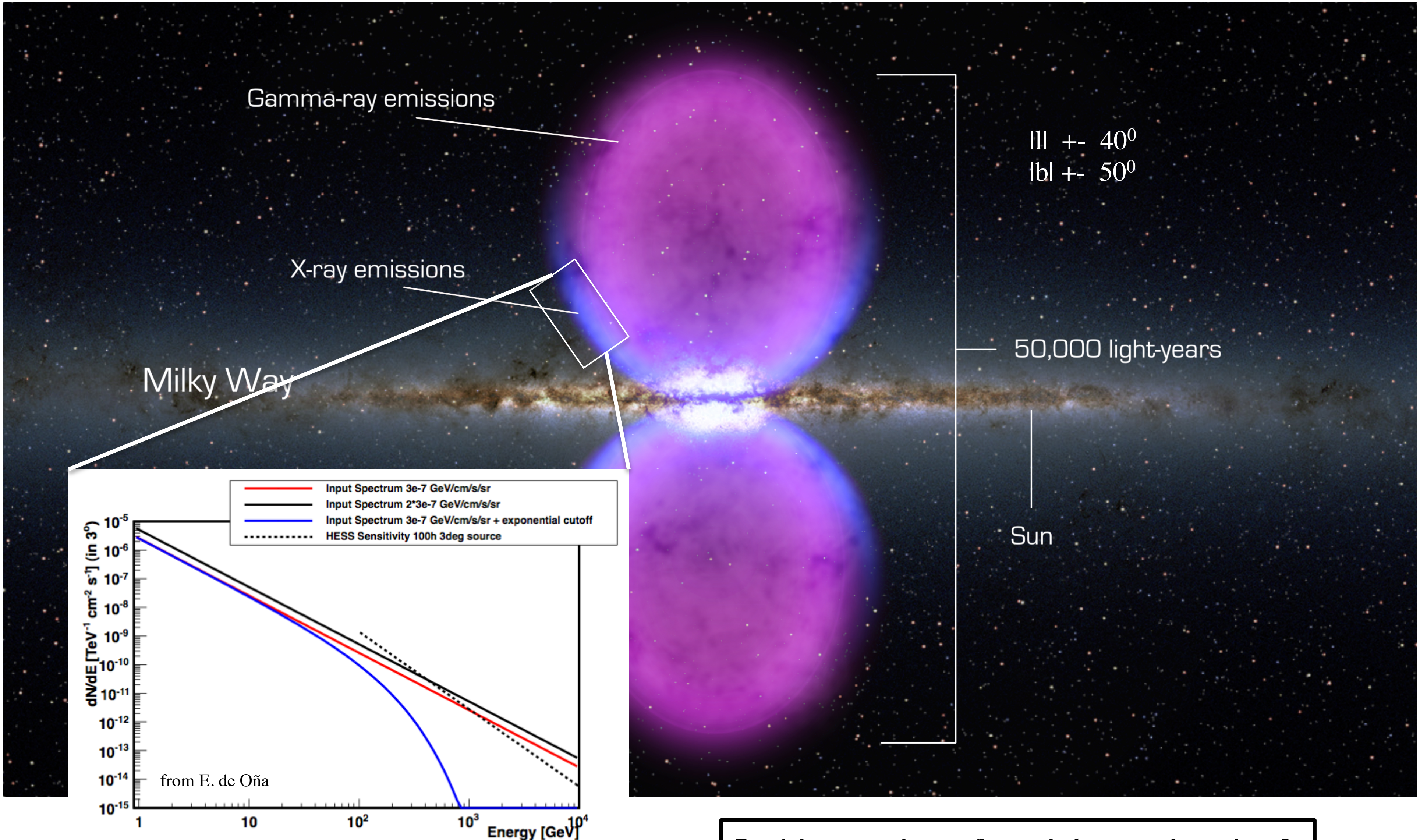

Is this a region of particle acceleration?

Fermi Bubbles, and jets?

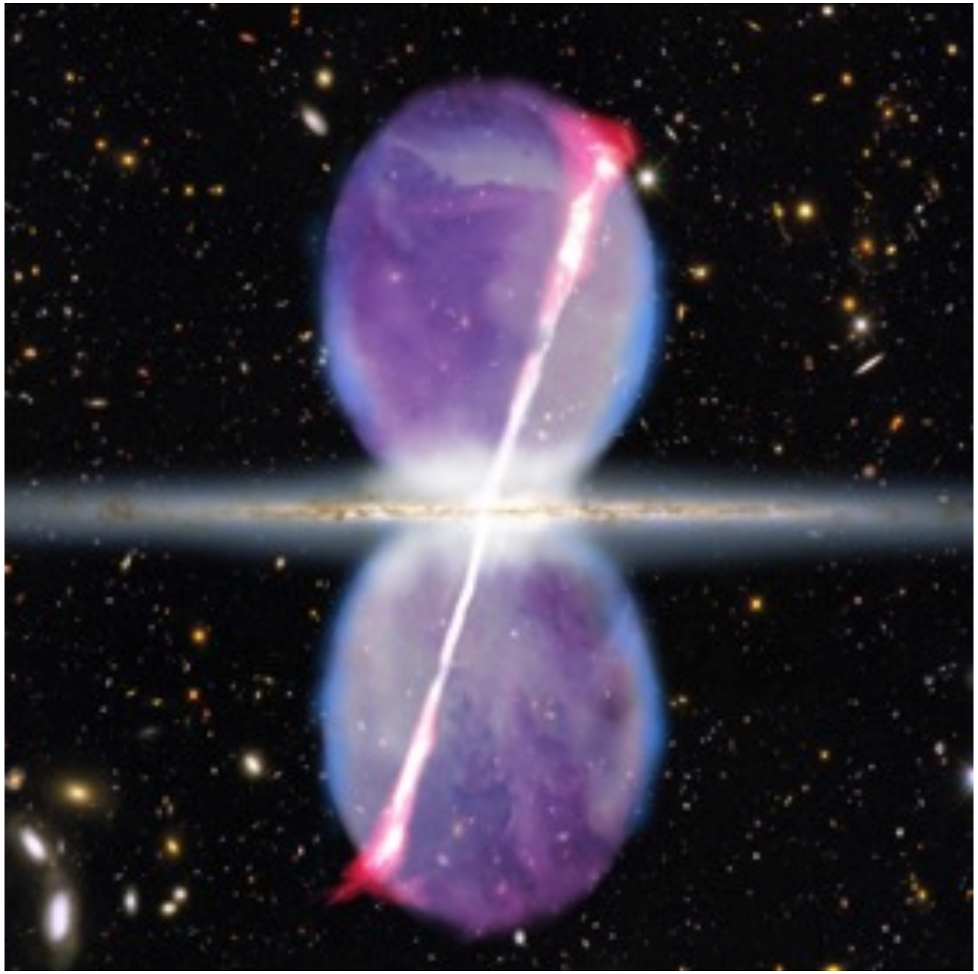

Are jet features real?

Require a hard CR electron population, which may lead to VHE emission depending on electron cutoff.

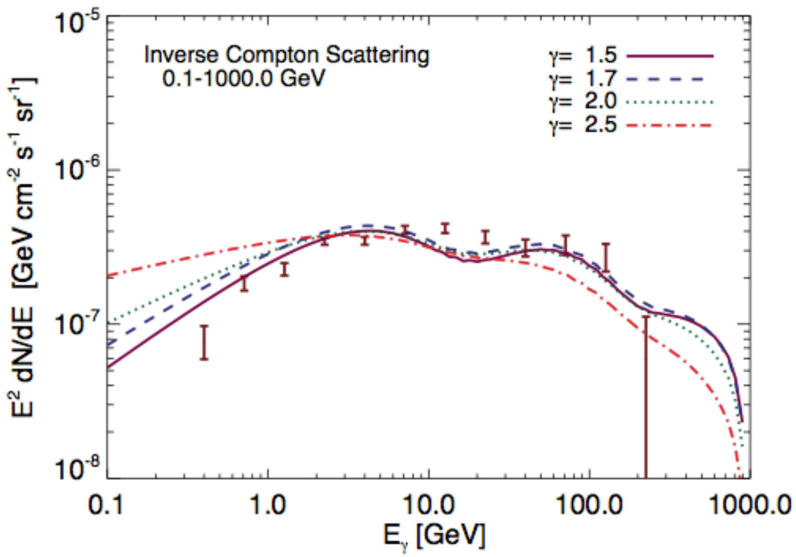

Cosmic-rays in SNRs

- Believed to be the origin of Galactic cosmic rays, essentially because of energetics:

- Galactic CR luminosity = $L_{CR} \sim 10_{41}$ erg/s $\rightarrow$ achievable via ~10% efficiency

$$\eta_{CR} \sim 0.1 \times (R_{SN}/0.03\ \mathrm{yr}^{-1}) \times (10^{51}\ \mathrm{erg}/E_{SN})$$

- The by-product of CRs acceleration is gamma-ray (& neutrino) emission
  - Trace the particle distribution from GeV to TeV
  - Point to their origin

- Shell and filled SNRs observed
  - Hadronic origin of GeV photons in some cases
  - Still no observations of PeV particles in the shells

Hadronic emission explains GeV photons in middle-aged SNRs

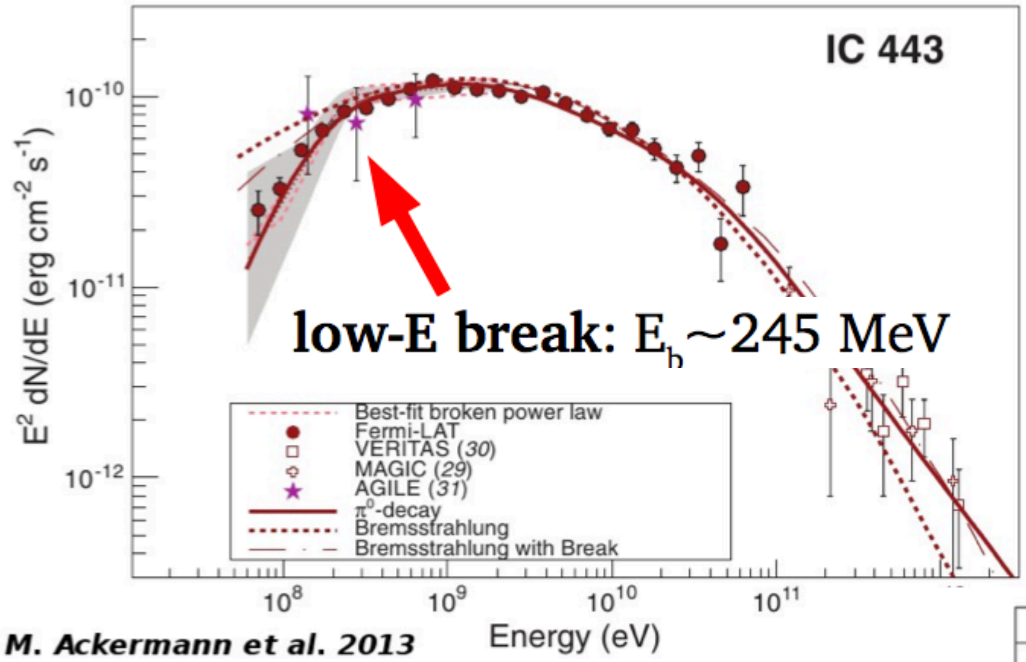

M. Ackermann et al. 2013

Low energy breaks impossible to model with electron Bremsstrhalung unless ad-hoc cutoffs in the e-population are introduced

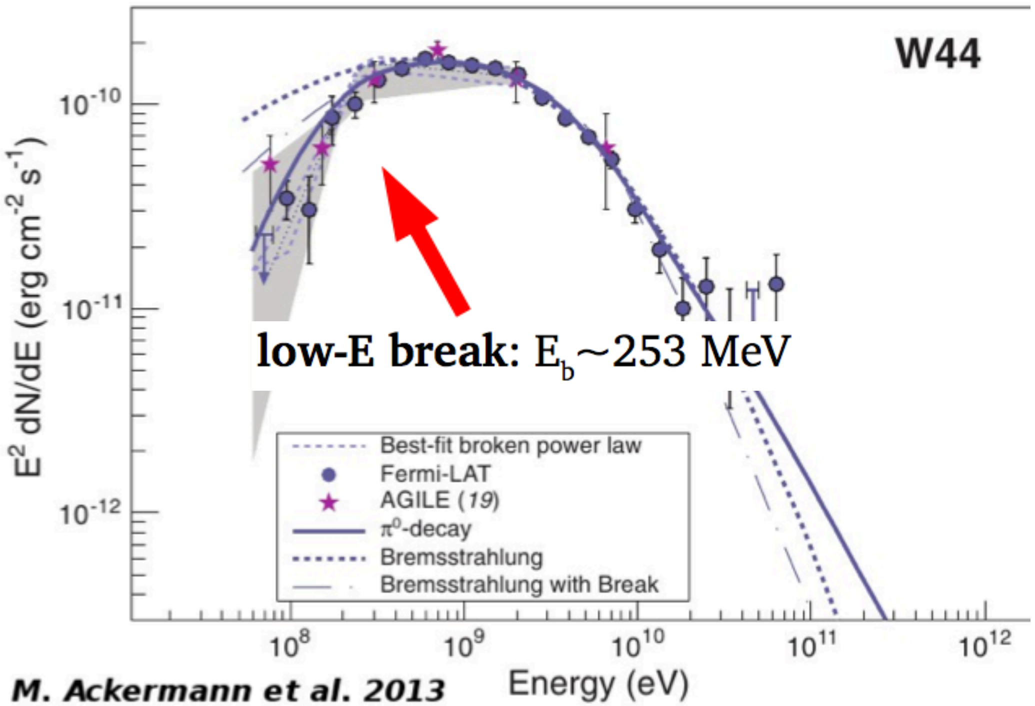

M. Ackermann et al. 2013

Middle-aged SNRs are not pevatrons

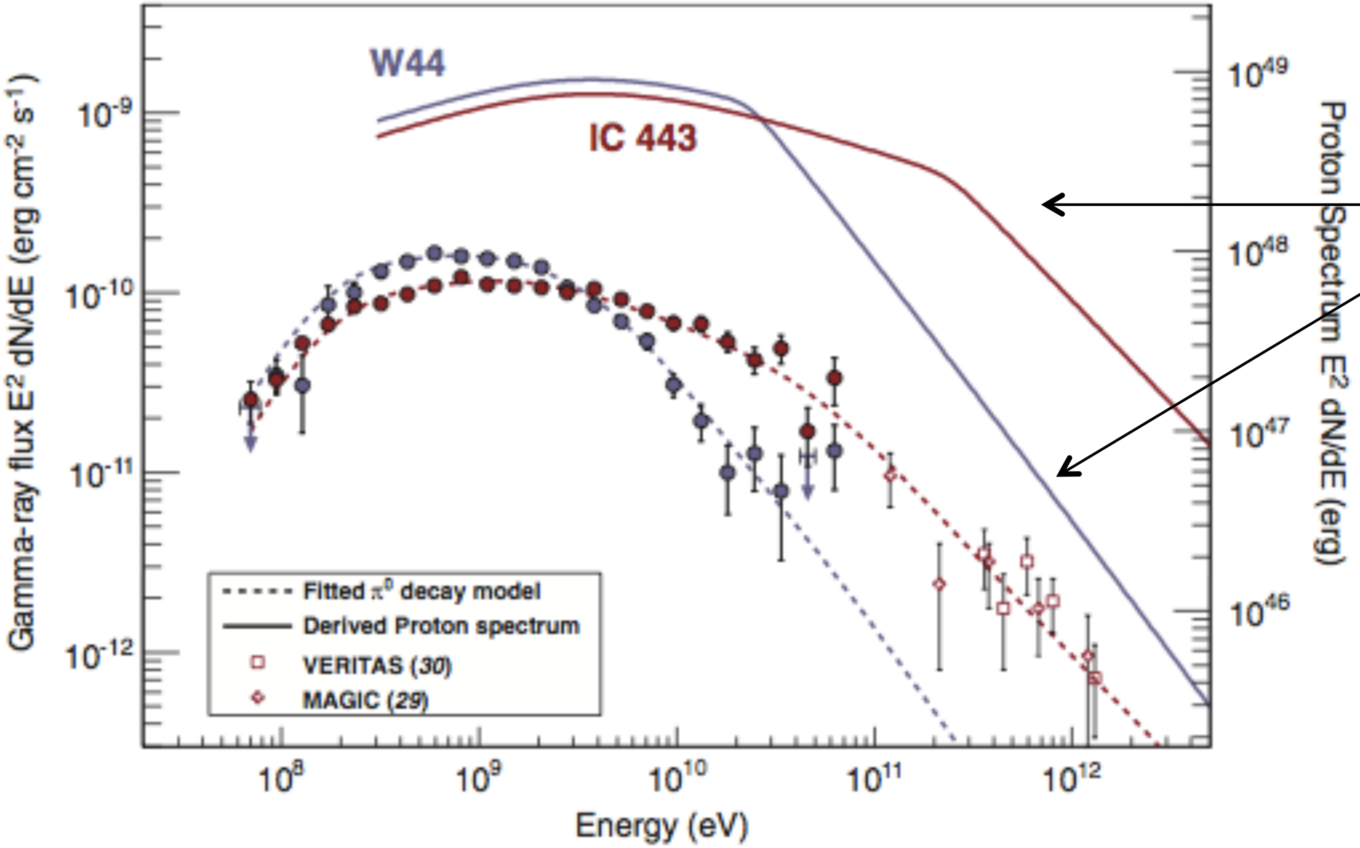

Proton spectra is very steep

TeV emission is cut for W44 and very steep for IC443.

And no shell pevatrons: e.g., Vela Jr.

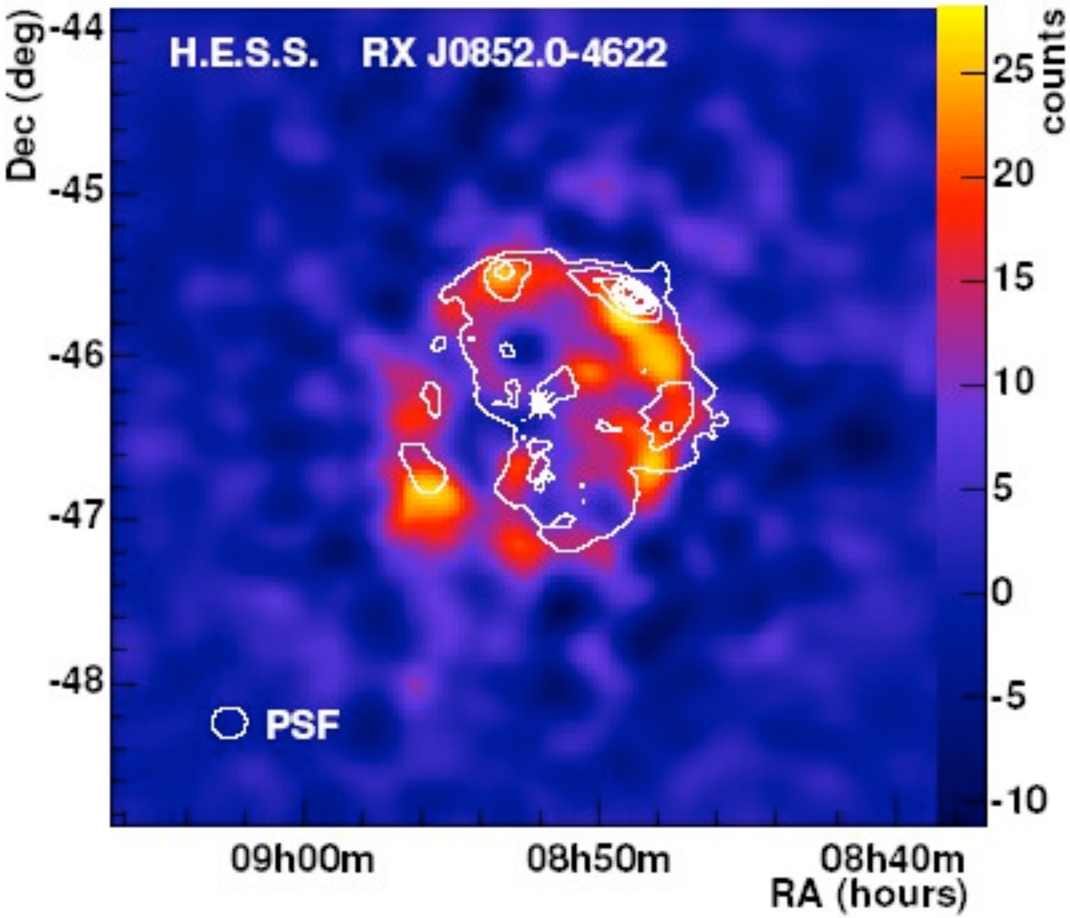

And no shell pevatrons: e.g., Vela Jr.

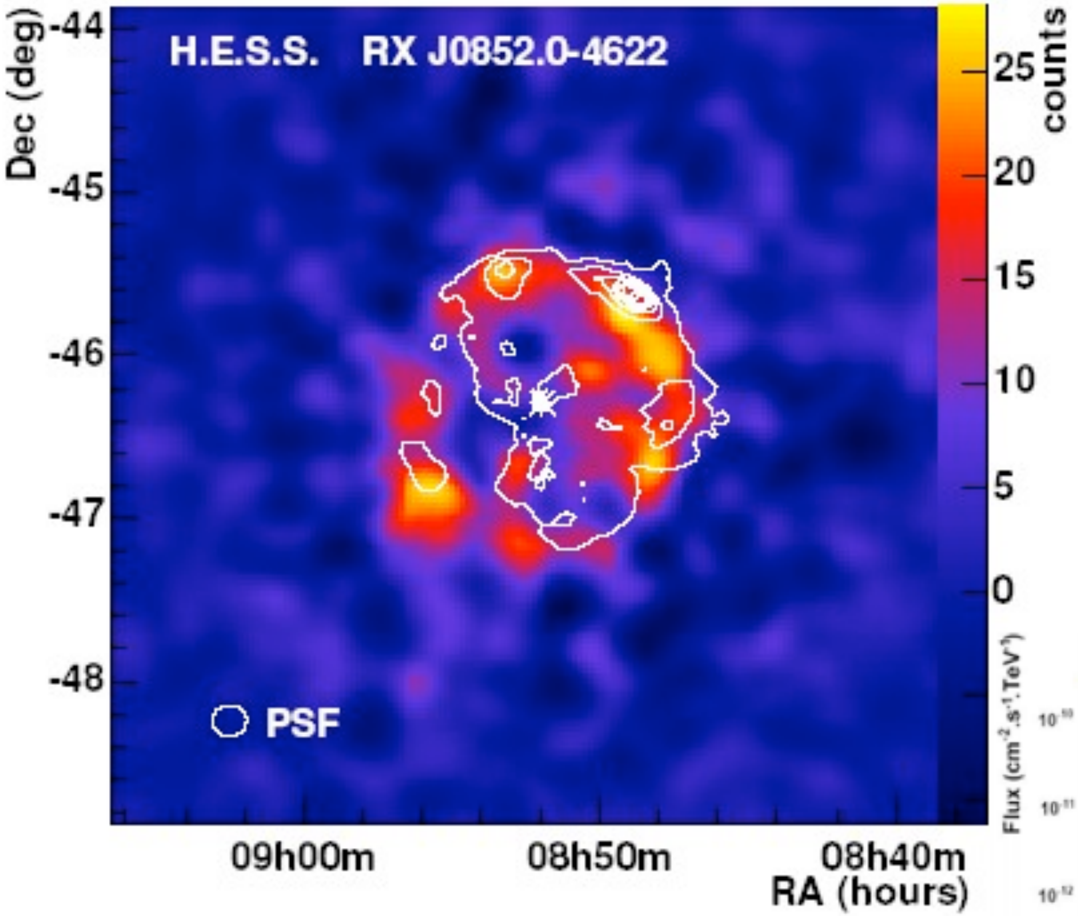

Cutoff suspected.

[And no thermal X-rays as expected in hadronic Models]

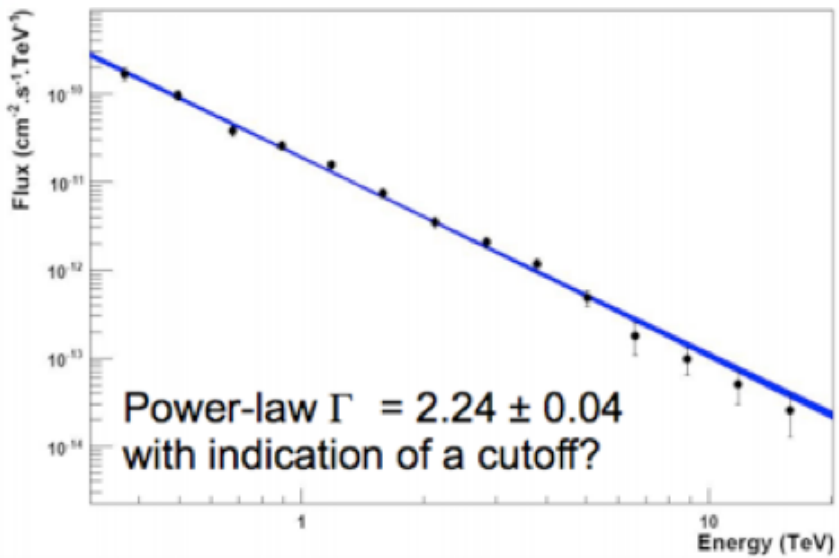

And no shell pevatrons: e.g., RX J 1713-3947

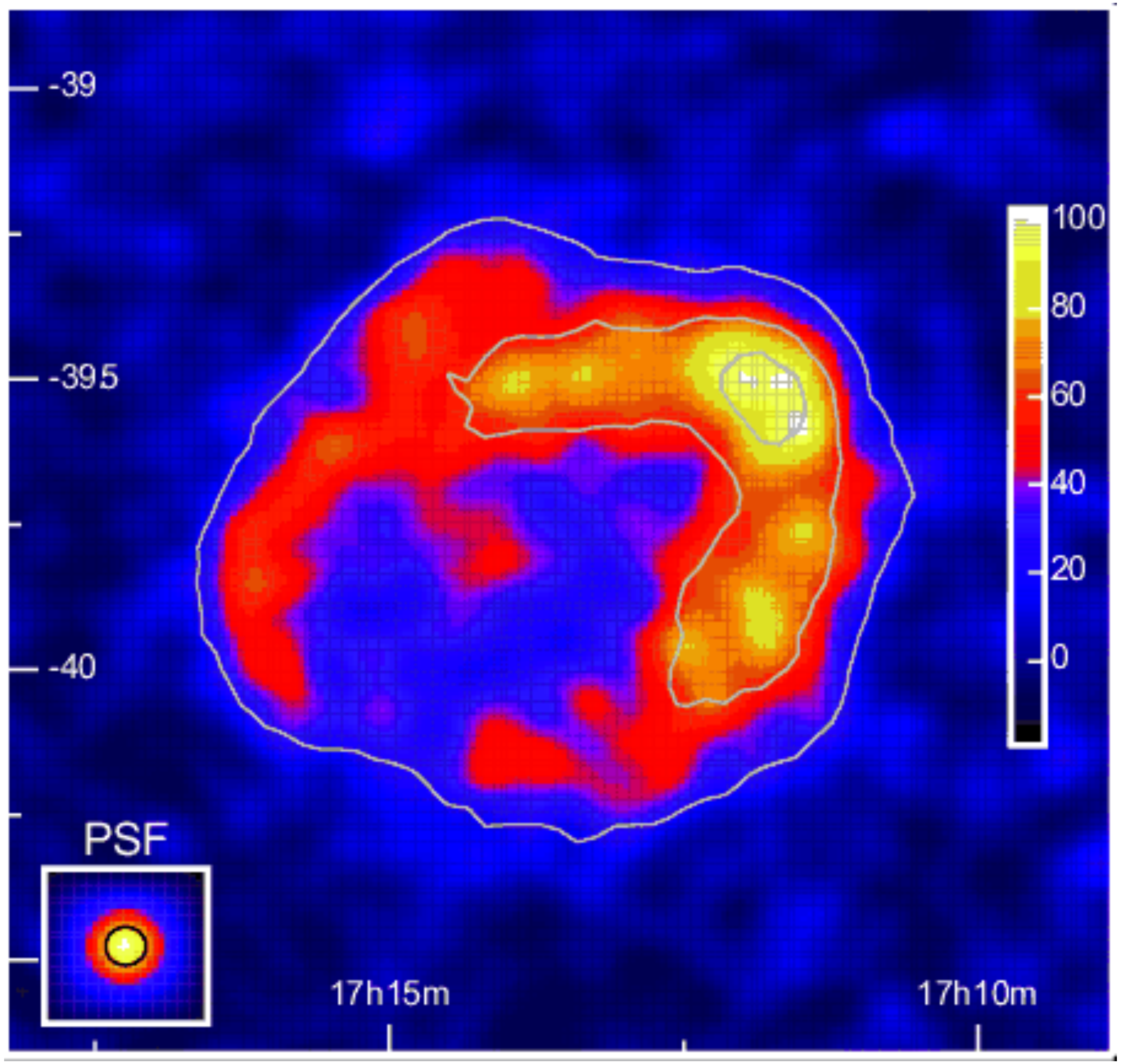

And no shell pevatrons: e.g., RX J 1713-3947

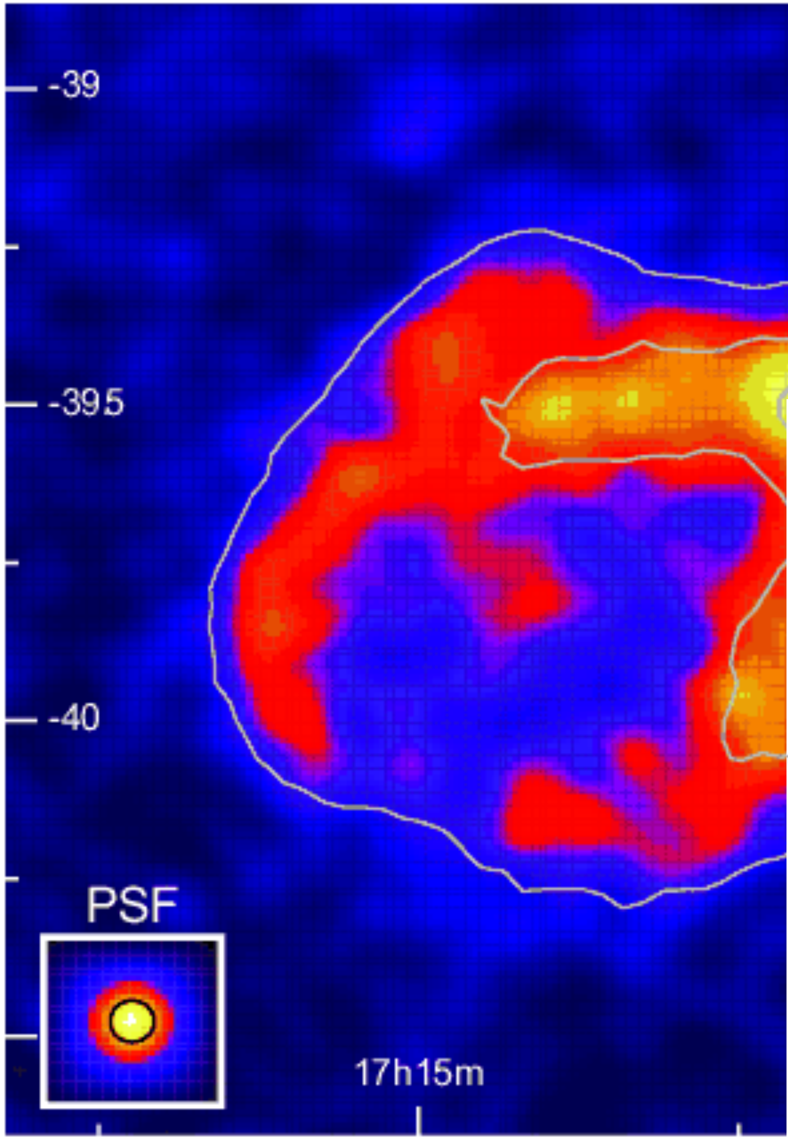

Cutoff detected.

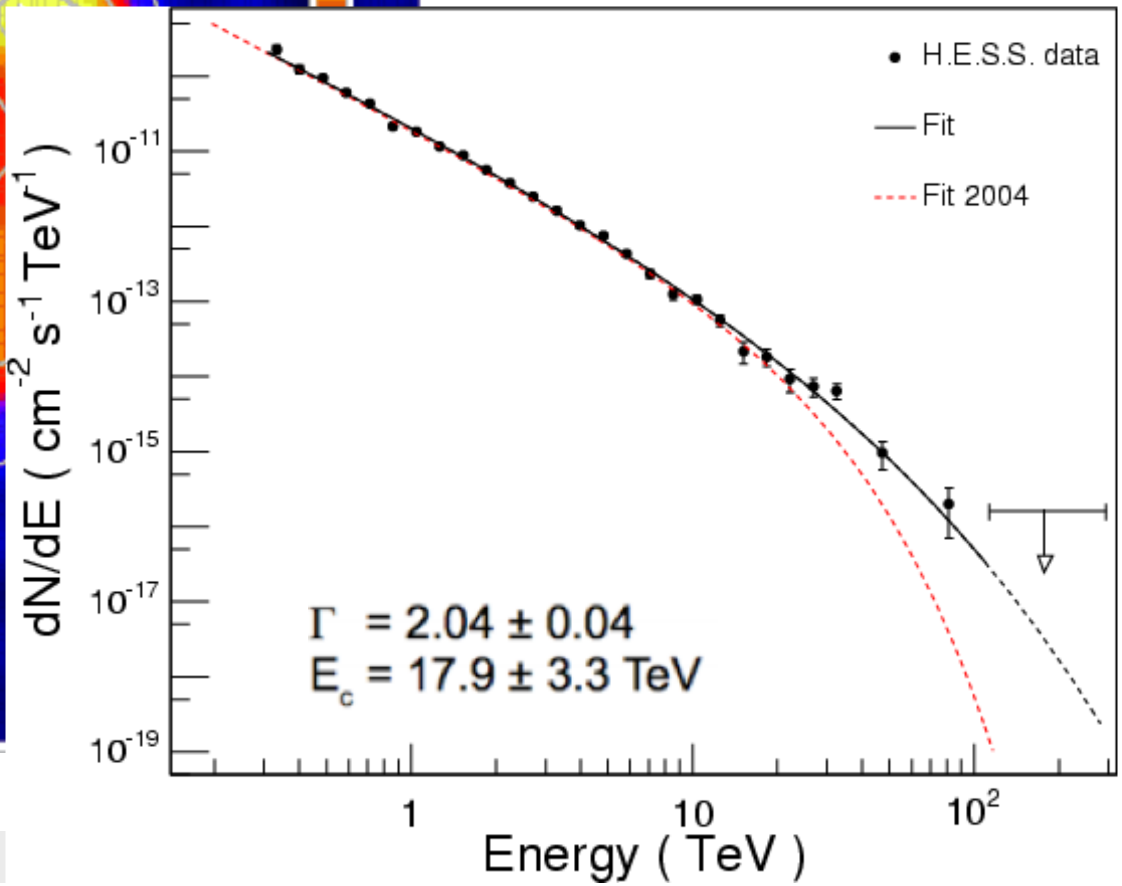

HESS Collaboration

And no shell pevatrons: e.g., RX J 1713-3947

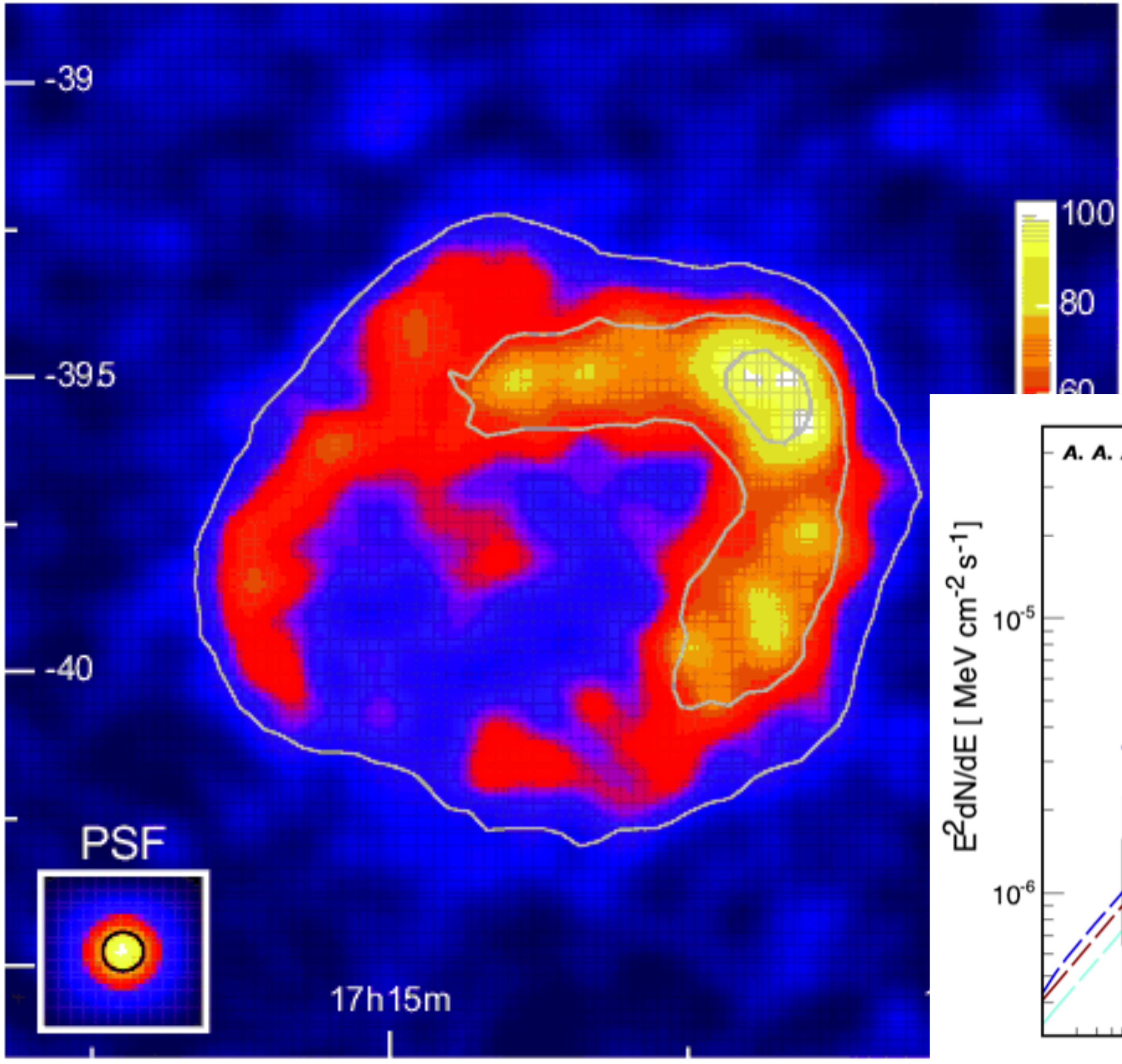

Leptons can dominate the gamma-ray emission.

That does not mean there are no hadrons! η~0.2

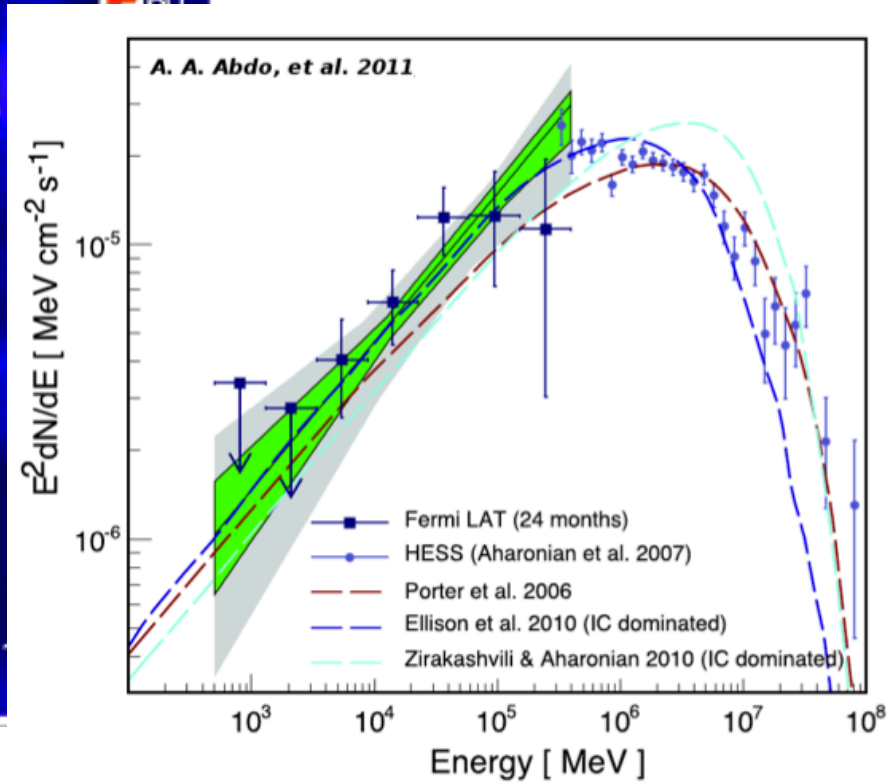

Where are the efficient CR accelerators?

GeV-hard, TeV-bright SNRs
(RX J1713, Vela Jr, RCW 86, etc):
'Leptonic-like shape' /
not necessarily an efficient CR source up to PeV

GeV/TeV-faint SNRs
(Cas A, Tycho, SN 1006?) :
'Hadronic-like shape' /
not necessarily an efficient CR source up to PeV

GeV bright TeV-soft SNRs, interacting with MCs
(W44,W51C, IC443,W49B, etc) :
'Hadronic-like shape' /
not necessarily an efficient CR source up to PeV

Catch them in the act, in TeV gamma-rays

- PeV particles accelerated at the beginning of the Sedov phase (~200 years, when the shock velocity is high):

    - In SNR shocks with relatively low acceleration rate, the synchrotron losses prevent acceleration of electrons to energies beyond 100 TeV.

    - The IC component is suppressed because of the Klein–Nishina effect.
    - Therefore, the contribution of the IC gamma-rays to the radiation above 10 TeV should gradually die out. Above 100 TeV, the hadronic origin of radiation would be established.

    - Blind pevatron search to be conducted with CTA

Catch them in the act, in hard X-rays

- Perhaps possible with Nustar or ASTRO-H

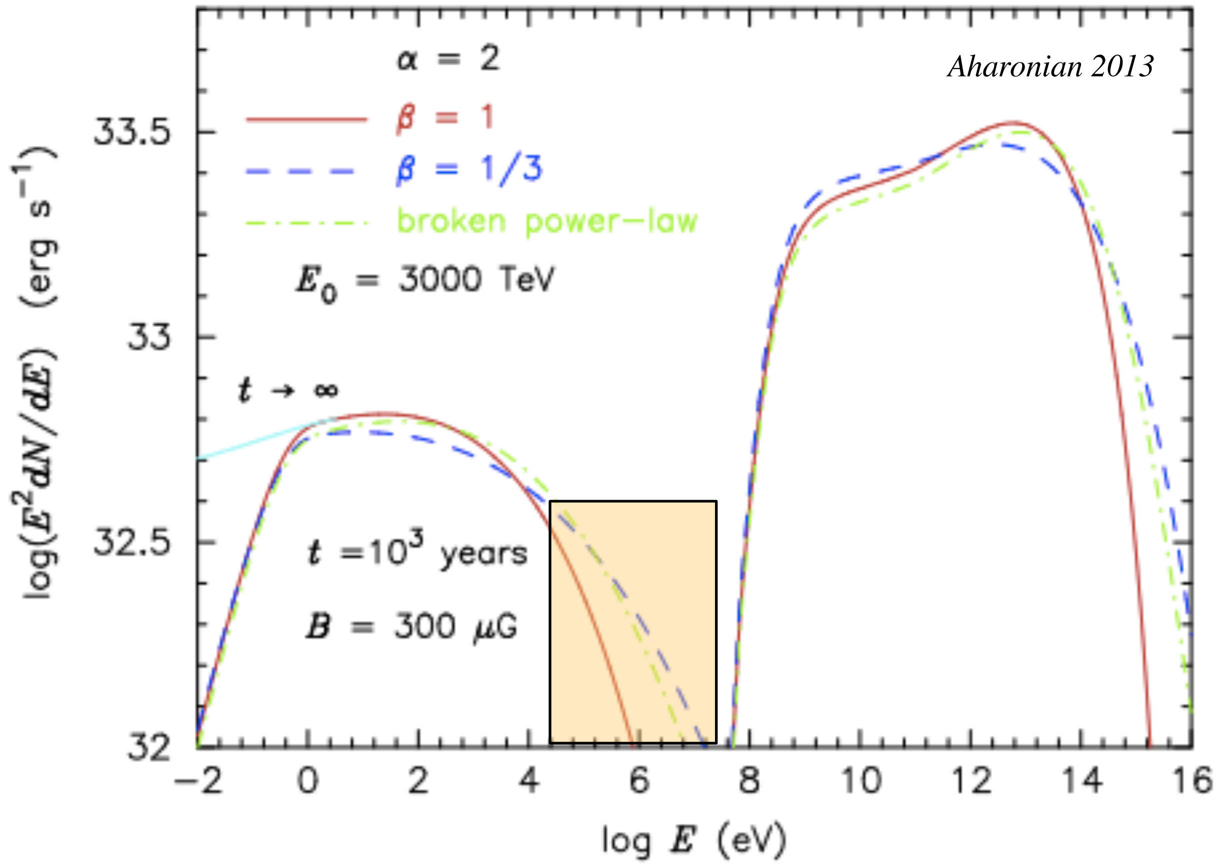

1000yrs-pevatron with injection of 10^{39} erg/s with three different injection spectra of protons, leading to similar results.

Synchrotron emission in X-rays produced by secondary electrons and positrons.

Several SNRs interacting with Molecular Clouds detected, but at lower energies by Fermi and IACTs

- Examples are W28, W51, W44, etc. Protons up to the knee not required -- Interaction of formerly released high-E particles

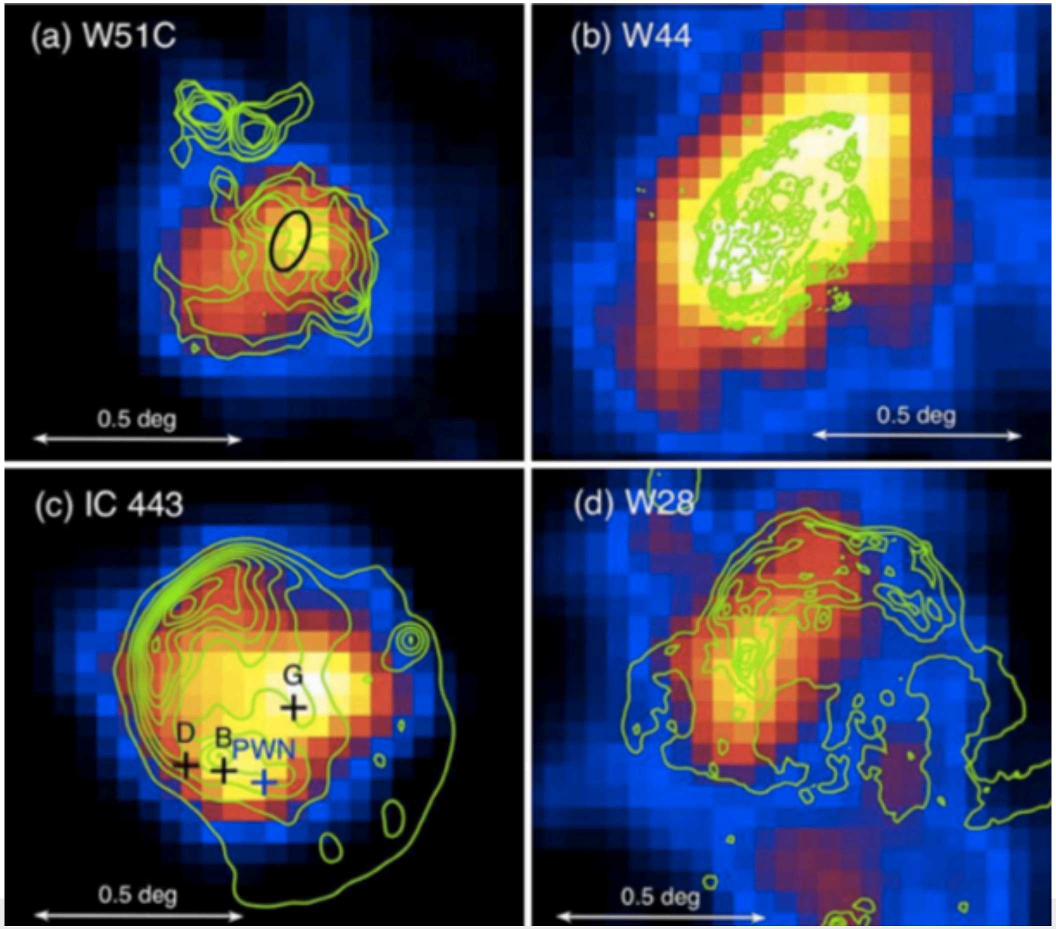

Where are the cutoffs? E.g., in W44? How do they correlate with age?

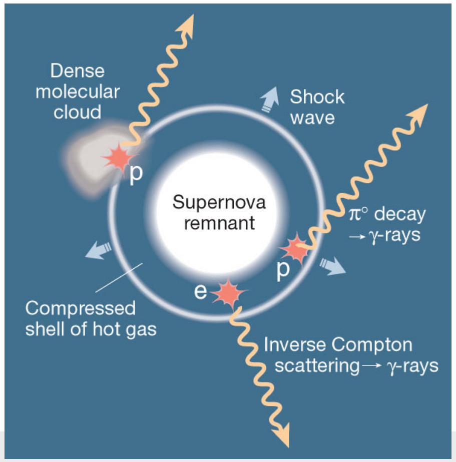

Catch formerly emitted high-energy protons

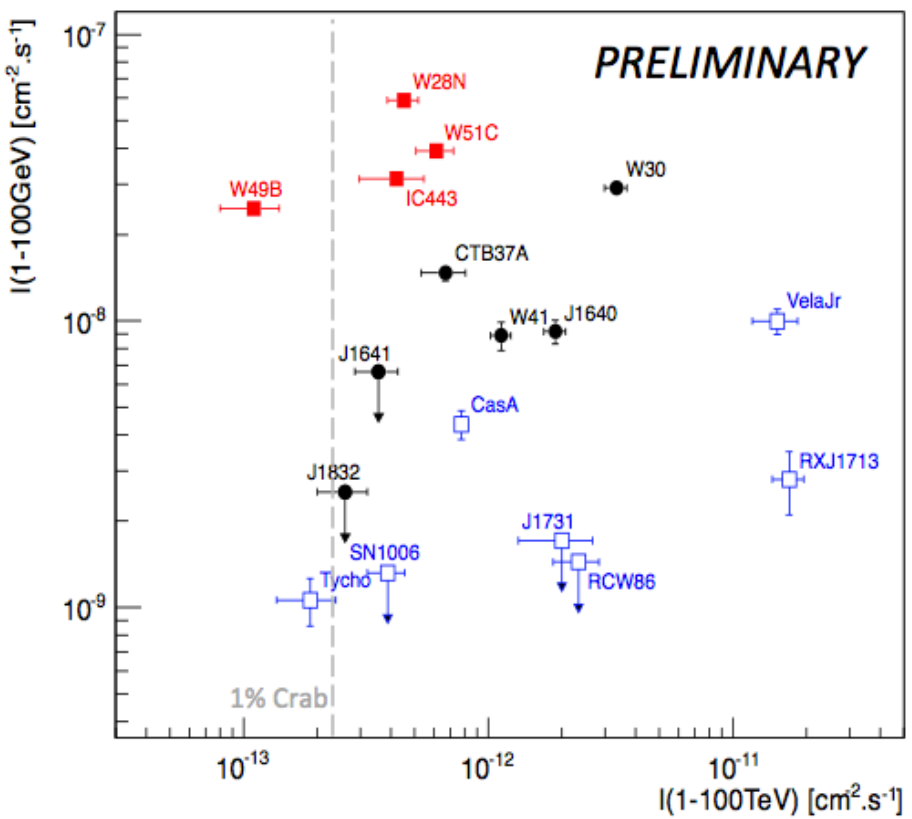

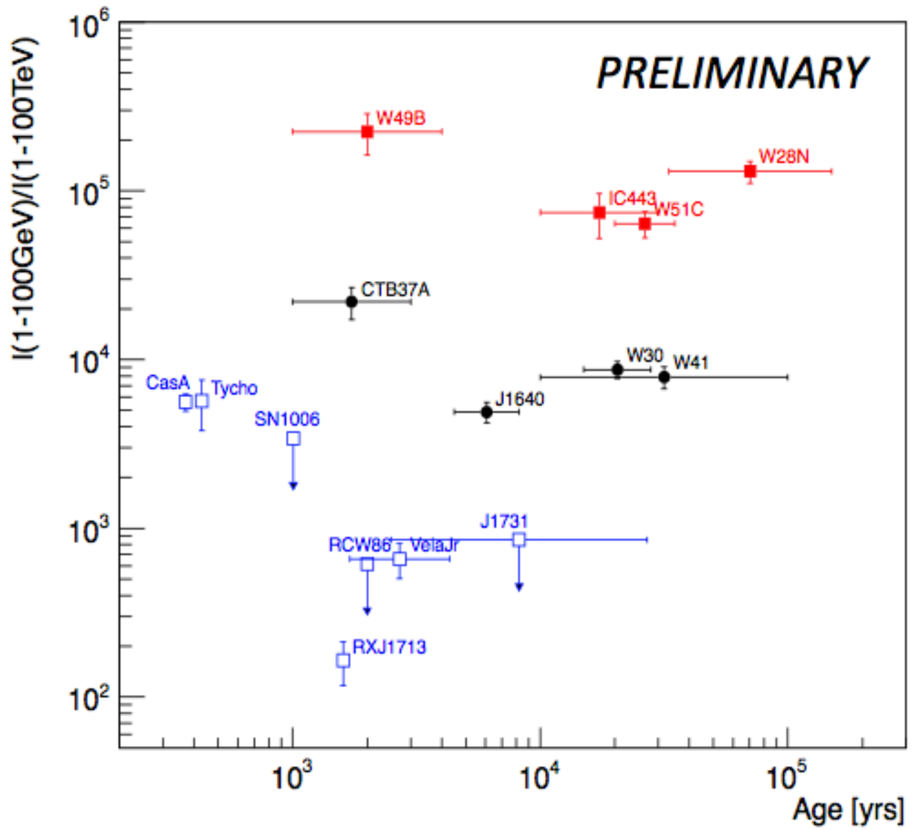

HESS II will be exploring the GeV – TeV trends in SNR with and without Molecular clouds interaction

Mixed lepto-hadronic cases: ionization level is key (e.g., CTB 109)

Hadronic model requires high density and small distance, ionization states overpredicted due to the density required to fit the gamma-rays

Leptonic model requires low density and larger distance, and as a result the ionization states are underpredicted

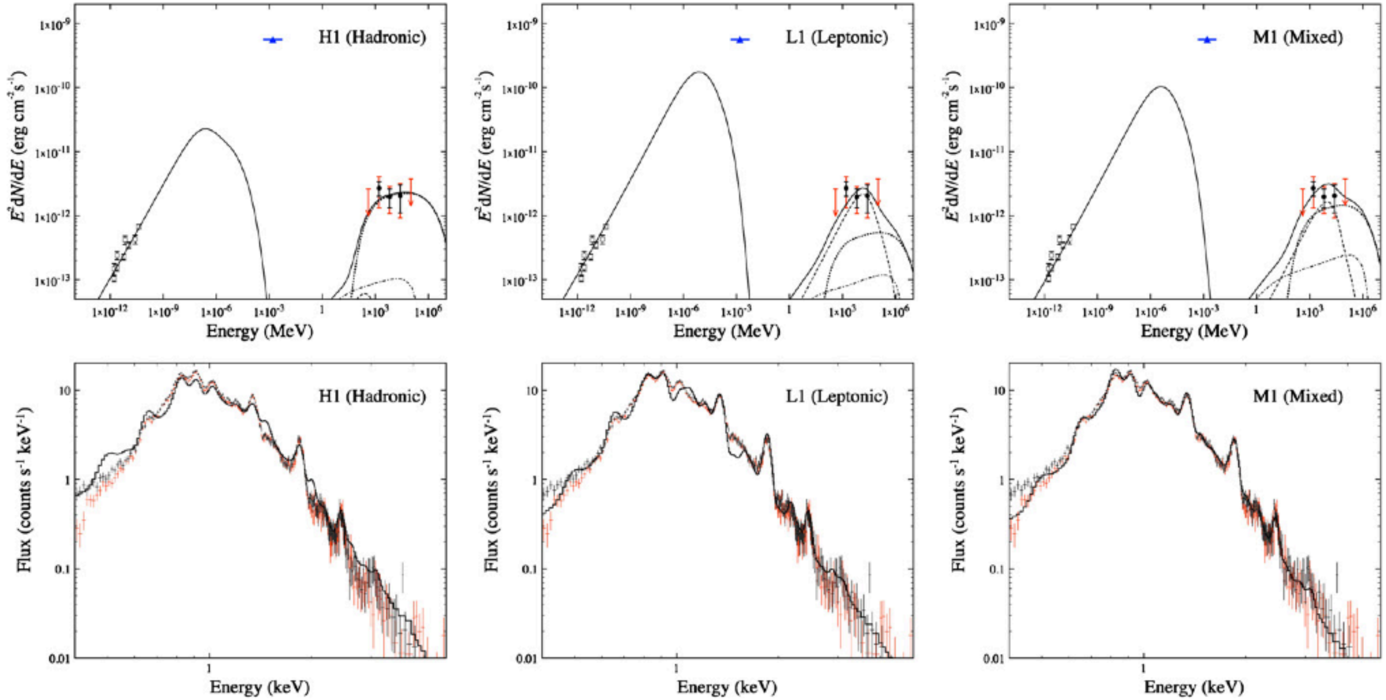

CR-Hydro-NEI Parameters

Model	K_{ep}	s	n_0 (cm^{-3})	D_{SNR} (kpc)	t_{SNR} (10^3yr)	B_{amp}	ε_{CR} (%)	R_{FS} (pc)	R_{tot}	B_2[a] (μG)	E_{CR}/E_{SN}	F_π/F_{IC}[b]
H1 (Hadronic)	0.01	0	1.1	2.7	15	7.0	23	14.2	4.4	67	0.40	14
L1 (Leptonic)	0.02	0	0.2	3.0	8.5	2.7	33	15.6	4.7	26	0.42	0.35
M1 (Mixed)	0.015	0	0.5	2.8	11	2.6	35	14.6	4.7	26	0.49	1.0

Notes.
[a] B_2 is the magnetic field immediately behind the shock.
[b] F_π/F_{IC} is the ratio of the pion decay flux to the inverse Compton flux in the energy range 100 MeV to 1 TeV.

Castro et al. 2012

Crab flares

- AGILE and Fermi collaborations have reported flaring activity (30 times larger flux) above 1 GeV from the nebula: duration of days, doubling times in <8 hours

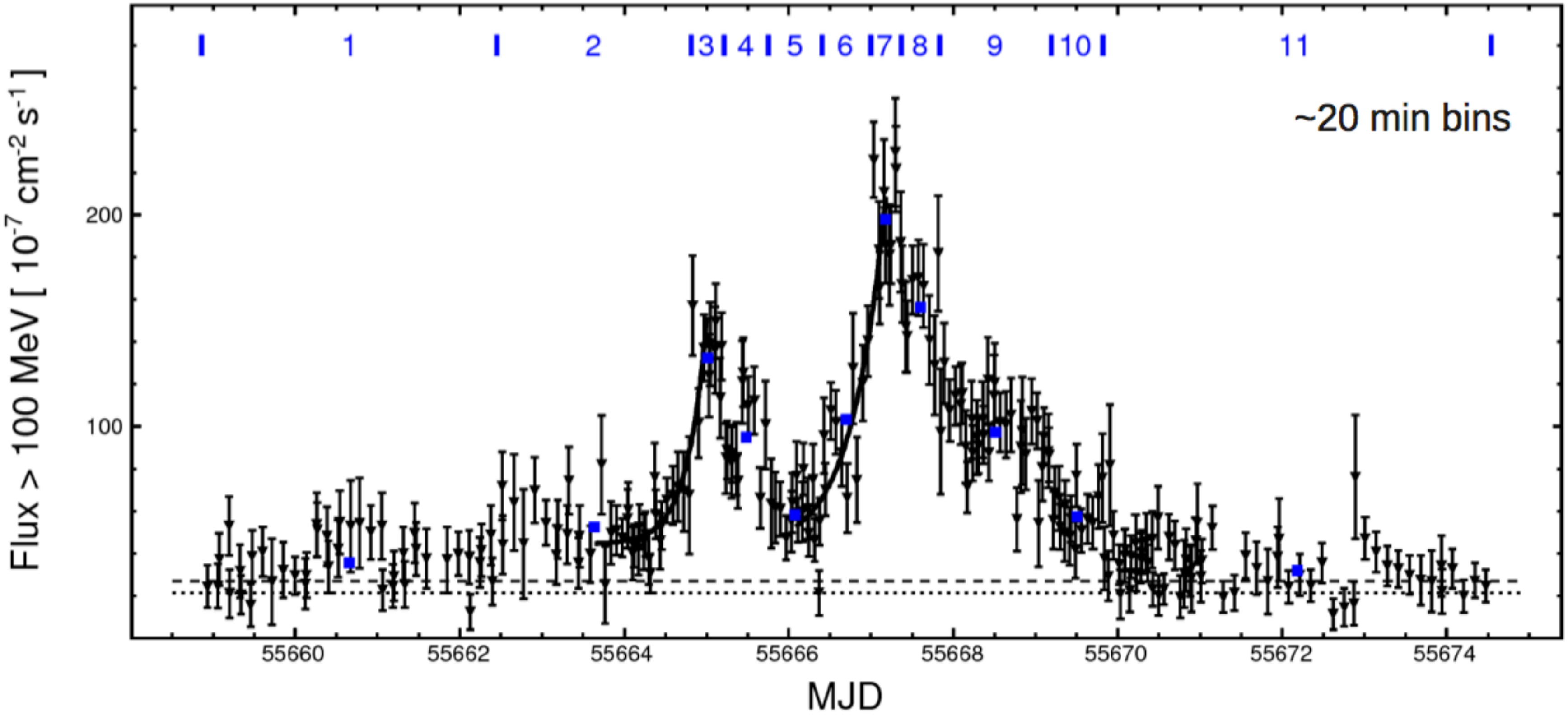

Crab flares

The emitted (un-pulsed) isotropic power at the peak of the flare of ~ 4×10^{36} erg s^{-1} corresponds to ~1% of the total spin-down power of the pulsar.

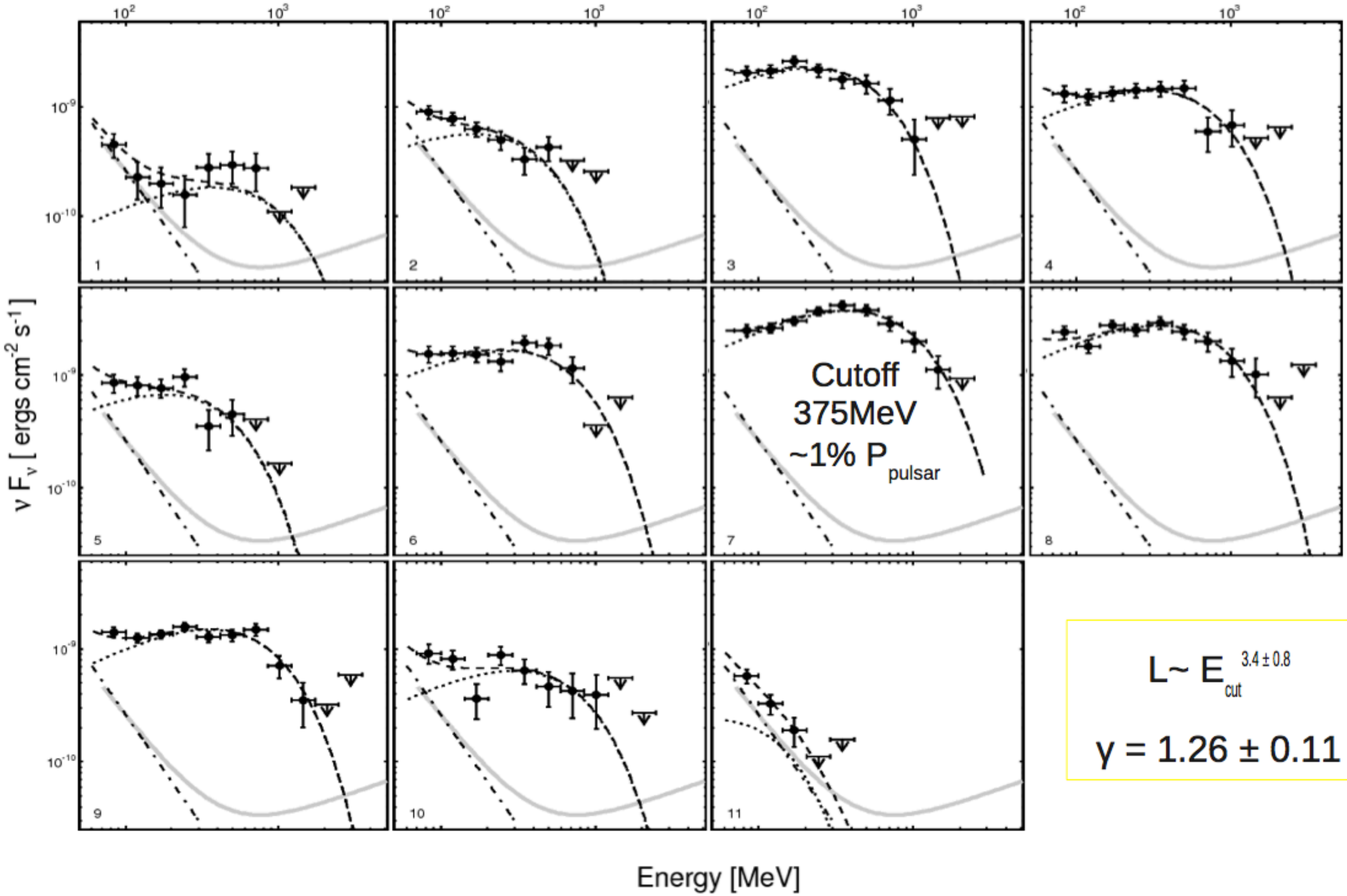

$L \sim E_{cut}^{3.4 \pm 0.8}$

$\gamma = 1.26 \pm 0.11$

Crab flares

The observation of peak synchrotron energy of 380 MeV is among the highest seen from an astrophysical source. The observation is surprising as particle acceleration in the presence of synchrotron cooling is expected to limit synchrotron emission to photon energies below ~150 MeV (Guilbert et al. 1983; de Jager et al. 1996).

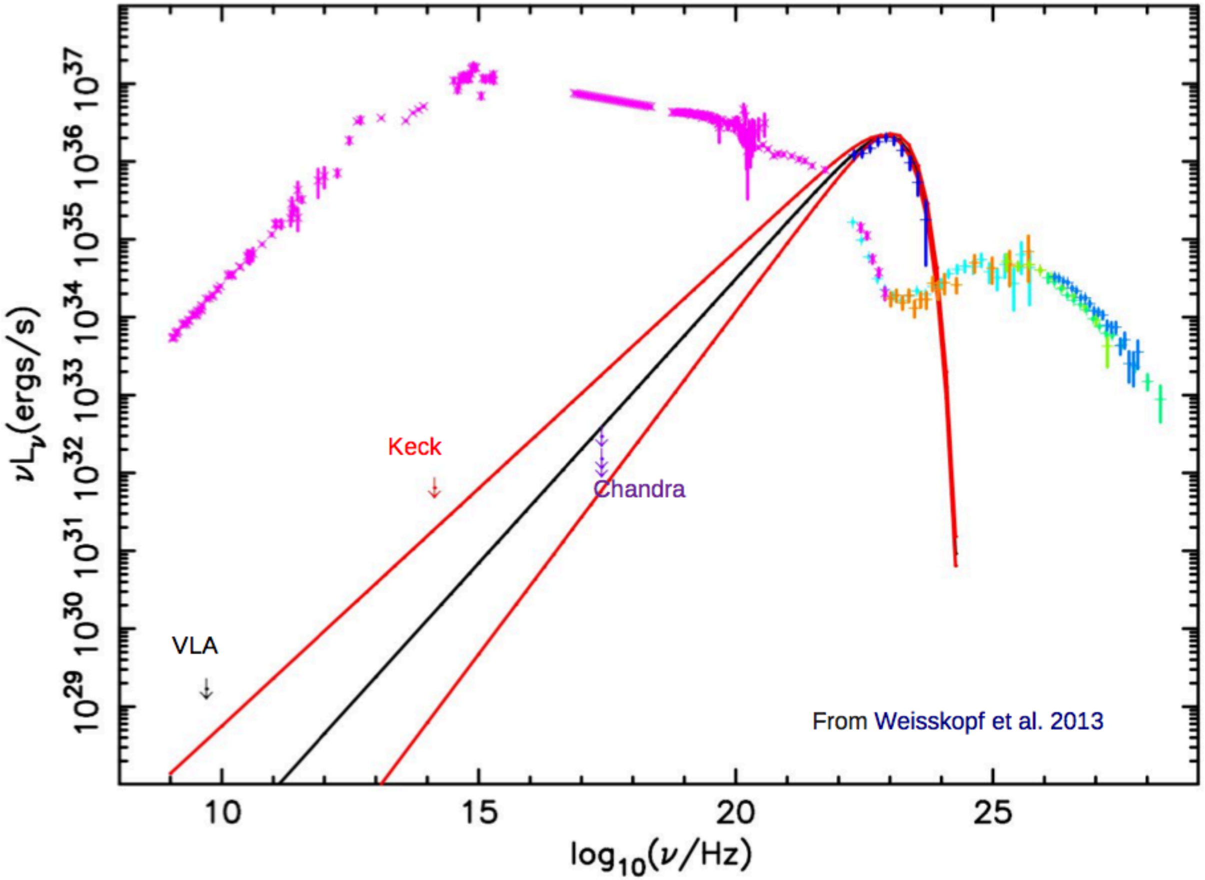

Crab flares

- If these are related to synchrotron emission of electrons, only the highest energy electrons above 100 TeV can be responsible for this and only these electrons can provide changes on scales of days for any reasonable assumption about the magnetic field.

- That implies a corresponding IC photon flux above at least 10 TeV.
  - Possibility of distinguishing boosted blobs ($\Gamma > 30$)

Likely not a direct detection in TeV,
High B would lead to strong suppression

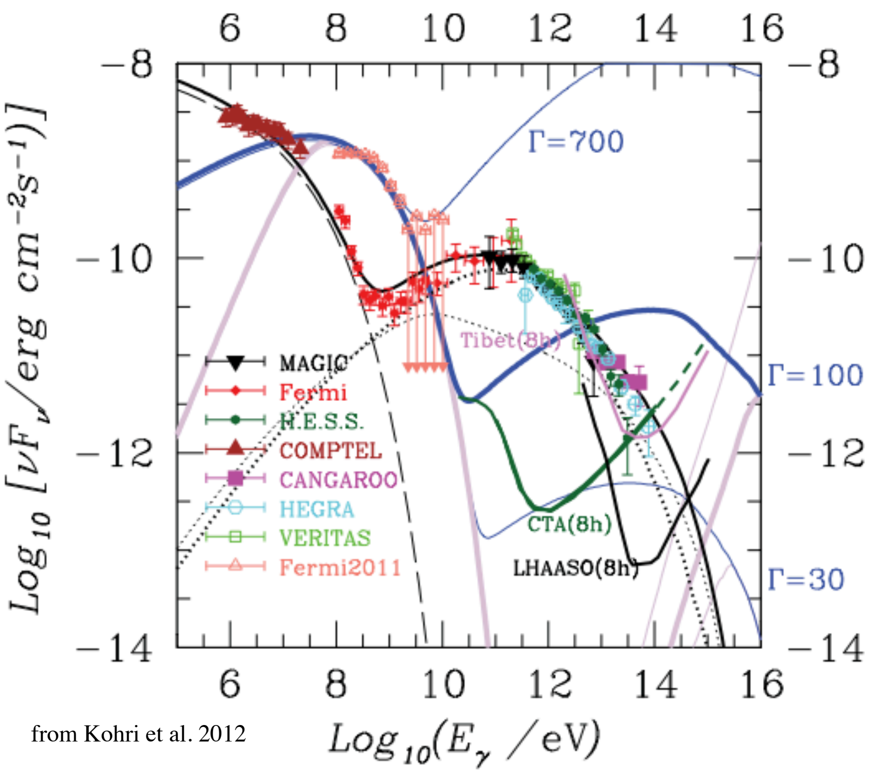

from Kohri et al. 2012

Crab flares

Enhanced TeV gamma ray flux from the Crab Nebula observed by the ARGO-YBJ experiment

ATel #4258; B. Bartoli, P. Bernardini, X. J. Bi, I. Bolognino, P. Branchini, A. Budano, A. K. Calabrese Melcarne, P. Camarri, Z. Cao, R. Cardarelli, S. Catalanotti, C. Cattaneo, S. Z. Chen, T. L. Chen, Y. Chen, P. Creti, S. W. Cui, B. Z. Dai, G. D'AlÃÂ¬ Staiti , A. D'Amone, Danzengluobu, I. De Mitri, B. D'Ettorre Piazzoli, T. Di Girolamo, X. H. Ding, G. Di Sciascio, C. F. Feng, Zhaoyang Feng ,Zhenyong Feng, F. Galeazzi, E. Giroletti, Q. B. Gou, Y. Q. Guo, H. H. He, Haibing Hu, Hongbo Hu, Q. H Y. Jia, Labaciren, H. J. Li, J. Y. Li, X. X. Li, G. H. Lu, L. L. Ma, X. H. Ma, G. Mancarella, Mastroianni, P. Montini, C. C. Ning, A. Pagli Pistilli, F. Ruggieri, P. Salvini, R. Santonico, S. Surdo, Y. H. Tan, P. Vallania, S. Vernetto, C. V Wu, B. Xu, L. Xue, Q. Y. Yang, X. C. Yang, Z. Jilong Zhang, Jianli Zhang, L. Zhang, P. Zhaxiciren, Zhaxisangzhu, X. X. Zhou
on 16 Jul 2012
Credential Certification: Songzh

Subjects: Gamma Ray, TeV, VHE, Neutron Star,

Following the detection by Fermi (ATel#4239) o Crab Nebula region on July 3rd, 2012, we report day by the ARGO-YBJ experiment. ARGO-YBJ at the Yangbajing Cosmic Ray Laboratory in Tib monitors the northern sky at energies above 0.3T duty cycle of about 85%. The Crab Nebula regio A preliminary analysis of the data shows an exce about 4 standard deviations from a direction con corresponding to a flux about 8 times higher thai about 1 TeV. The monitoring of the Crab Nebula significant excesses are detected in the following

No significant enhancement in the VHE gamma-ray flux of the Crab Nebula measured by MAGIC in September 2010

ATel #2967; Mose Mariotti (INFN and Univ. of Padova) on behalf of the MAGIC Collaboration
on 23 Oct 2010; 17:01 UT
Credential Certification: MosÃ¨ Mariotti (mariotti@pd.infn.it)

Subjects: Gamma Ray, TeV, Cosmic Rays, Supernova Ren

The MAGIC telescopes observed the Crab Nebula in stere enhanced activity reported by AGILE (ATel #2855) and Fe September 2010. The observations started at MJD 55459.2 minutes. The average flux and spectrum during these obse reference Crab Nebula data sample taken between 2009 O significant change was detected in flux or spectral shape: t TeV in the flare sample and the reference sample is dN/dE(1TeV)_flare/dN/dE(1TeV)_ref=1.06+/-0.15_stat+/-(the photon indices, fitting data with energies between 1 an Alpha_flare=0.06+/-0.14_stat+/-0.15_syst. Within statistica support the evidence of an increase in the flux of the Crab factor 3 to 4 as reported by ARGO-YBJ (ATel #2921), if th consists of two 17m diameter imaging air Cherenkov teles Islands, Spain. Questions regarding the MAGIC observatio Mariotti (mose.mariotti@pd.infn.it).

Search for an Enhanced TeV Gamma-Ray Flux from the Crab Nebula with VERITAS

ATel #2968; Rene A. Ong (UCLA) for the VERITAS Collaboration
on 23 Oct 2010; 19:25 UT
Credential Certification: Rene Ong (rene@astro.ucla.edu)

Subjects: Gamma Ray, >GeV, TeV, VHE, Neutron Star, Supernova Remnant, Pulsar

Both the AGILE (ATEL #2855) and Fermi-LAT (ATEL #2861) teams have reported an increased >100 MeV gamma-ray flux from a source positionally coincident with the Crab Nebula over the time period from September 19 to September 21, 2010. The ARGO-YBJ air shower detector has reported a gamma-ray excess from the region at the 4 standard deviation level, corresponding to a flux about 3-4 times higher than usual. The ARGO-YBJ result covers the period from September 17 to September 22, at a median energy of about 1 TeV (ATEL #2921).

VERITAS observations of the Crab Nebula in the energy range from 200 GeV to 3 TeV were made on the four nights of September 17, 18, 19, and 20, 2010, totaling 120 minutes. We detect a strong gamma-ray signal corresponding to 40 standard deviations above background. The measured flux level is consistent with VERITAS observations of the Crab Nebula from the previous year (the 2009-2010 observing season). There is no evidence for enhanced emission during the period of time that VERITAS observed the source region; the VERITAS observation times are given in the table below. Statistical errors (one standard deviation) on the average and nightly fluxes above 1 TeV are at the 9% and 20% level, respectively.

Table of VERITAS Observations of the Crab Nebula between Sept 17 and Sept 20, 2010:

Start (MJD)	End (MJD)	Duration (secs)
55456.4471	55456.4610	1202.14
55456.4717	55456.4856	1202.12
55457.4790	55457.4929	1202.15
55458.4529	55458.4669	1202.13
55458.4710	55458.4849	1202.14
55459.4729	55459.4868	1202.11

Mild variability from the nebulae

- Potentially detect IC variability (~1% per year as in x-rays?)
- Results from changes in acceleration efficiency? Magnetic field of the nebulae?
- Is this common to all nebulae? Is there a pattern?

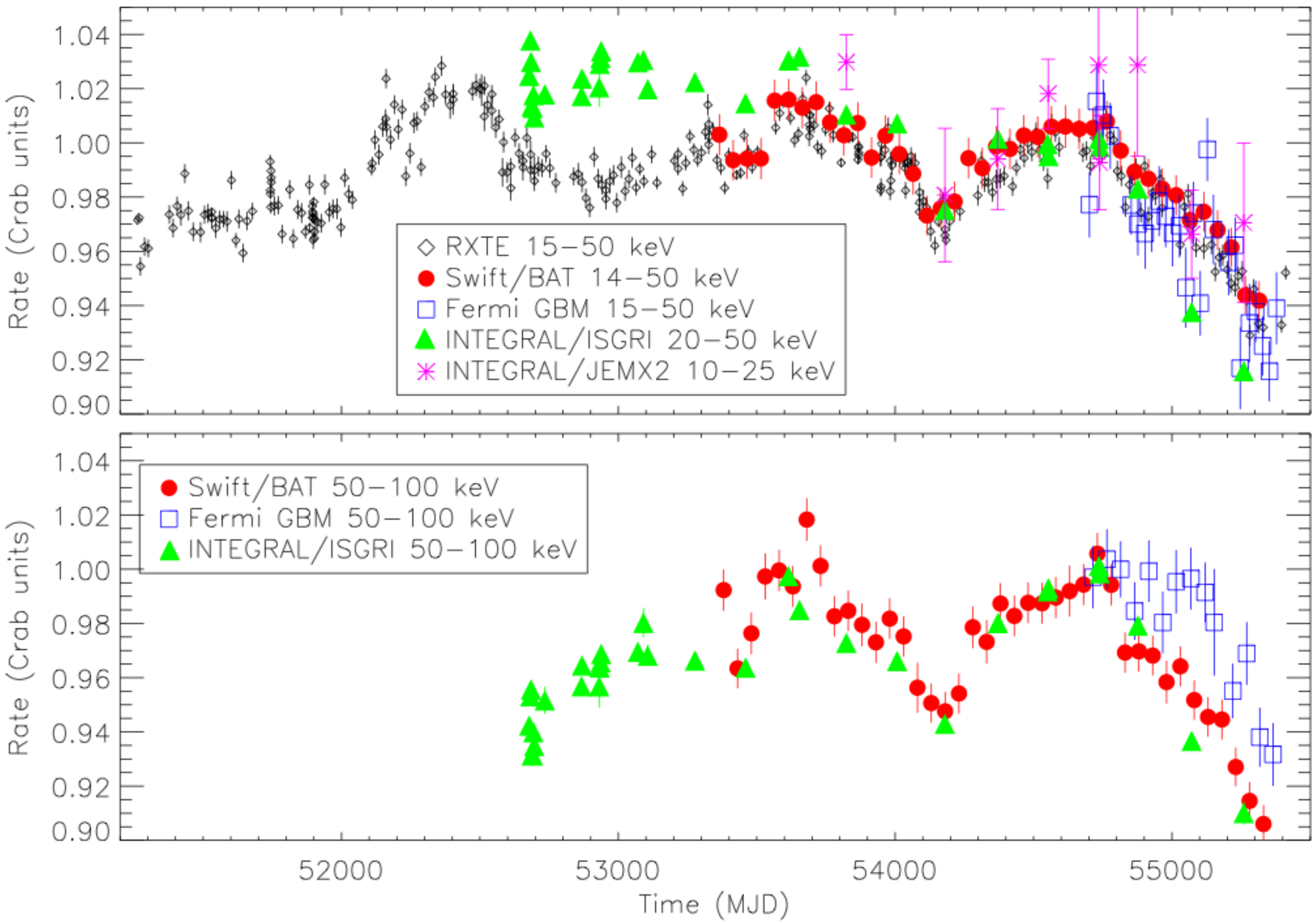

Wilson-Hodge et al. 2011, Kouzu et al. 2013

Pulsations up to 400 GeV

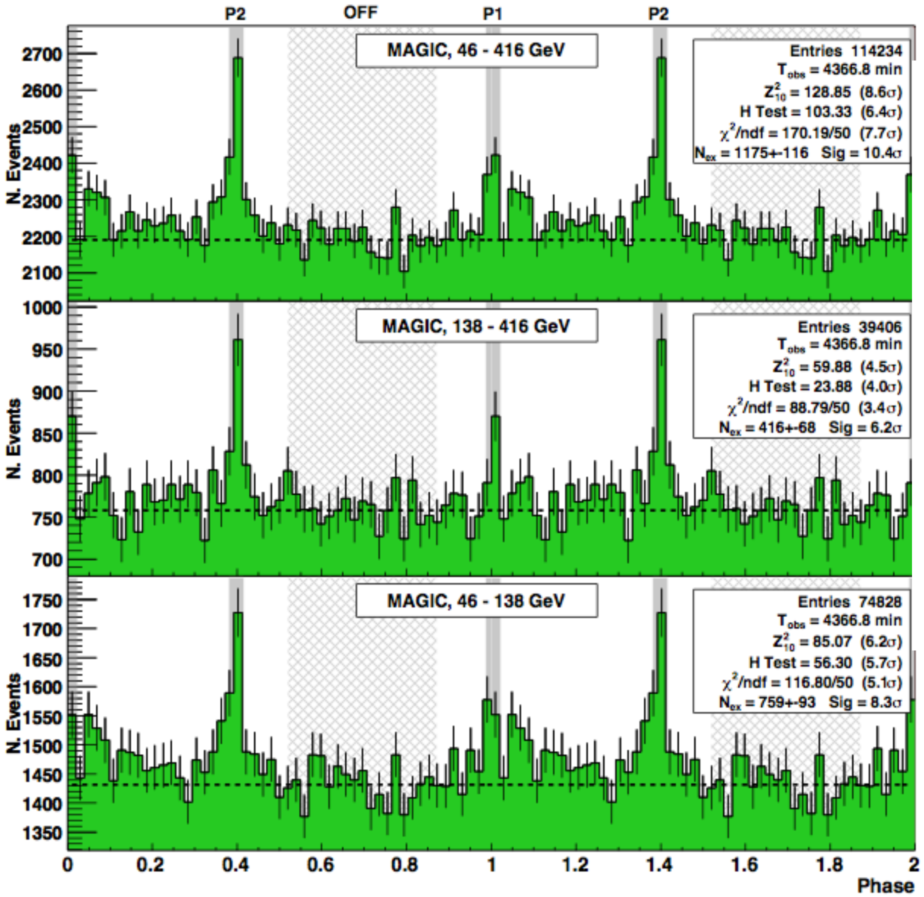

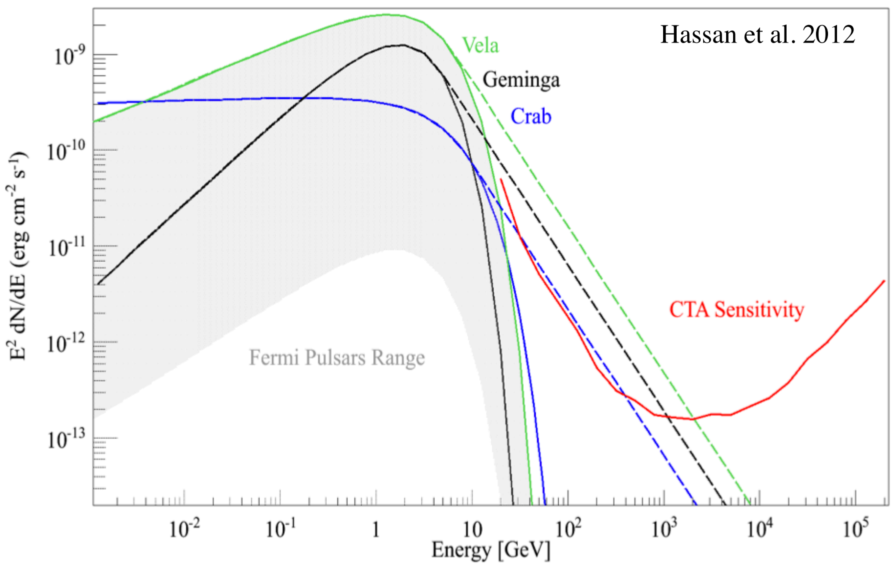

A few pulsars in the detectable region for HESS II. Particlularly, Vela.

MAGIC and VERITAS compatible detection of pulsed radiation >100 GeV

The Crab tail

Explanation proposed:

- SSC from secondary electron-positron pairs created in the magnetosphere (Hirotani)
- IC scattering close to the magnetosphere (Lyutikov)
- IC of the relativistic wind (monoenergetic electron population) with pulsed low-energy (X-ray) emission (Aharonian et al)

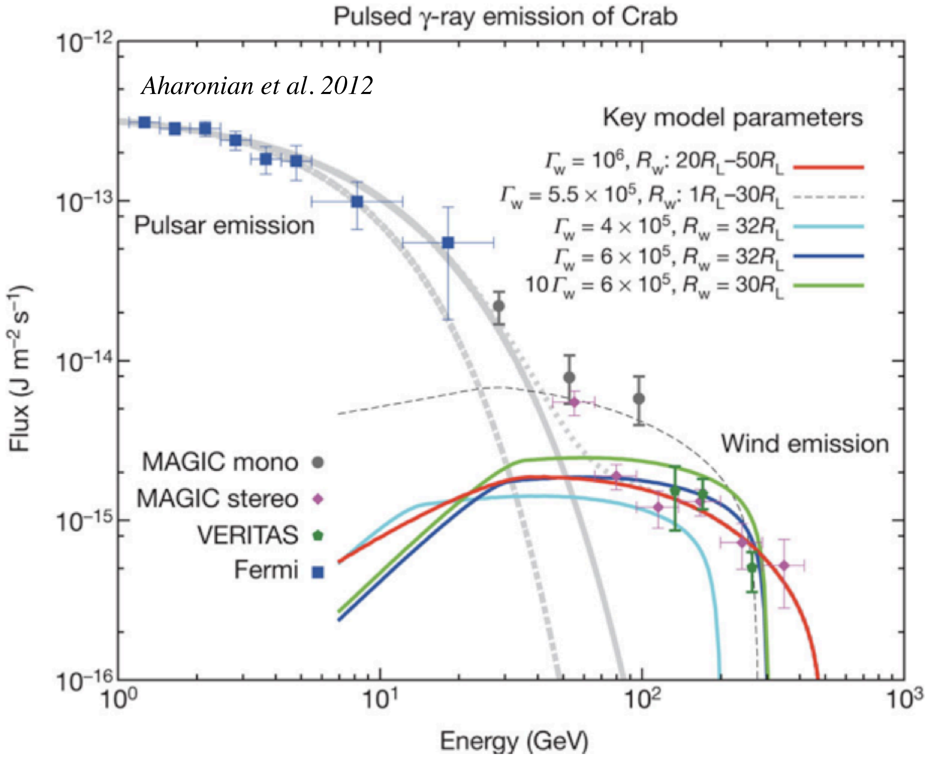

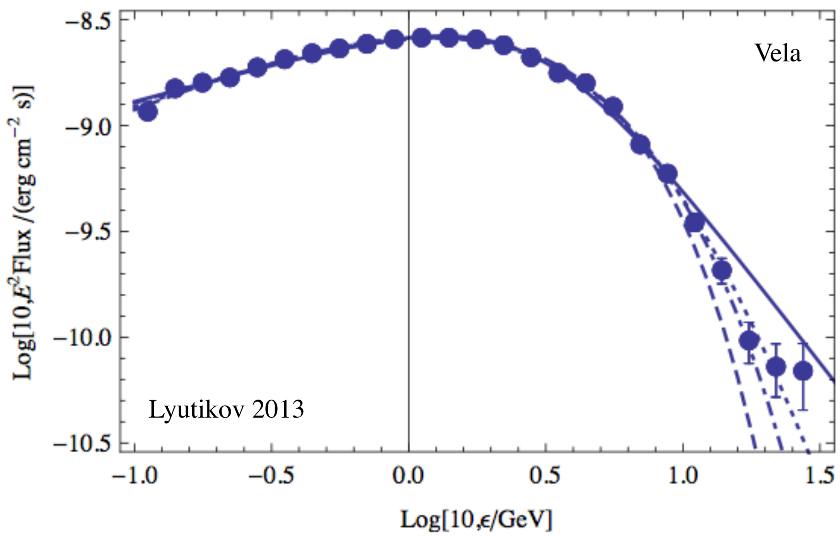

At least for Crab, Vela, and Geminga a power law tail is tenable.

Can PSRs provide DM-like signals? Are they needed?

Is the evidence of a line-like spectral features at 130 GeV real? If it is, can it be the result of a Comptonization of a cold ultrarelativistic electron-positron pulsar wind in the deep Klein-Nishina regime ($\Delta E/E \leq 0.2$)?

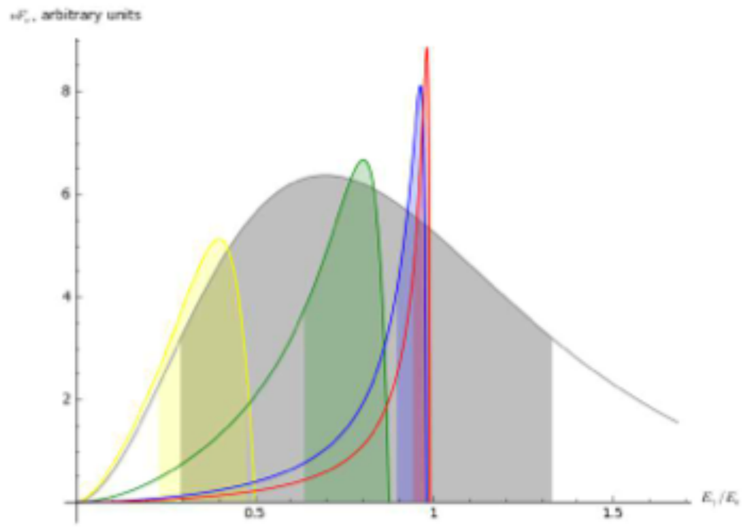

Should we then expect a plethora of gamma-ray lines above 100 GeV in all cases where Lorentz factors and high photon backgrounds are appropriate – Galactic center?

Dark matter hunters, be aware.

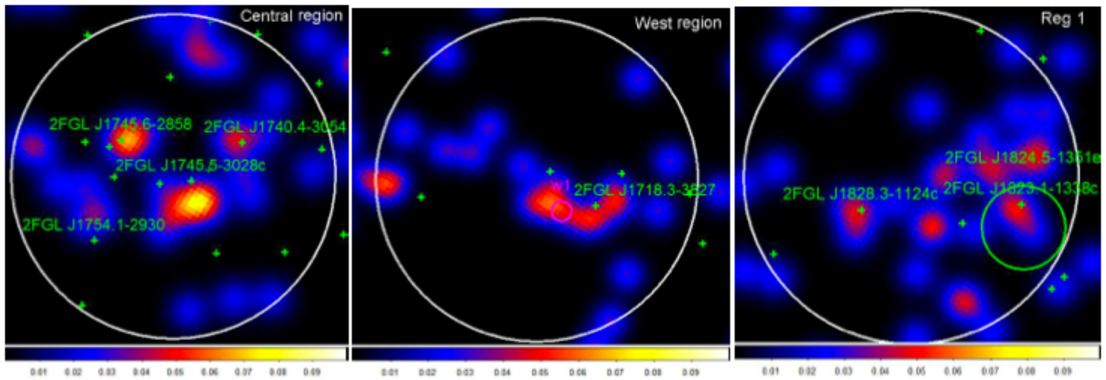

120-140 GeV Fermi-LAT counts towards the Galactic center

A similar analysis lead to discard that PWZ models of gamma-ray binaries prompted by mono-energetic electrons, at least for a single e population (Sierpowska & DFT 2008, Dubus 2009)

Aharonian, Khangulyan and Malishev 2012

Towards understanding order parameters in PWN detectability

ATNF pulsars with less than 10 kyrs of characteristic age

Name J...	P s	$\dot{P}$ s s^{-1}	D kpc	τ yrs	B_d G	$\dot{E}$ erg s^{-1}	$\dot{E}/D^2$ erg s^{-1} kpc^{-2}	TeV Obs.?	TeV PWN?	T_τ^{Crab} yrs	$\dot{E}_{Crab}(T_\tau^{Crab})$ erg s^{-1}	CFP %
1808−2024 †	7.5559	5.49×10^{-10}	13.0	218	2.06×10^{15}	5.0×10^{34}	3.0×10^{32}	H	J1809-194/G11.0+0.08	...	...	...
1846−0258	0.3265	7.10×10^{-12}	5.8	728	4.88×10^{13}	8.1×10^{36}	2.4×10^{35}	H	Kes 75	238	1.6×10^{39}	0.5
1907+0919 †	5.1983	9.20×10^{-11}	...	895	7.00×10^{14}	2.6×10^{34}	...	H	J1908+063/G40.1-0.89	459	1.0×10^{39}	0.003
1714−3810 †	3.8249	5.88×10^{-11}	...	1030	4.80×10^{14}	4.1×10^{34}	...	H	J1718-385/CTB37A	638	7.2×10^{38}	0.006
0534+2200	0.0334	4.21×10^{-13}	2.0	1258	3.78×10^{12}	4.5×10^{38}	1.2×10^{38}	HMV	Crab Nebula	940	4.5×10^{38}	100
1550−5418	2.0698	2.32×10^{-11}	9.7	1410	2.22×10^{14}	1.0×10^{35}	1.1×10^{33}	H	...	1141	3.5×10^{38}	0.03
1513−5908	0.1512	1.53×10^{-12}	4.4	1560	1.54×10^{13}	1.7×10^{37}	9.0×10^{35}	H	J1514-281/MSH 15-52	1340	2.8×10^{38}	6
1119−6127	0.4079	4.02×10^{-12}	8.4	1610	4.10×10^{13}	2.3×10^{36}	3.3×10^{34}	H	J1119-6127/G292.1-0.54	1406	2.6×10^{38}	0.9
0540−6919	0.0504	4.79×10^{-13}	53.7	1670	4.98×10^{12}	1.5×10^{38}	5.1×10^{34}	H	...	1486	2.4×10^{38}	63
0525−6607	8.0470	6.50×10^{-11}	...	1960	7.32×10^{14}	4.9×10^{33}	...	...	...	1871	1.6×10^{38}	0.003
1048−5937	6.4520	3.81×10^{-11}	9.0	2680	5.02×10^{14}	5.6×10^{33}	6.9×10^{31}	H	...	2825	7.8×10^{37}	0.007
1124−5916	0.1354	7.52×10^{-13}	5.0	2850	1.02×10^{13}	1.2×10^{37}	4.8×10^{35}	H	...	3050	6.8×10^{37}	18
1930+1852	0.1368	7.50×10^{-13}	7.0	2890	1.03×10^{13}	1.2×10^{37}	2.4×10^{35}	V	J1930+188/G54.1+0.3	3103	6.6×10^{37}	18
1622−4950	4.3261	1.70×10^{-11}	9.1	4030	2.74×10^{14}	8.3×10^{33}	9.9×10^{31}	H	...	4614	3.0×10^{37}	0.03
1841−0456	11.7789	4.47×10^{-11}	9.6	4180	7.34×10^{14}	1.1×10^{33}	1.2×10^{31}	H	...	4813	2.8×10^{37}	0.004
1023−5746	0.1115	3.84×10^{-13}	8.0	4600	6.62×10^{12}	1.1×10^{37}	1.7×10^{35}	H	J1023+575	5370	2.2×10^{37}	50
1833−1034	0.0618	2.02×10^{-13}	4.10	4850	3.58×10^{12}	3.4×10^{37}	2.0×10^{36}	H	J1833-105/G21.5-0.9	5701	2.0×10^{37}	170
1838−0537	0.1457	4.72×10^{-13}	...	4890	8.39×10^{12}	6.0×10^{36}	...	H	...	5754	1.9×10^{37}	32
0537−6910	0.0161	5.18×10^{-14}	53.7	4930	9.25×10^{11}	4.9×10^{38}	1.7×10^{35}	H	N157B	5807	1.9×10^{37}	2579
1834−0845	2.4823	7.96×10^{-12}	...	4940	1.42×10^{14}	2.1×10^{34}	...	H	J1834-087/W41	5820	1.9×10^{37}	0.1
1747−2809	0.0521	1.55×10^{-13}	17.5	5310	2.88×10^{12}	4.3×10^{37}	1.4×10^{35}	H	J1747-281/G0.9+0.1	6311	1.6×10^{37}	269
0205+6449	0.0657	1.94×10^{-13}	3.2	5370	3.61×10^{12}	2.7×10^{37}	2.6×10^{36}	MV	...	6390	1.6×10^{37}	169
1813−1749	0.0446	1.26×10^{-13}	...	5600	2.41×10^{12}	5.6×10^{37}	...	H	J1813-178/G12.8-0.02	6695	1.4×10^{37}	400
0100−7211	8.0203	1.88×10^{-11}	62.4	6760	3.93×10^{14}	1.4×10^{33}	3.7×10^{29}	...	...	8233	9.1×10^{36}	0.02
1357−6429	0.1661	3.60×10^{-13}	4.1	7310	7.83×10^{12}	3.1×10^{36}	1.9×10^{35}	H	J1356-645/G309.9-2.51	8962	7.6×10^{36}	41
1614−5048	0.2316	4.94×10^{-13}	7.2	7420	1.08×10^{13}	1.6×10^{36}	3.0×10^{34}	H	...	9107	7.3×10^{36}	22
1734−3333	1.1693	2.28×10^{-12}	7.4	8130	5.22×10^{13}	5.6×10^{34}	1.0×10^{33}	H	...	10048	5.9×10^{36}	0.9
1617−5055	0.0693	1.35×10^{-13}	6.4	8130	3.10×10^{12}	1.6×10^{37}	3.8×10^{35}	H	J1616-508	10048	5.9×10^{36}	271
2022+3842	0.0242	4.32×10^{-14}	10.0	8910	1.04×10^{12}	1.2×10^{38}	1.2×10^{36}	...	...	11082	4.8×10^{36}	2500
1708−4009 †	11.0013	1.93×10^{-11}	3.8	9010	4.67×10^{14}	5.7×10^{32}	4.0×10^{31}	H	J1708-443/G343.1-2.69	11215	4.7×10^{36}	0.01

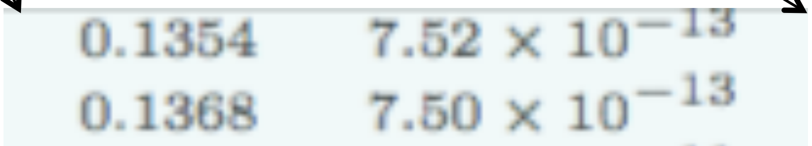

0.1354	7.52×10^{-13}
0.1368	7.50×10^{-13}

Crab Nebula model

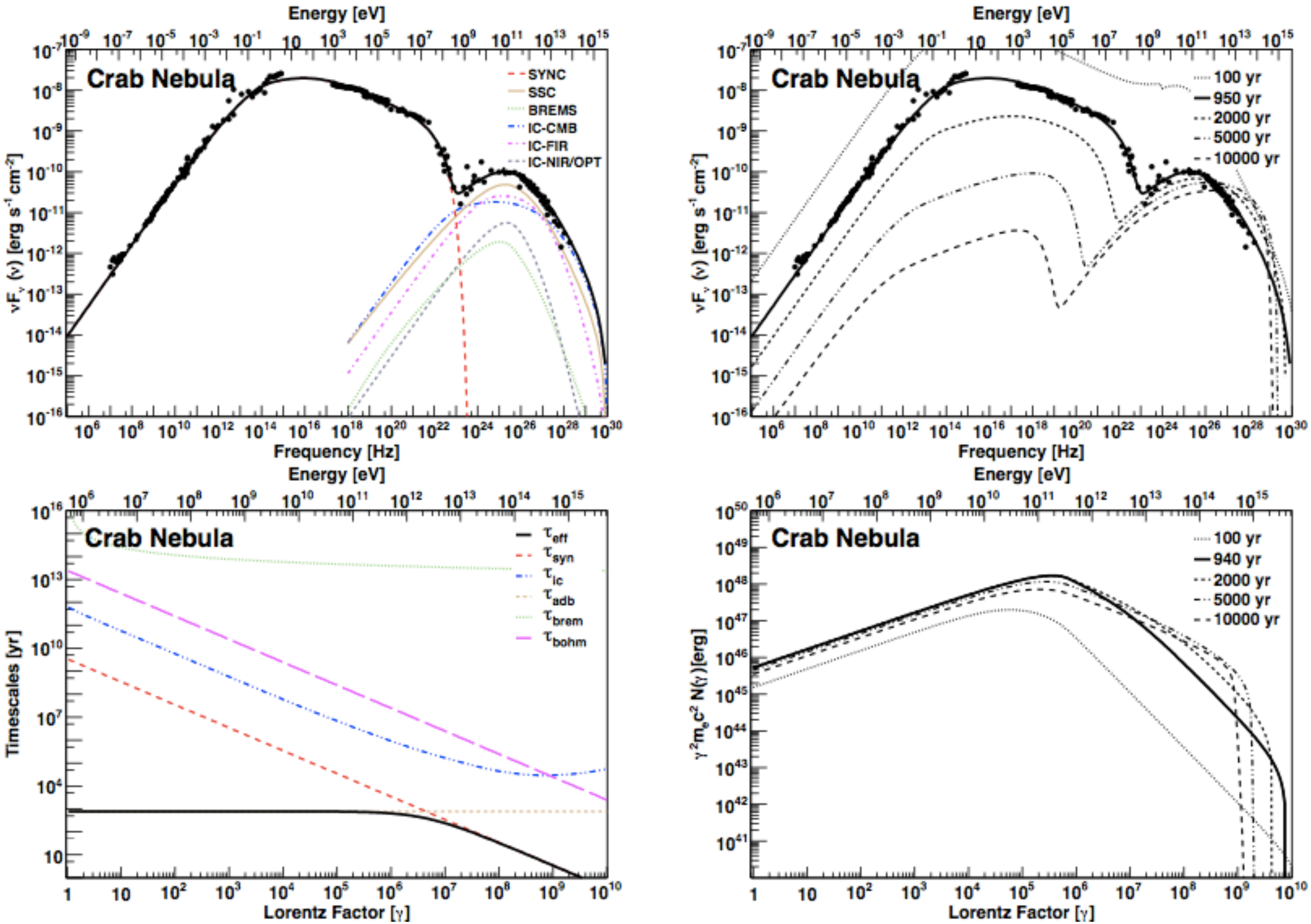

Torres et al. 2013b

Systematic analysis of TeV-detected, young PWNe

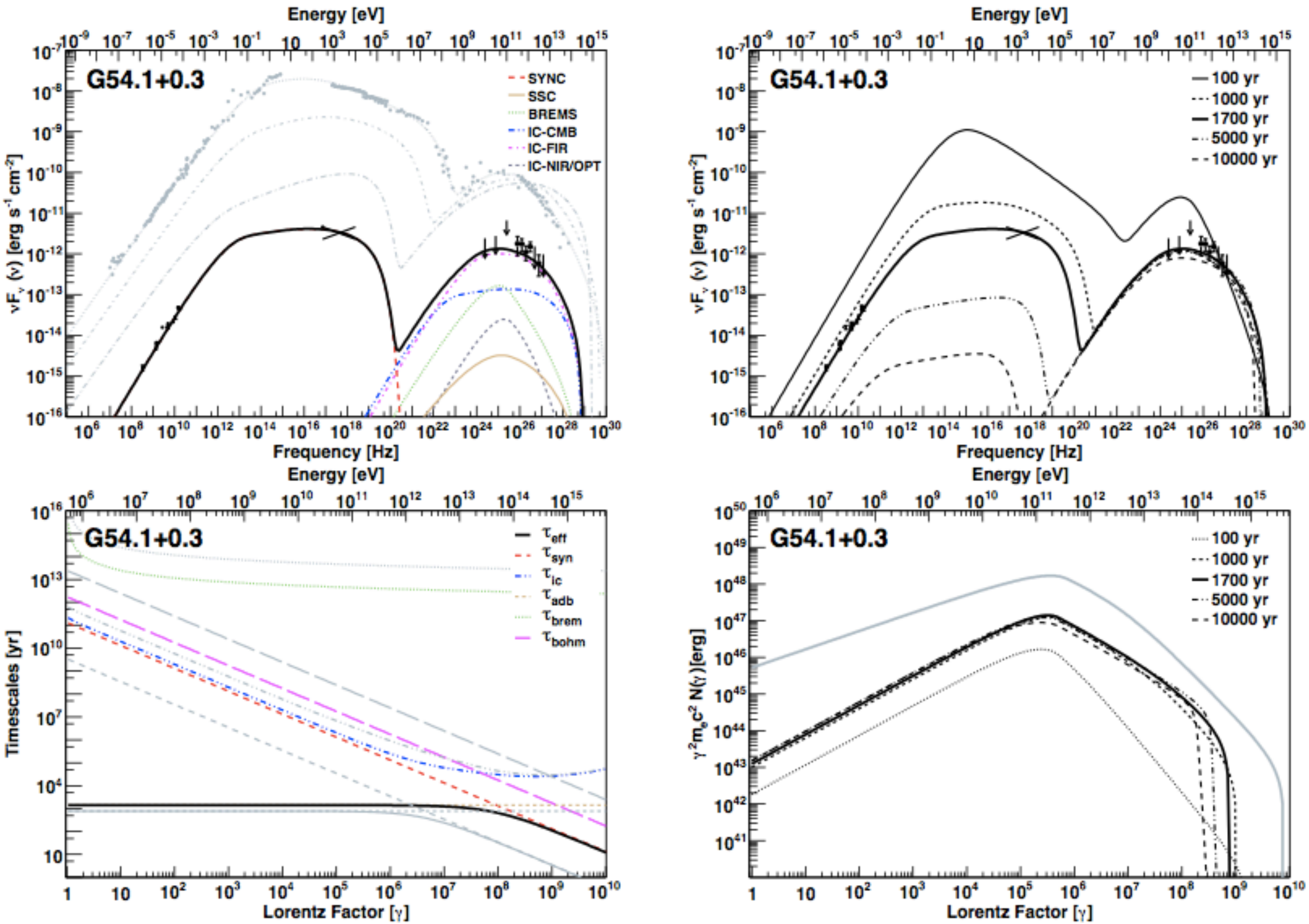

Torres et al. 2013b

Systematic analysis of TeV-detected, young PWNe

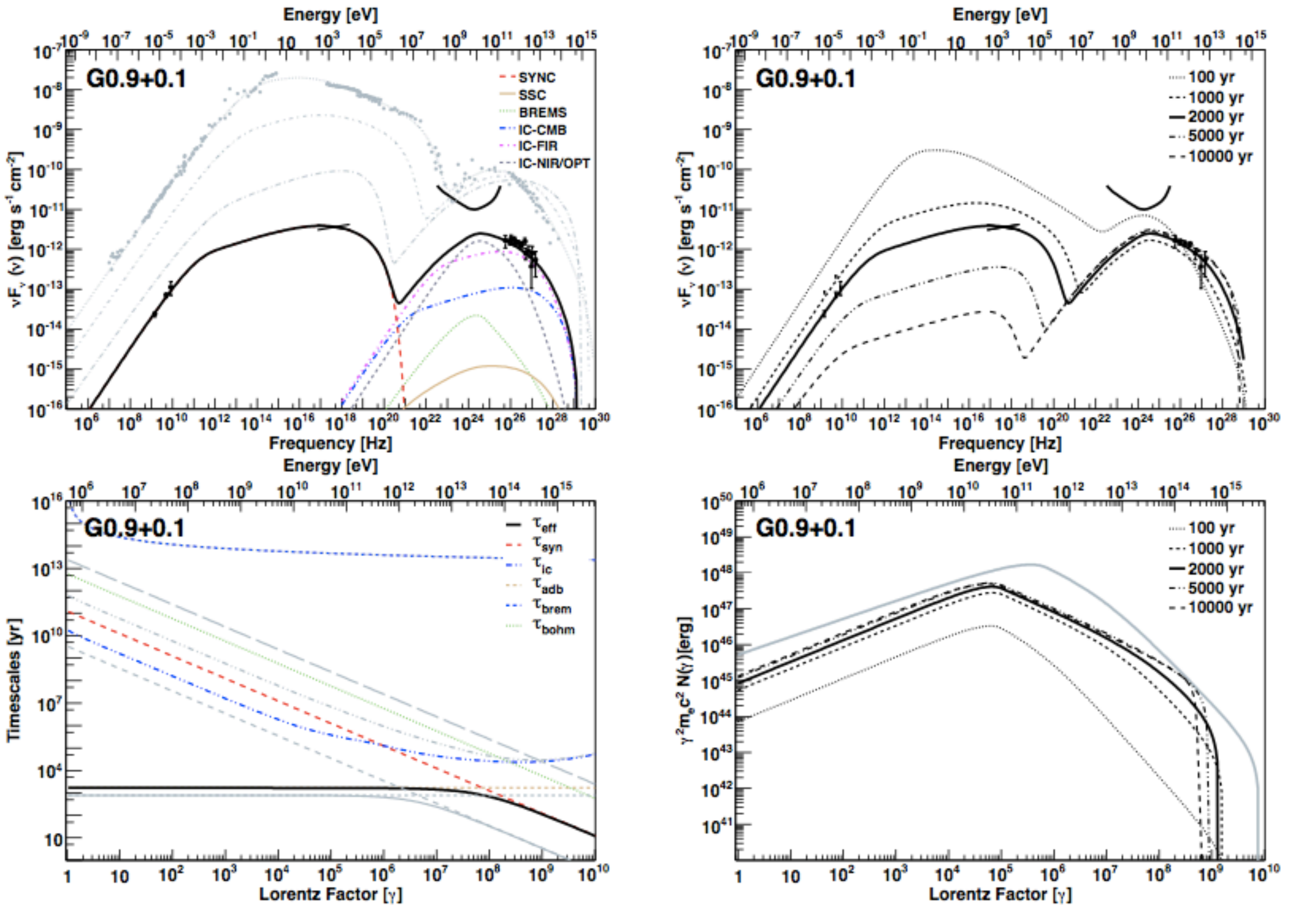

Systematic analysis of TeV-detected, young PWNe

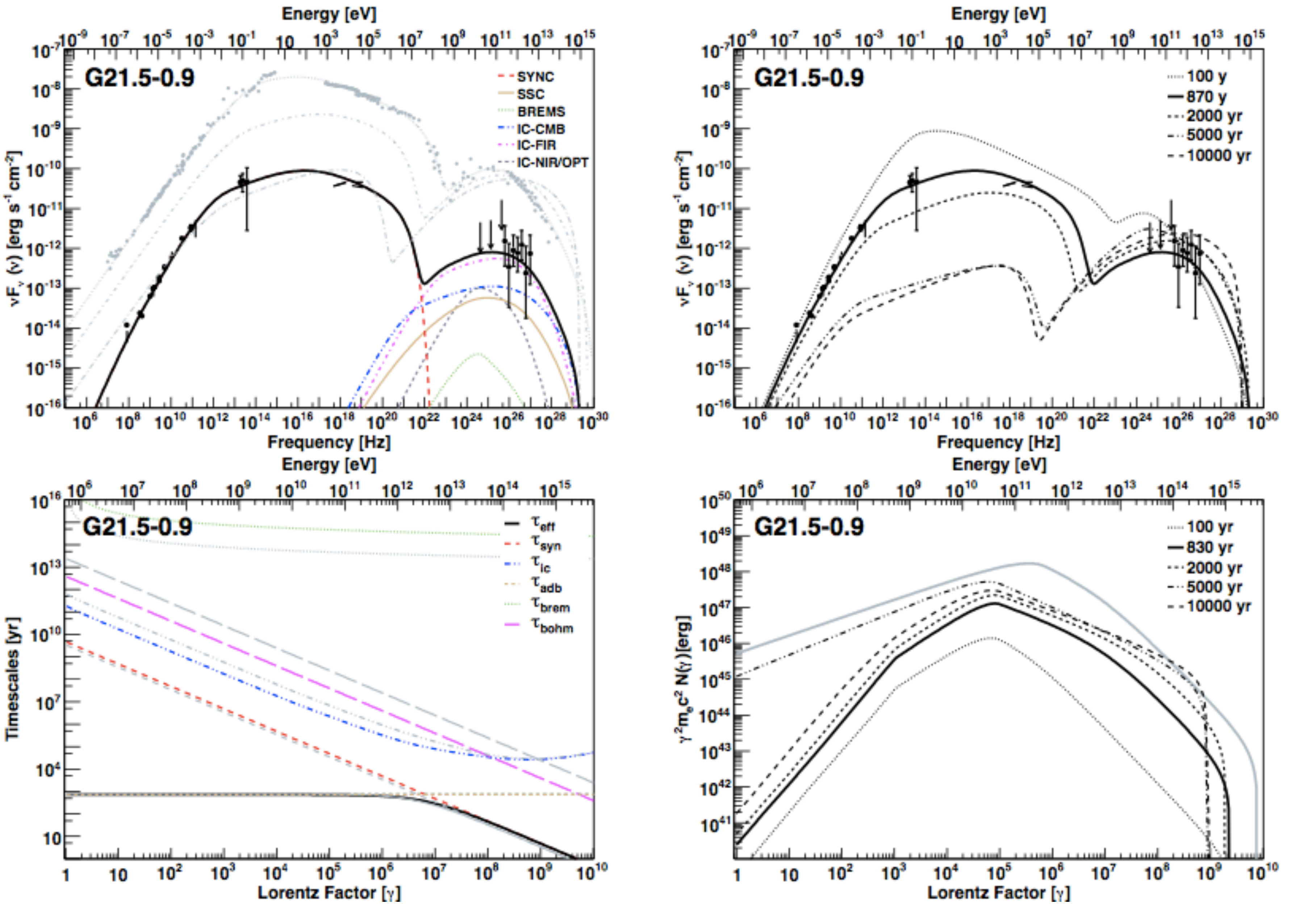

Systematic analysis of TeV-detected, young PWNe

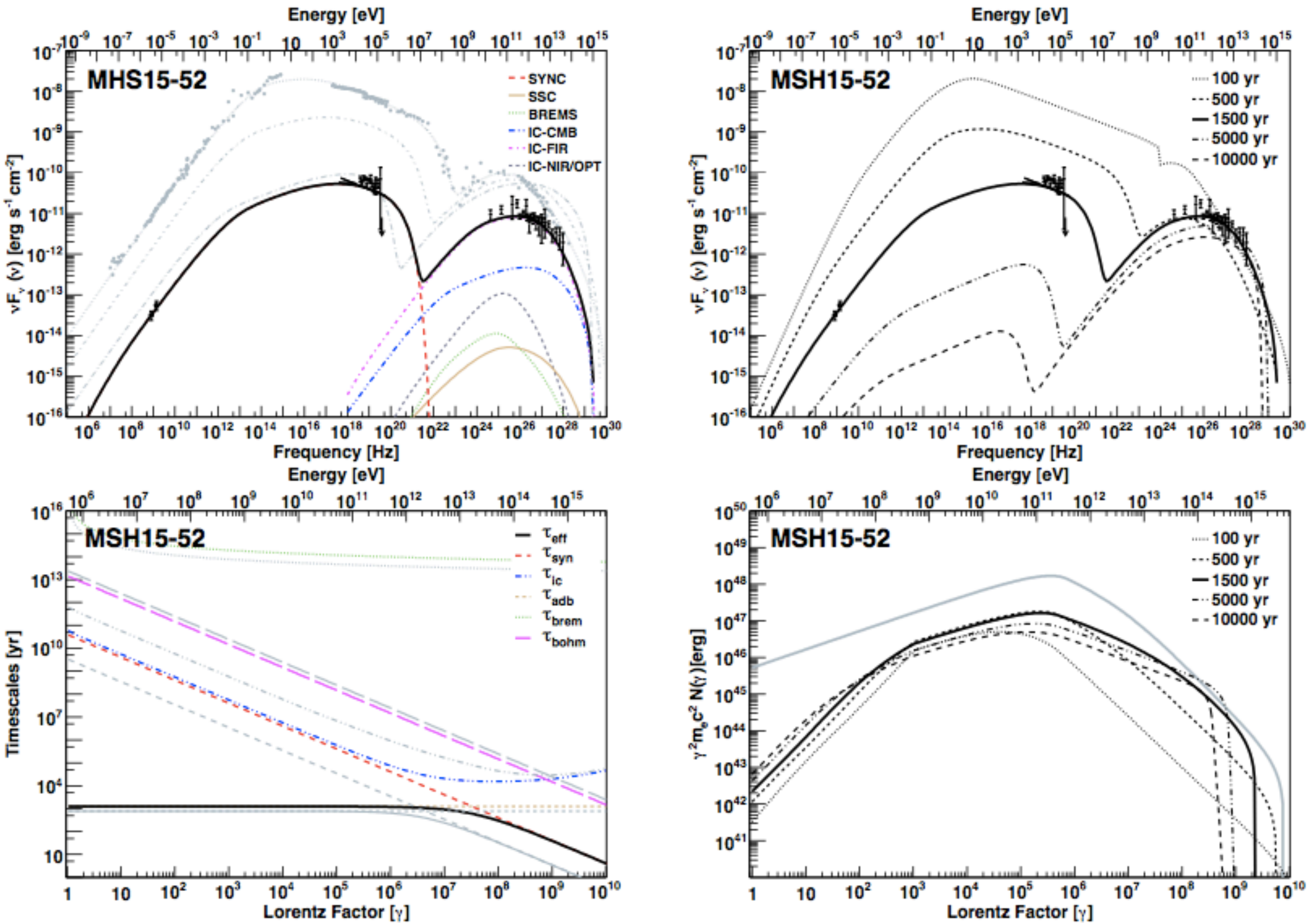

Torres et al. 2013b

Systematic analysis of TeV-detected, young PWNe

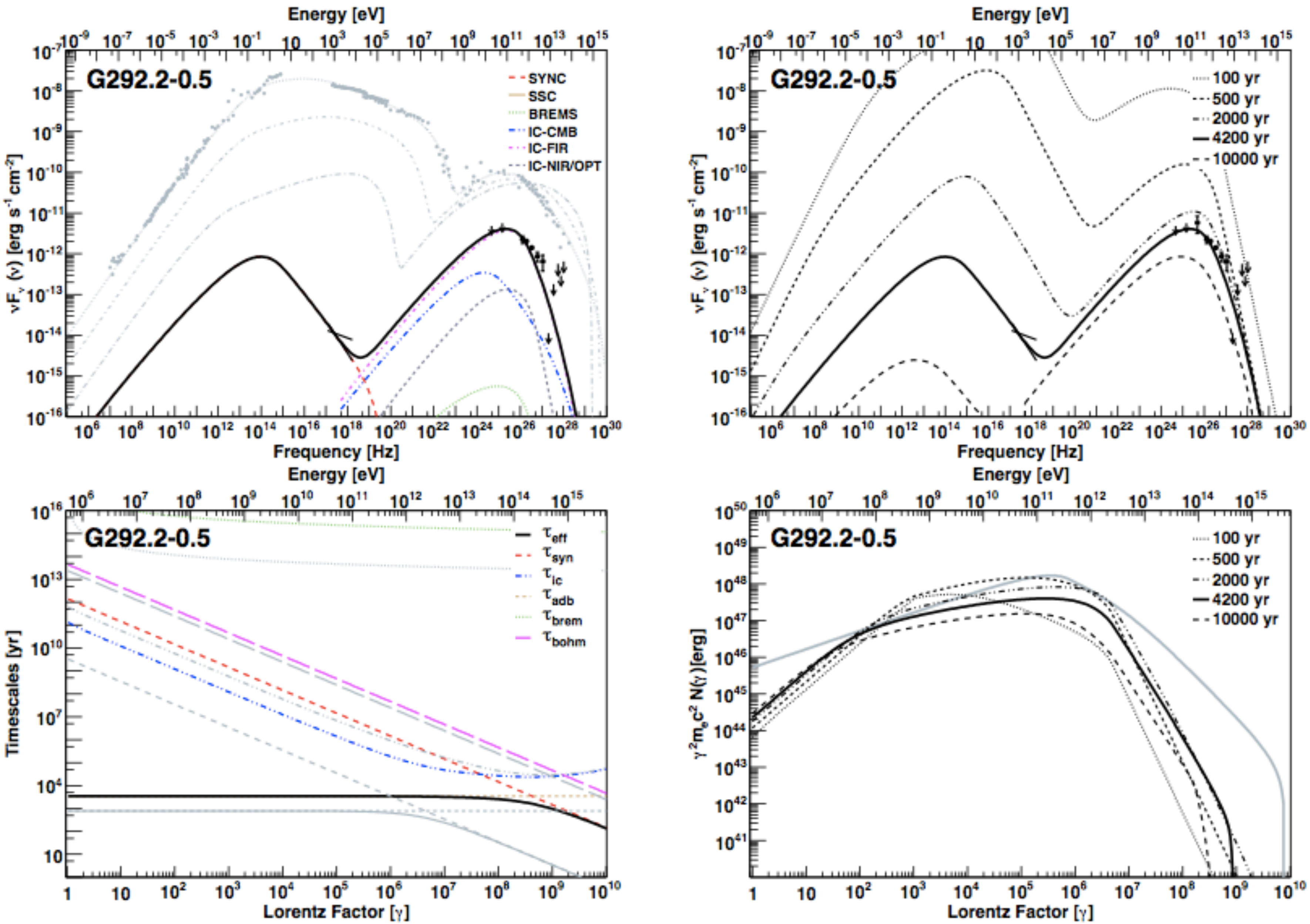

Torres et al. 2013b

Systematic analysis of TeV-detected, young PWNe

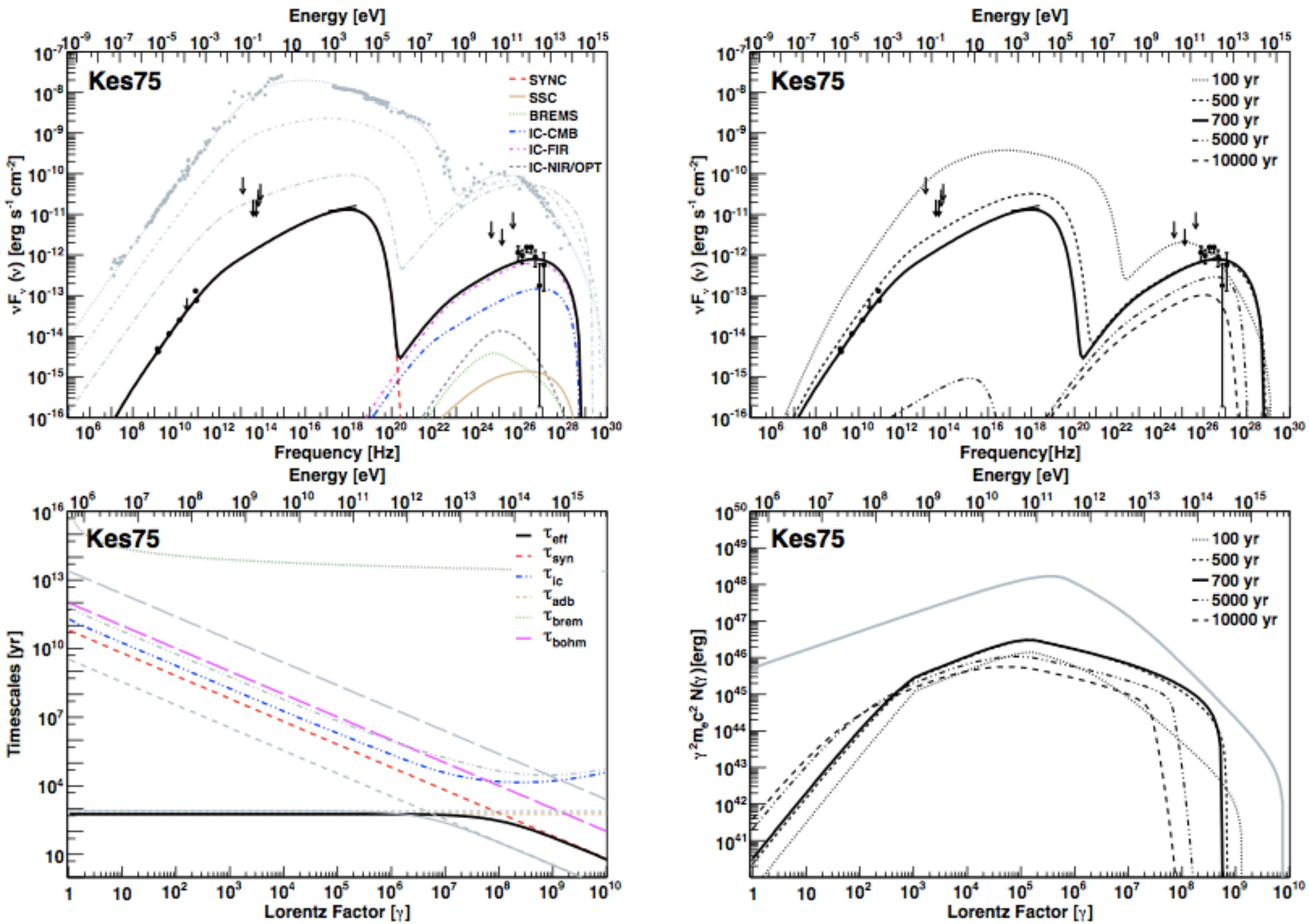

Torres et al. 2013b

Systematic analysis of TeV-detected, young PWNe

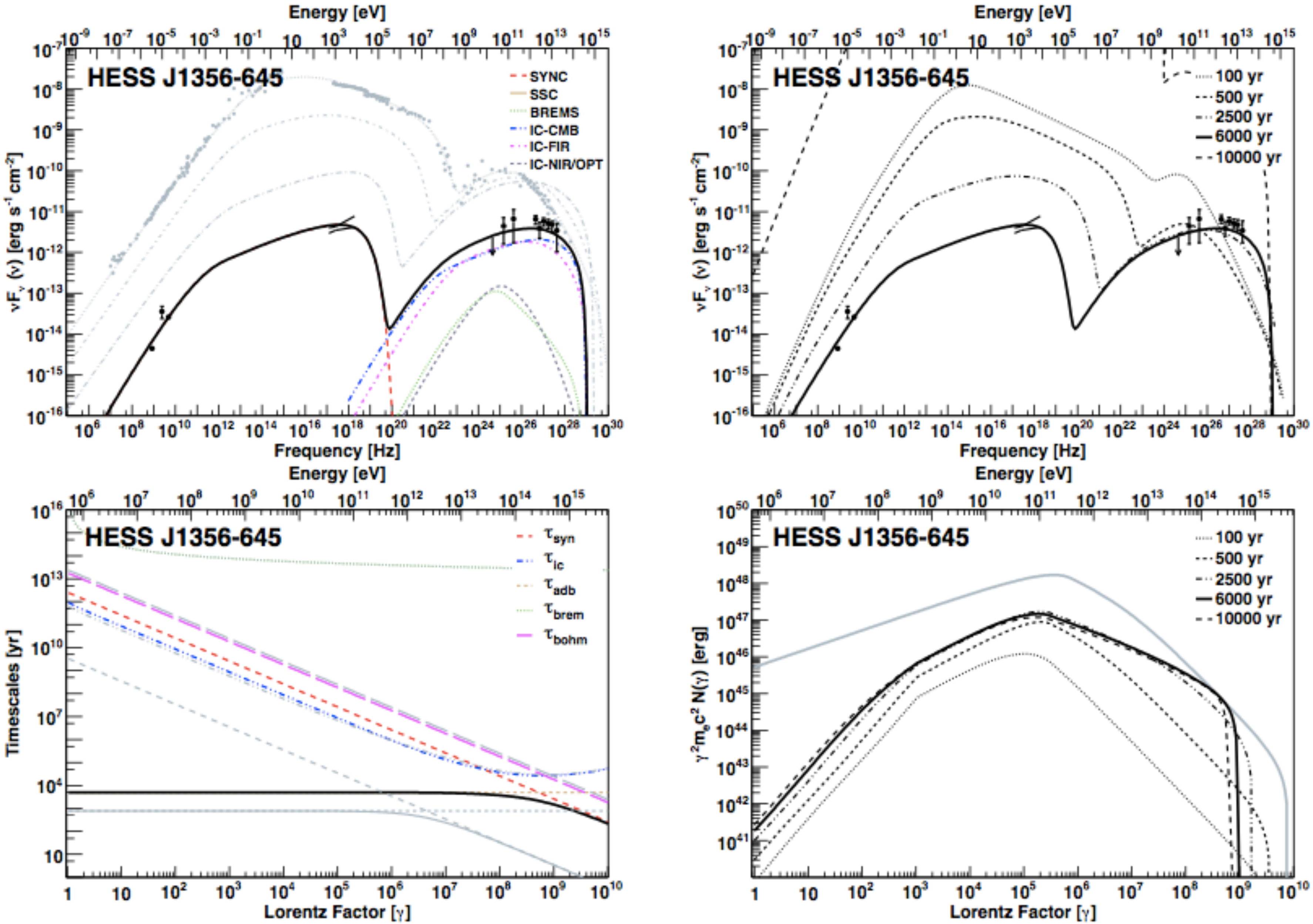

Systematic analysis of TeV-detected, young PWNe

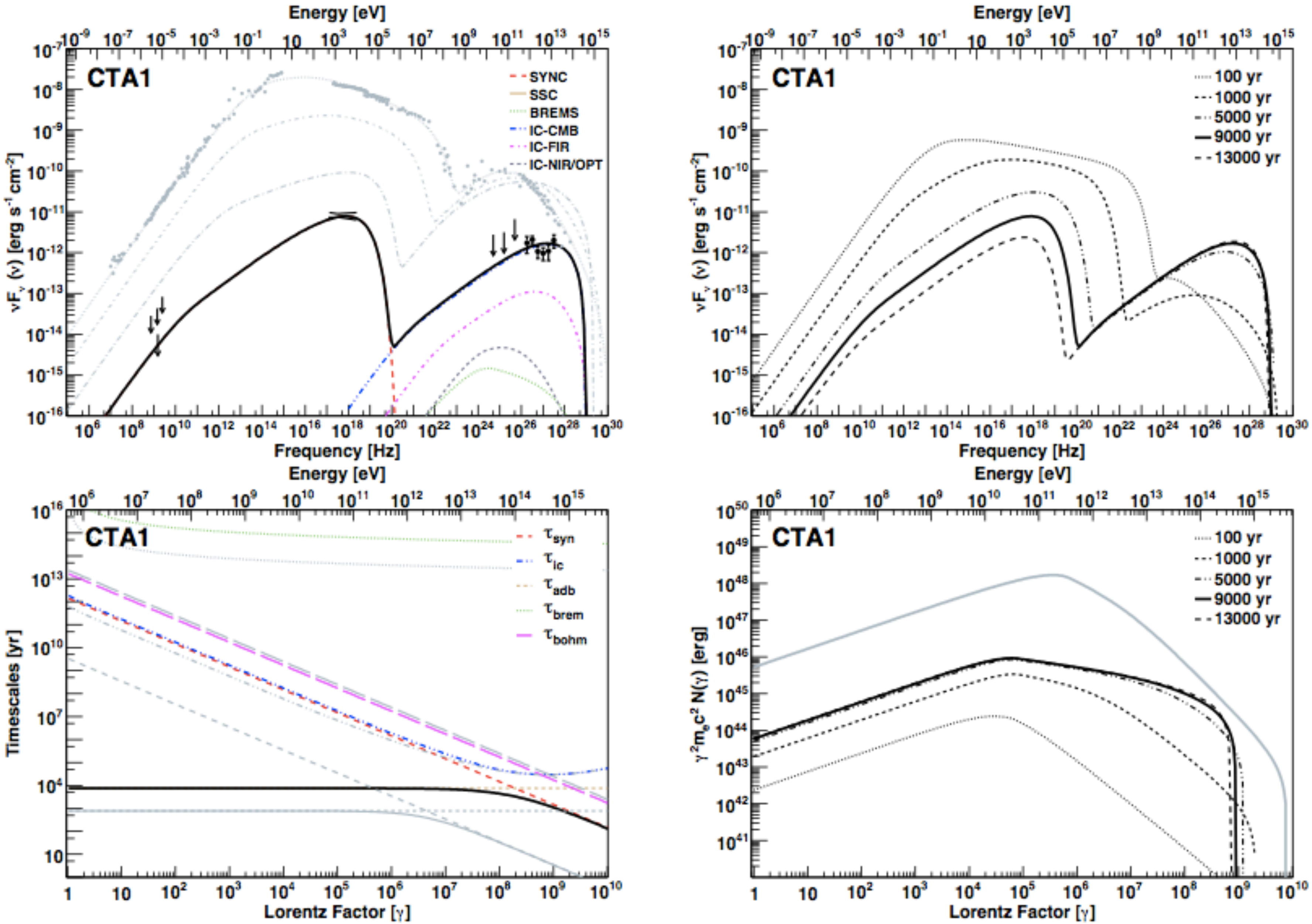

Torres et al. 2013b

Face-value observations

- Large variety of SED shapes and flux level
  - a lot to think about from a population standpoint
- Only Crab is SSC dominated. Most others are FIR-IC dominated and SSC is (very) irrelevant.
- All PWNe are particle dominated (magnetization in the order of a few percent is common; there is only one case with high magnetization, almost equipartion)
- Detected PWNe have high multiplicity
- GALPROP codes tend to undepredict local values of FIR and NIR needed for PWNe to shine up in TeV as they do
- Very similar injection parameters and break energies for all

Torres et al. 2013b

Searching for a more meaningful comparison of PWNe SEDs

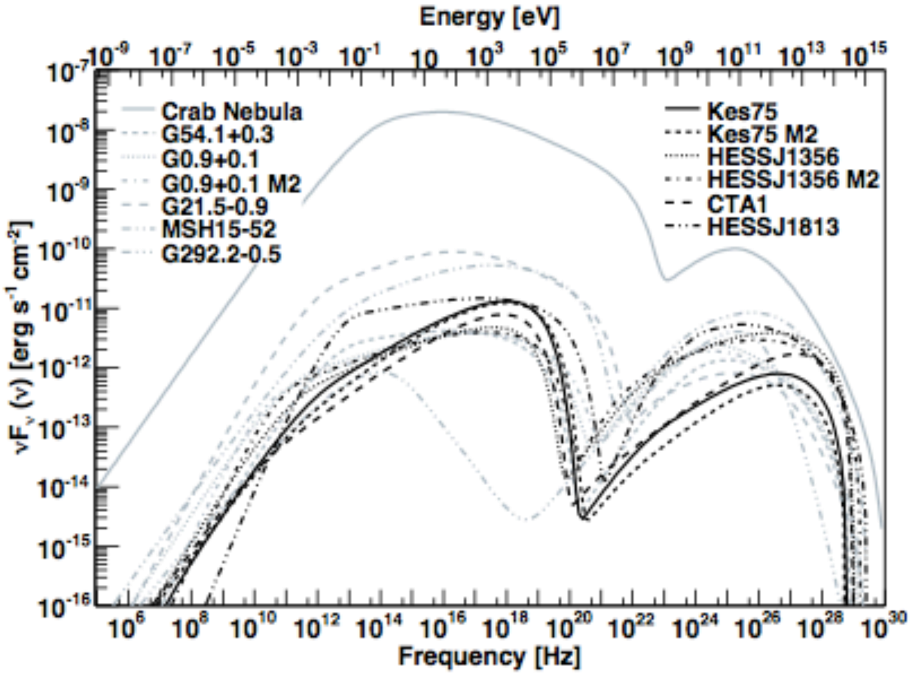

PWNe SEDs today

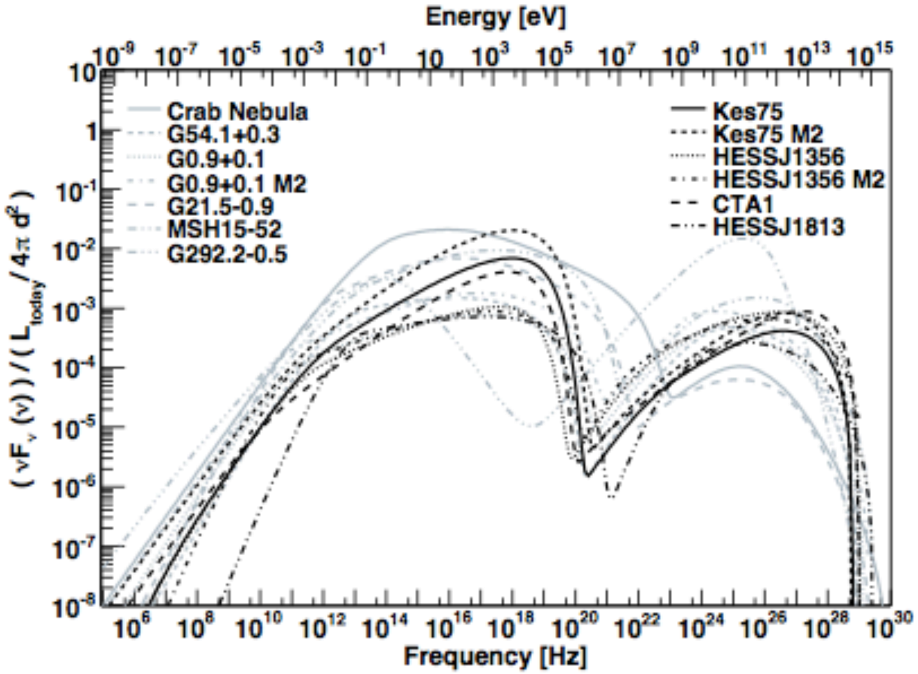

PWNe SEDs today, normalized by spin-down power

Searching for a more meaningful comparison of PWNe SEDs

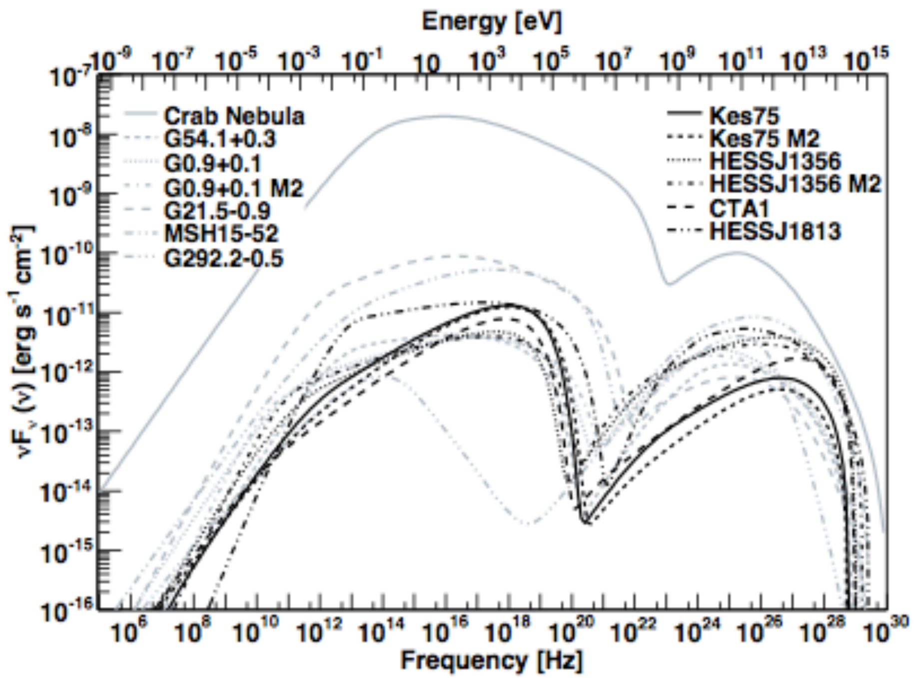

PWNe SEDs today

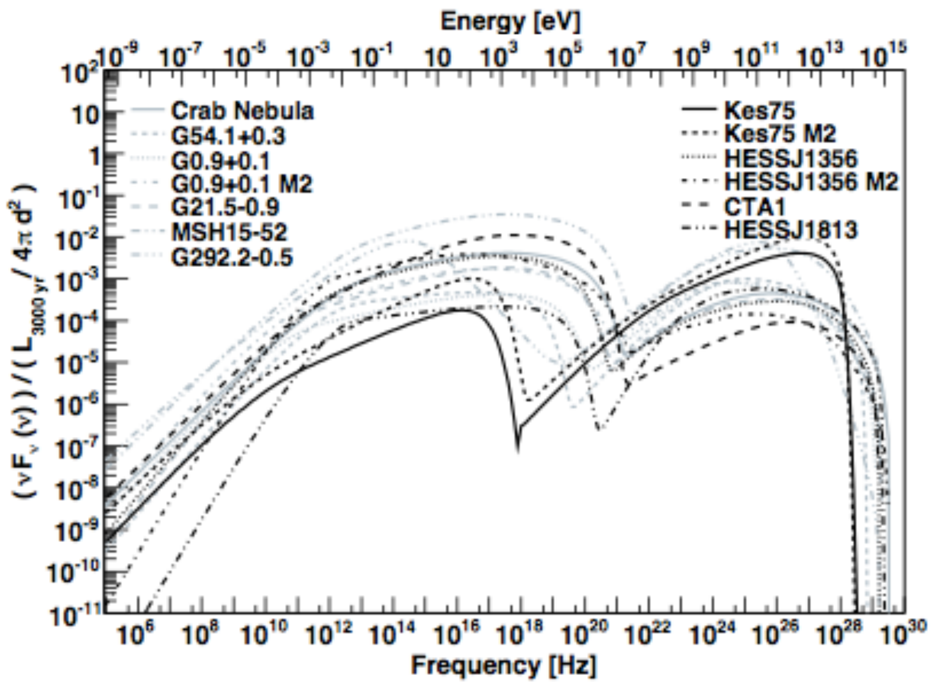

PWNe SEDs today, normalized by spin-down power and compared at the same age

We see particle dominated nebulae

	Crab Nebula	G54.1+0.3 Model 1	G0.9+0.1 Model 1	... Model 2	G21.5−0.9	MSH 15−52 Model 1	G292.2−0.5
Pulsar & Ejecta							
$P(t_{age})$ (ms)	33.40	136	52.2	...	61.86	150	408
$\dot{P}(t_{age})$ (s s^{-1})	4.2×10^{-13}	7.5×10^{-13}	1.5×10^{-13}	...	2.0×10^{-13}	1.5×10^{-12}	4.0×10^{-12}
τ_c (yr)	1296	2871	5305	...	4860	1600	1610
$L(t_{age})$ (erg/s)	$4.5\ \times10^{38}$	1.2×10^{37}	4.3×10^{-37}	...	3.4×10^{37}	$1.8\ \times10^{37}$	$2.3\ \times10^{36}$
n	2.509	3	3	...	3	2.839	1.7
t_{age} (yr)	940	1700	2000	3000	870	1500	4200
d (kpc)	2.0	6	8.5	13	4.7	5.2	8.4
τ_0 (yr)	730	1171	3305	2305	3985	224	270
L_0 (erg/s)	$3.1\ \times10^{39}$	7.2×10^{37}	1.1×10^{38}	2.3×10^{38}	5.0×10^{37}	1.3×10^{39}	$9.2\ \times10^{40}$
M_{ej} $(M_\odot)$	9.5	20	11	17	8	10	35
$R_{PWN}(t_{age})$ (pc)	2.1	1.4	2.5	3.8	0.9	3	13
Environment							
T_{FIR} (K)	70	70	70	...	70	70	70
w_{FIR} (eV/cm^3)	0.5	2.8	4	5	2	10	3
T_{NIR} (K)	5000	5000	5000	...	5000	5000	4000
w_{NIR} (eV/cm^3)	1.0	0.5	35	40	2	1.4	1.4
n_H	1.0	10	1	...	0.1	0.4	0.02
Particles and field							
$\gamma_{max}(t_{age})$	7.9×10^9	7.5×10^8	1.3×10^9	1.9×10^9	2.4×10^9	2.3×10^9	8.0×10^8
γ_b	7×10^5	5×10^5	1.0×10^5	0.5×10^5	1.0×10^5	5.0×10^5	5.0×10^6
α_1	1.5	1.20	1.4	1.2	1.0	1.5	1.5
α_2	2.5	2.77	2.65	2.53	2.53	2.4	4.1
ϵ	0.2	0.3	0.2	...	0.2	0.2	0.3
$B(t_{age})$ (μG)	84	14	14	15	71	25	4
η	0.03	0.005	0.01	0.02	0.04	0.07	0.03

Torres et al. 2013b

SED dependence with magnetic fraction

1% Crab

10% Crab

940 yrs

3000 yrs

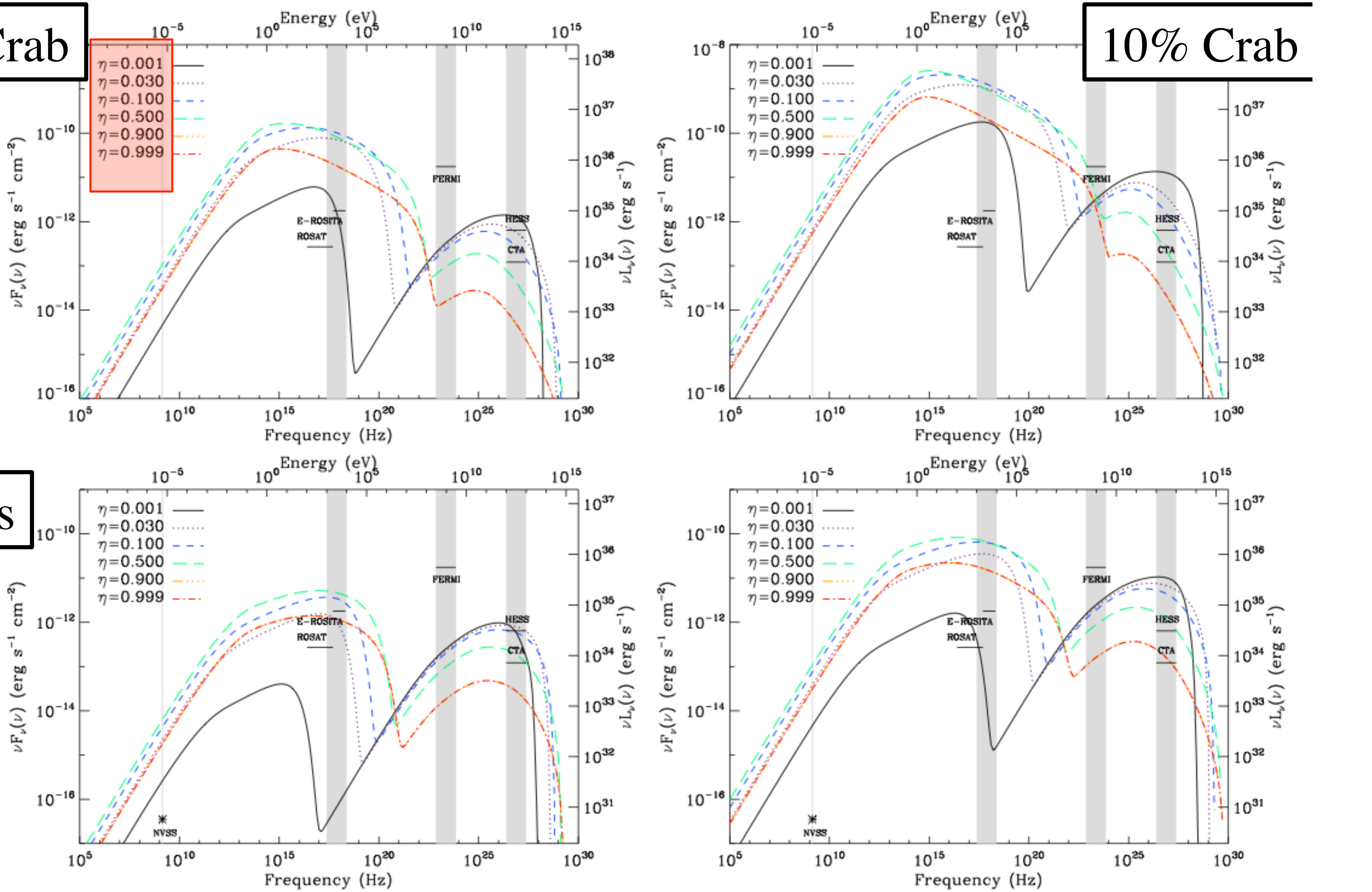

Can we see magnetically dominated nebulae?

Conclusion of PWN phase-space analysis (100 PWN models):

- We would not see any magnetic dominated nebula unless very energetic in terms of spin down, with hard spectrum, in a high FIR background.

- We could barely see a nebula in equipartition if the spin-down is ~10% of Crab, for nebulae of similar injection slope, and living in normal backgrounds (<~1-2 eV cm^{-3})
  - Now, many PWN are indeed in high backgrounds – absence of detection of high magnetization cannot be fully ascribed to biases

Two new PWNe likely to be detected: PSR J1124-5916 & J1614-642

As a result of the phase space analysis

Name J...	P s	$\dot{P}$ s s^{-1}	D kpc	τ yrs	B_d G	$\dot{E}$ erg s^{-1}	$\dot{E}/D^2$ erg s^{-1} kpc^{-2}	TeV Obs.?	TeV PWN?	T_τ^{Crab} yrs	$\dot{E}_{Crab}(T_\tau^{Crab})$ erg s^{-1}	CFP %
1808−2024 †	7.5559	5.49×10^{-10}	13.0	218	2.06×10^{15}	5.0×10^{34}	3.0×10^{32}	H	J1809-194/G11.0+0.08	...	...	...
1846−0258	0.3265	7.10×10^{-12}	5.8	728	4.88×10^{13}	8.1×10^{36}	2.4×10^{35}	H	Kes 75	238	1.6×10^{39}	0.5
1907+0919 †	5.1983	9.20×10^{-11}	...	895	7.00×10^{14}	2.6×10^{34}	...	H	J1908+063/G40.1-0.89	459	1.0×10^{39}	0.003
1714−3810 †	3.8249	5.88×10^{-11}	...	1030	4.80×10^{14}	4.1×10^{34}	...	H	J1718-385/CTB37A	638	7.2×10^{38}	0.006
0534+2200	0.0334	4.21×10^{-13}	2.0	1258	3.78×10^{12}	4.5×10^{38}	1.2×10^{38}	HMV	Crab Nebula	940	4.5×10^{38}	100
1550−5418	2.0698	2.32×10^{-11}	9.7	1410	2.22×10^{14}	1.0×10^{35}	1.1×10^{33}	H	...	1141	3.5×10^{38}	0.03
1513−5908	0.1512	1.53×10^{-12}	4.4	1560	1.54×10^{13}	1.7×10^{37}	9.0×10^{35}	H	J1514-281/MSH 15-52	1340	2.8×10^{38}	6
1119−6127	0.4079	4.02×10^{-12}	8.4	1610	4.10×10^{13}	2.3×10^{36}	3.3×10^{34}	H	J1119-6127/G292.1-0.54	1406	2.6×10^{38}	0.9
0540−6919	0.0504	4.79×10^{-13}	53.7	1670	4.98×10^{12}	1.5×10^{38}	5.1×10^{34}	H	...	1486	2.4×10^{38}	63
0525−6607	8.0470	6.50×10^{-11}	...	1960	7.32×10^{14}	4.9×10^{33}	...	...	...	1871	1.6×10^{38}	0.003
1048−5937	6.4520	3.81×10^{-11}	9.0	2680	5.02×10^{14}	5.6×10^{33}	6.9×10^{31}	H	...	2825	7.8×10^{37}	0.007
1124−5916	0.1354	7.52×10^{-13}	5.0	2850	1.02×10^{13}	1.2×10^{37}	4.8×10^{35}	H	...	3050	6.8×10^{37}	18
1930+1852	0.1368	7.50×10^{-13}	7.0	2890	1.03×10^{13}	1.2×10^{37}	2.4×10^{35}	V	J1930+188/G54.1+0.3	3103	6.6×10^{37}	18
1622−4950	4.3261	1.70×10^{-11}	9.1	4030	2.74×10^{14}	8.3×10^{33}	9.9×10^{31}	H	...	4614	3.0×10^{37}	0.03
1841−0456	11.7789	4.47×10^{-11}	9.6	4180	7.34×10^{14}	1.1×10^{33}	1.2×10^{31}	H	...	4813	2.8×10^{37}	0.004
1023−5746	0.1115	3.84×10^{-13}	8.0	4600	6.62×10^{12}	1.1×10^{37}	1.7×10^{35}	H	J1023+575	5370	2.2×10^{37}	50
1833−1034	0.0618	2.02×10^{-13}	4.10	4850	3.58×10^{12}	3.4×10^{37}	2.0×10^{36}	H	J1833-105/G21.5-0.9	5701	2.0×10^{37}	170
1838−0537	0.1457	4.72×10^{-13}	...	4890	8.39×10^{12}	6.0×10^{36}	...	H	...	5754	1.9×10^{37}	32
0537−6910	0.0161	5.18×10^{-14}	53.7	4930	9.25×10^{11}	4.9×10^{38}	1.7×10^{35}	H	N157B	5807	1.9×10^{37}	2579
1834−0845	2.4823	7.96×10^{-12}	...	4940	1.42×10^{14}	2.1×10^{34}	...	H	J1834-087/W41	5820	1.9×10^{37}	0.1
1747−2809	0.0521	1.55×10^{-13}	17.5	5310	2.88×10^{12}	4.3×10^{37}	1.4×10^{35}	H	J1747-281/G0.9+0.1	6311	1.6×10^{37}	269
0205+6449	0.0657	1.94×10^{-13}	3.2	5370	3.61×10^{12}	2.7×10^{37}	2.6×10^{36}	MV	...	6390	1.6×10^{37}	169
1813−1749	0.0446	1.26×10^{-13}	...	5600	2.41×10^{12}	5.6×10^{37}	...	H	J1813-178/G12.8-0.02	6695	1.4×10^{37}	400
0100−7211	8.0203	1.88×10^{-11}	62.4	6760	3.93×10^{14}	1.4×10^{33}	3.7×10^{29}	...	...	8233	9.1×10^{36}	0.02
1357−6429	0.1661	3.60×10^{-13}	4.1	7310	7.83×10^{12}	3.1×10^{36}	1.9×10^{35}	H	J1356-645/G309.9-2.51	8962	7.6×10^{36}	41
1614−5048	0.2316	4.94×10^{-13}	7.2	7420	1.08×10^{13}	1.6×10^{36}	3.0×10^{34}	H	...	9107	7.3×10^{36}	22
1734−3333	1.1693	2.28×10^{-12}	7.4	8130	5.22×10^{13}	5.6×10^{34}	1.0×10^{33}	H	...	10048	5.9×10^{36}	0.9
1617−5055	0.0693	1.35×10^{-13}	6.4	8130	3.10×10^{12}	1.6×10^{37}	3.8×10^{35}	H	J1616-508	10048	5.9×10^{36}	271
2022+3842	0.0242	4.32×10^{-14}	10.0	8910	1.04×10^{12}	1.2×10^{38}	1.2×10^{36}	...	...	11082	4.8×10^{36}	2500
1708−4009 †	11.0013	1.93×10^{-11}	3.8	9010	4.67×10^{14}	5.7×10^{32}	4.0×10^{31}	H	J1708-443/G343.1-2.69	11215	4.7×10^{36}	0.01

There is an excellent chance for them to be discovered in a reanalysis of HESS survey data; only way they would not show if they are magnetically dominated nebulae – anyway an excellent result.

Associations and their collective winds? Special binaries?

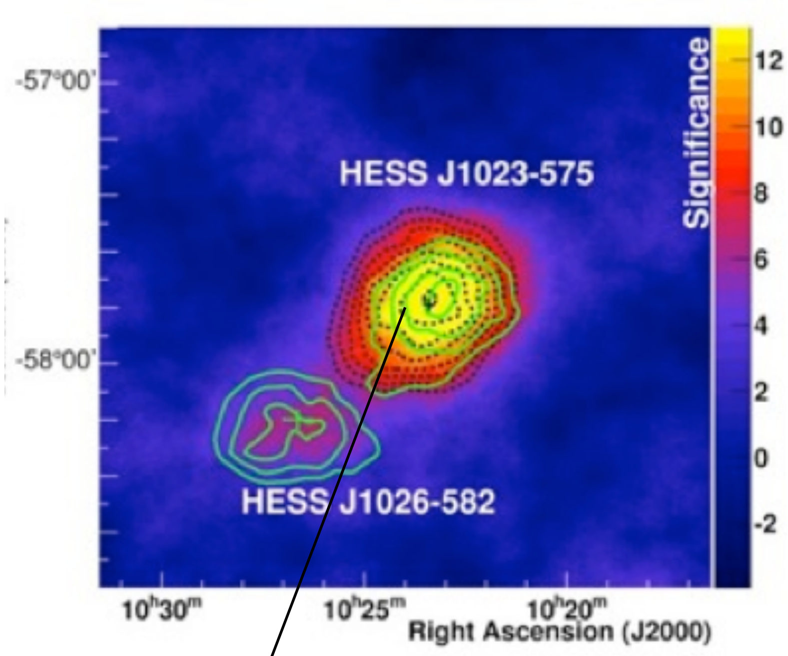

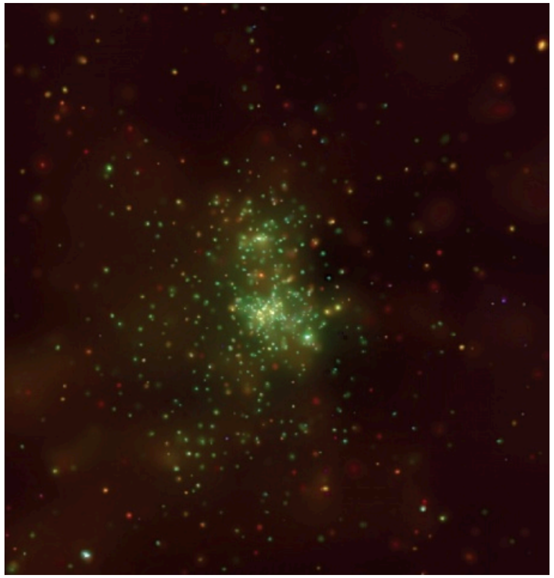

Westerlund 2, de Oña Wilhelmi et al. 2010

- WR20a among the more massive binary in the galaxy (2 stars of ~80 solar masses in a 3.8 day orbit!), also WR 20b nearby. But the TeV source is extended and steady

Associations and their collective winds?

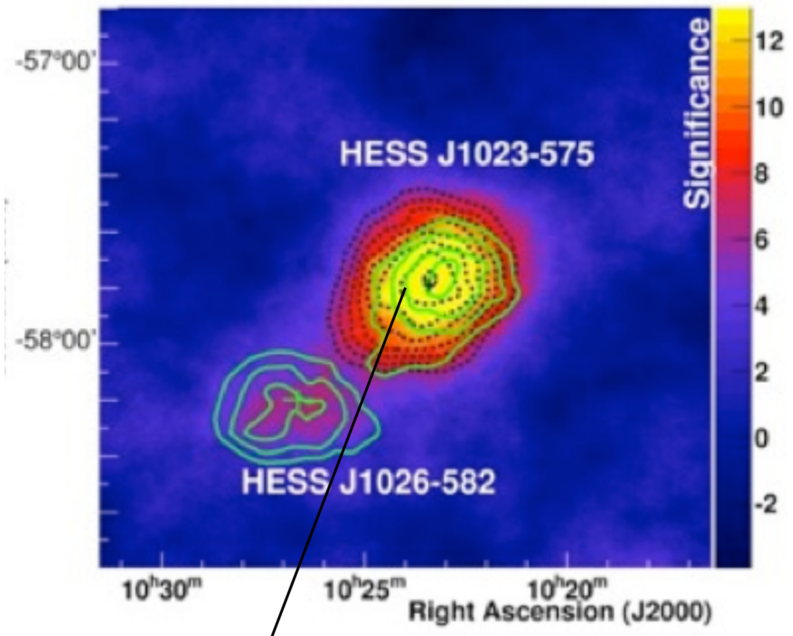

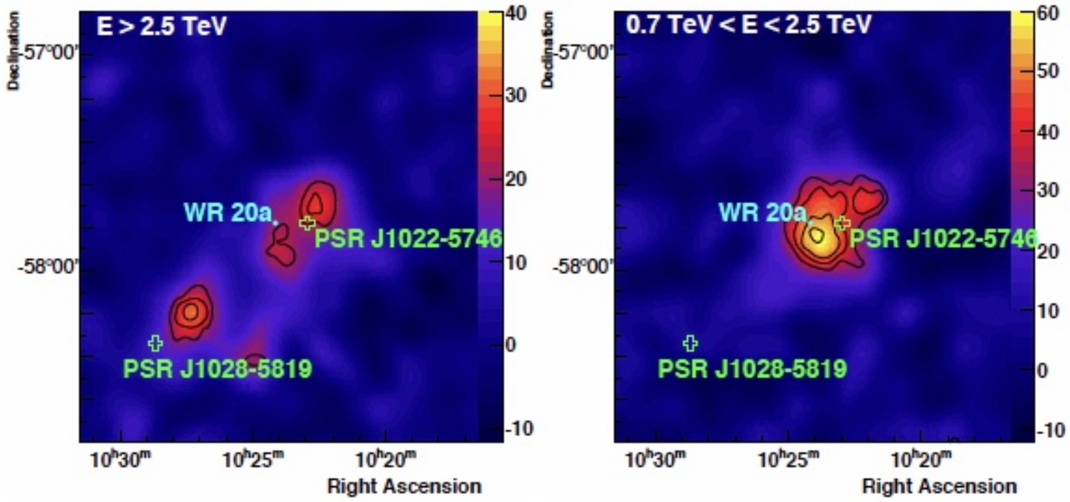

Westerlund 2, de Oña Wilhelmi et al. 2010

- WR20a among the more massive binary in the galaxy (2 stars of ~80 solar masses in a 3.8 day orbit!), also WR 20b nearby; but the source is extended and steady
- Increasing the observation time allows for source separation, and interesting energy dependent morphology; not clearly understood
  - PSRJ 1028 and J1022 are both Fermi pulsars

Associations and their collective winds?

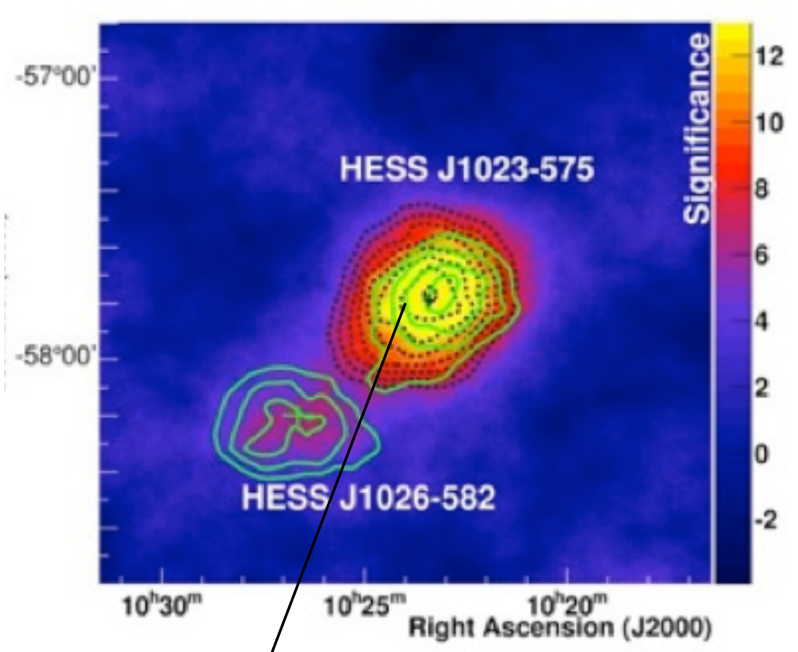

Westerlund 2, de Oña Wilhelmi et al. 2010

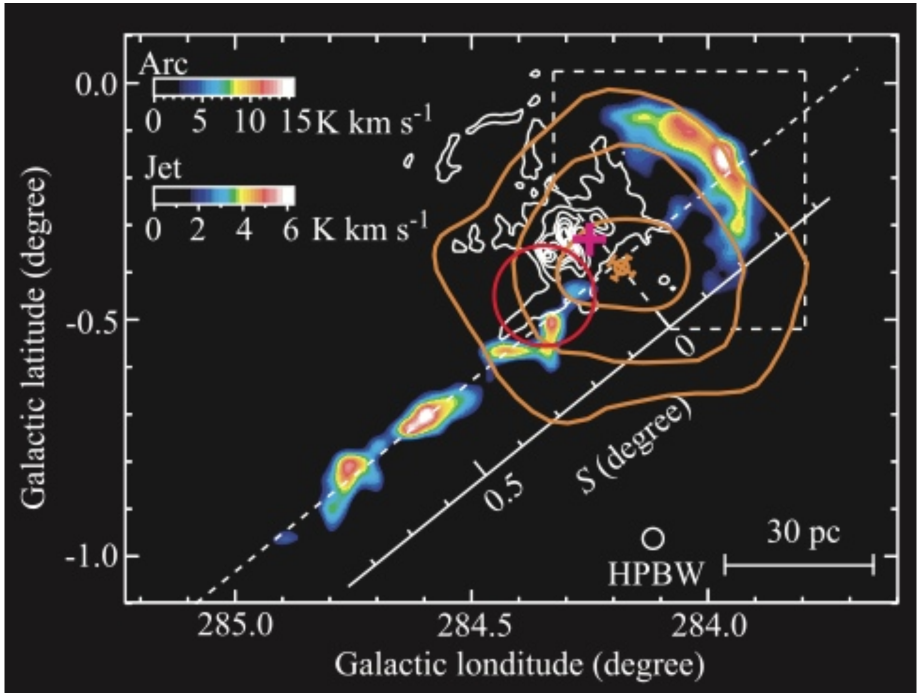

- WR20a among the more massive binary in the galaxy (2 stars of ~80 solar masses in a 3.8 day orbit!), also WR 20b nearby; but the source is extended and steady
- Very peculiar distribution of molecular clouds in the region, are they related to the gamma-ray emission from HESS J1026?

Fukui et al. 2009

Associations and their collective winds?

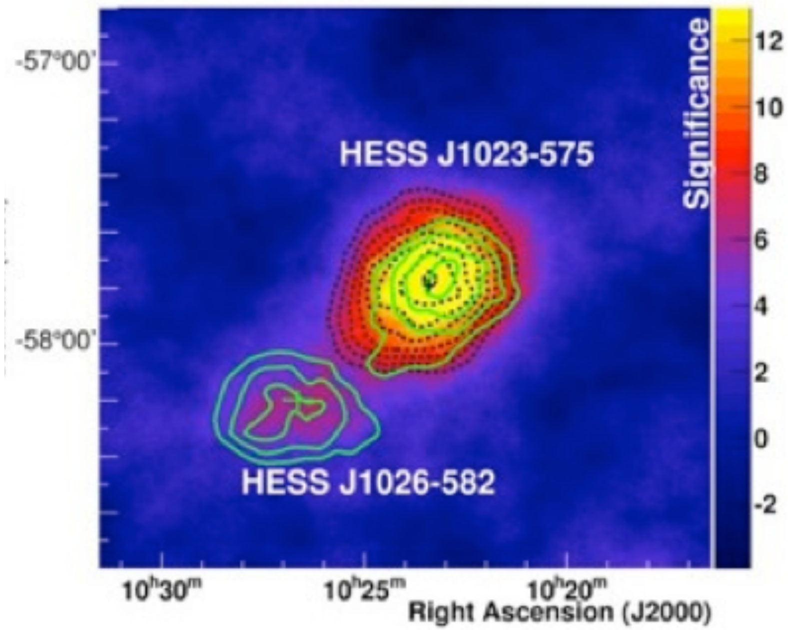

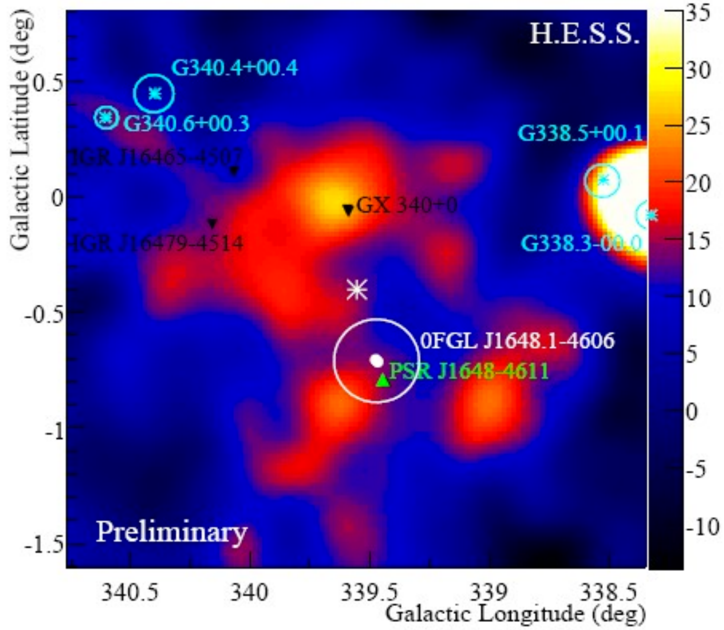

Westerlund 1, Ohm et al. 2011

- Wd1 is the most massive compact young star cluster in our Galaxy, with a total mass of around 60000 solar masses, at a distance of 4 to 5 kpc from Earth.
- Contains 24 Wolf-Rayet stars, as well as more than 80 blue supergiants.
- Age ~5 Myrs, thus some of the most massive stars will have evolved into supernovae, accelerating cosmic rays in their supernova remnant shocks.
- Winds of Wolf-Rayet stars and their termination shocks may also contribute to particle acceleration, dissipating an energy around 10^{39} ergs/s.

Associations and their collective winds?

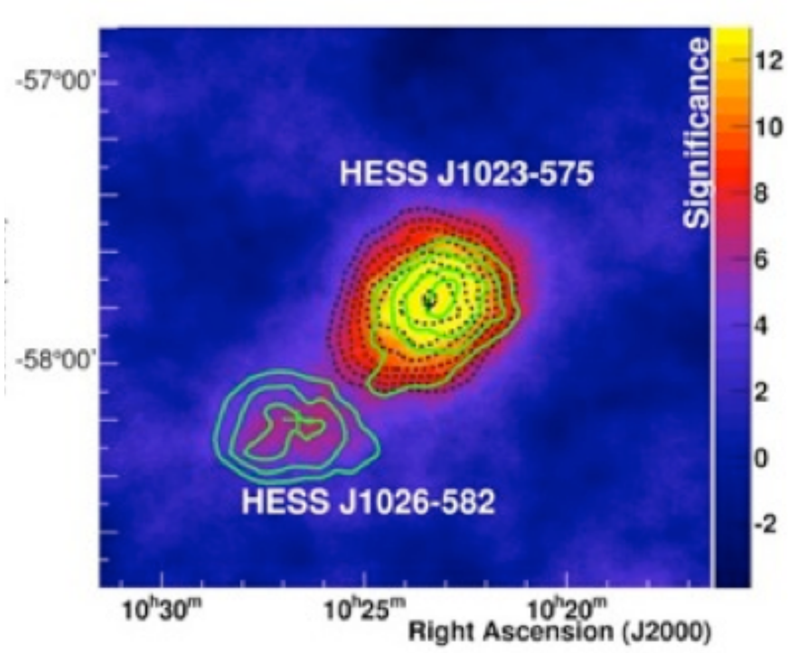

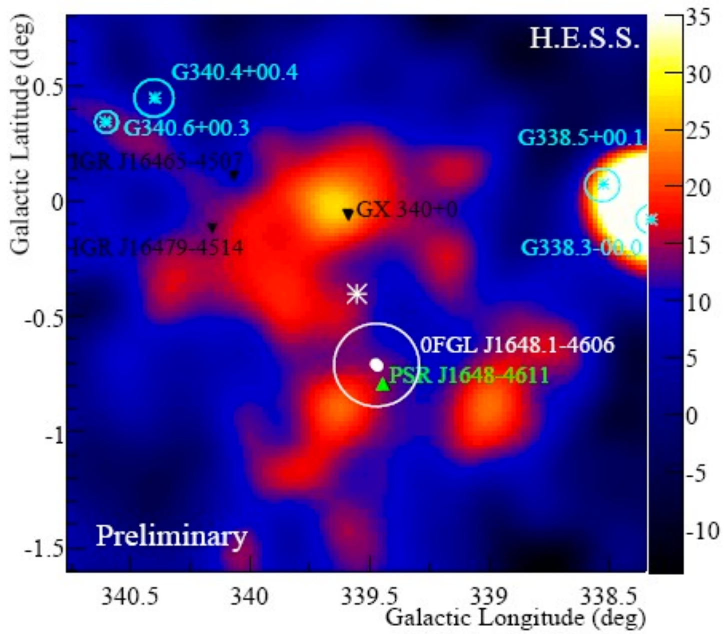

Westerlund 1, Ohm et al. 2011

- Wd1 one of the most extended sources in TeV
- Need of disentangling contributions
  - PWN?
  - Collective effects?

Associations and their collective winds?

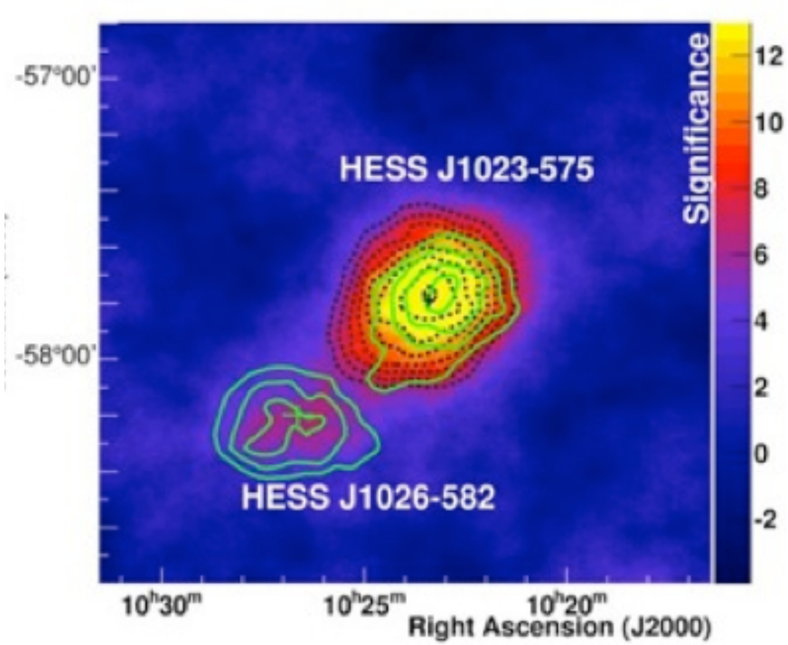

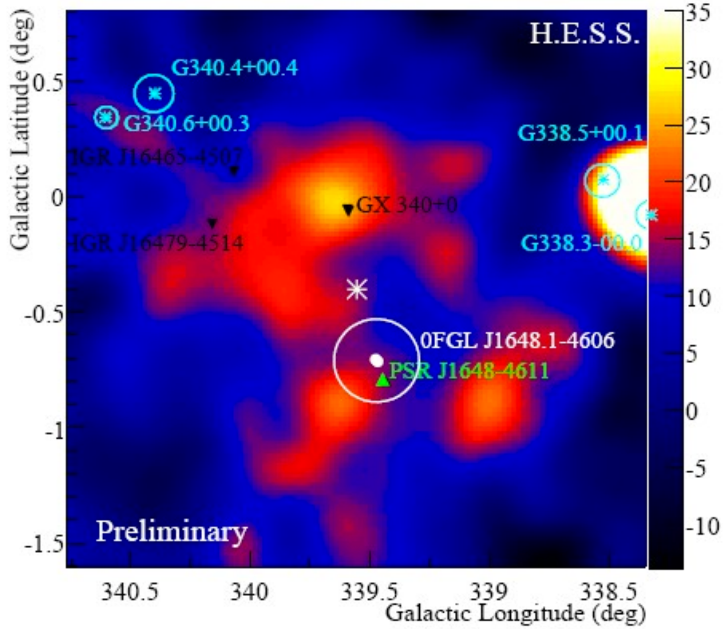

Westerlund 2, de Oña Wilhelmi et al. 2010
Westerlund 1, Ohm et al. 2011

Effects of modulation visible through energy dependent morphology?

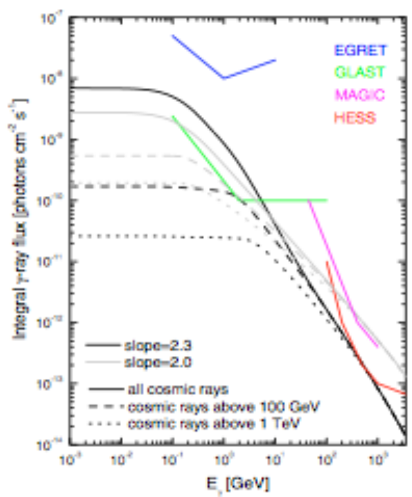

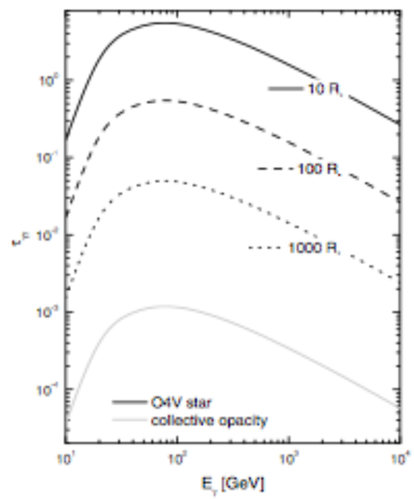

Special binaries: Eta carina / Colliding wind binary in GeV

AGILE flare detection, Tavani et al. 2009.
2 days integration time for each panel

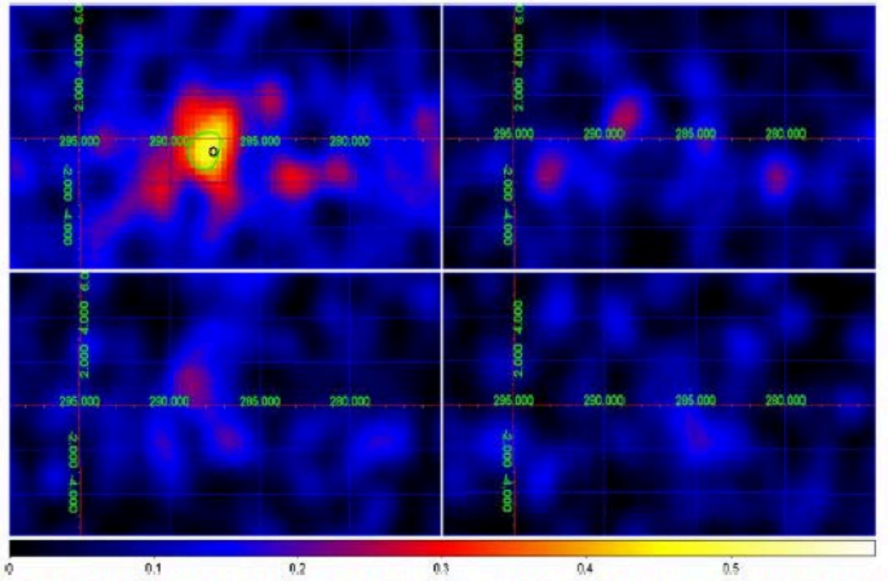

Reitberger et al. 2012, Fermi-LAT.
Average spectral energy distribution and variability

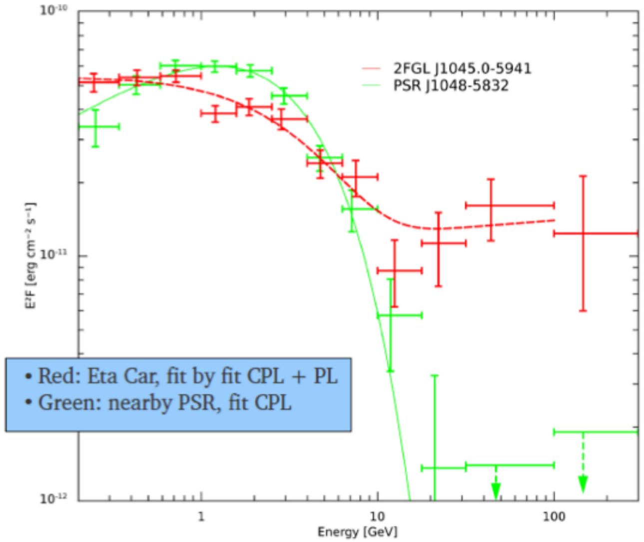

Reitberger et al. 2012, Fermi-LAT.

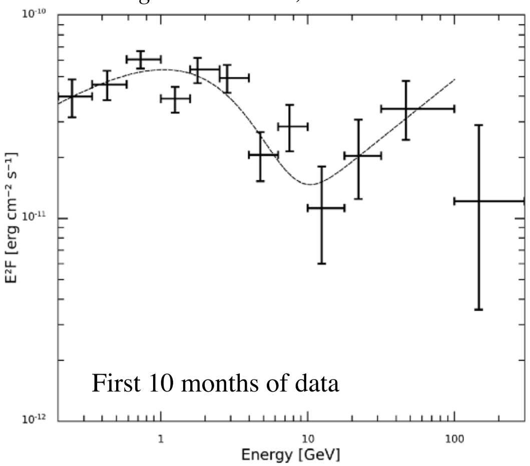

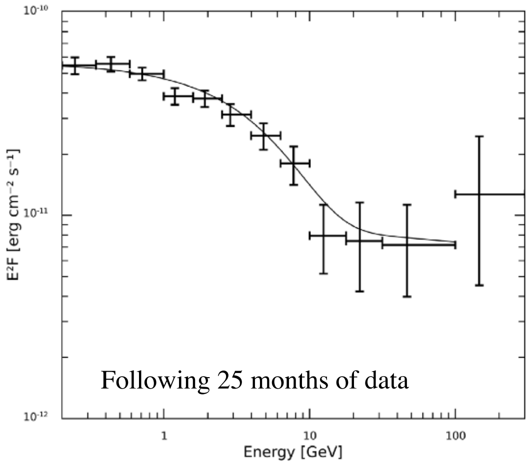

- Spectral and fluxes are variable, compatible with CWB and orbitally variable absorption
- Maximal energy of electrons? High energy spectra? Orbital variability?

Examples of possible Galactic short timescale phenomenology

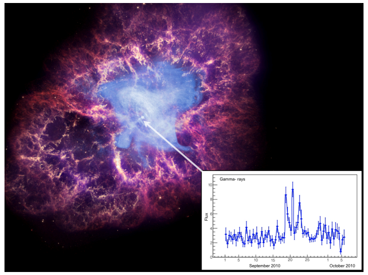

- Flares from pulsar nebulae?
  - Crab-flare-like phenomenology: What, if anything, happens at high energies?

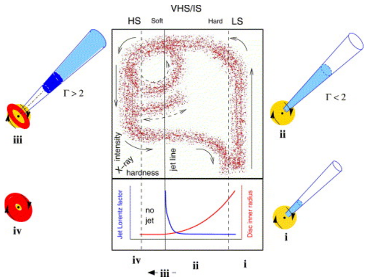

- Observing the accretion-ejection interface?
  - Possible counterparts of radio and X-ray transitions in binaries

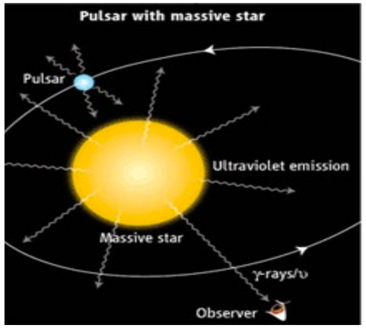

- Formation of relativistic outflows from highly magnetized binaries?
  - Short timescale phenomenology/sub-orbital changes in gamma-ray bin.

- Short timescale variability from black holes beyond the galaxy & GRBs
  - A strike of luck

Galactic short timescale phenomenology

- Fermi-LAT is signal limited above 10 GeV, and its sensitivity decreases rapidly with event duration.

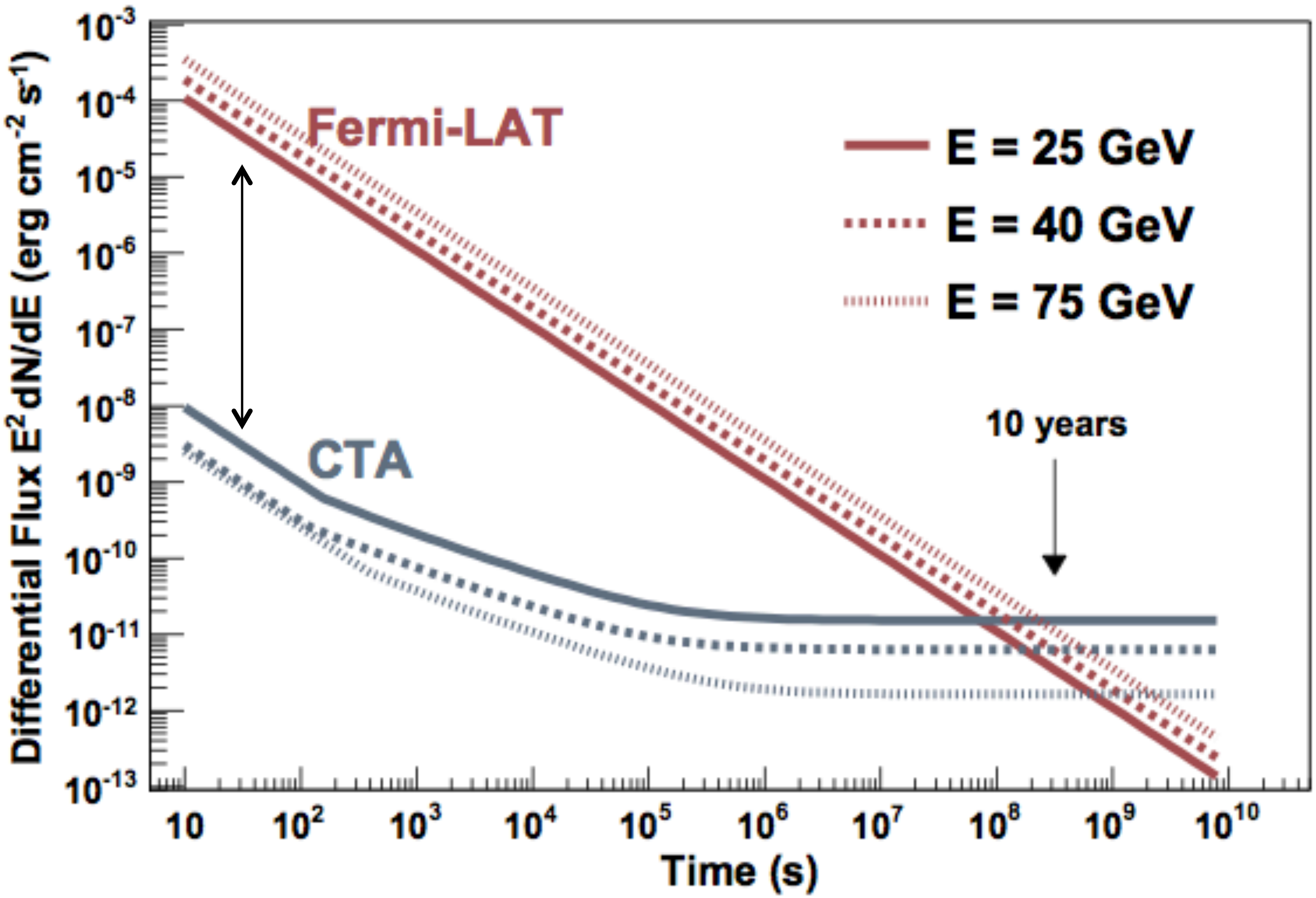

Plot from Funk, Hinton and the CTA collaboration 2012

Gamma-ray binaries: LS 5039 TeV snapshot

- Strong spectral modulation at 1 TeV, none at 200 GeV
- **Low-soft state:**
  2.53 ± 0.07
- **High hard state:**
  1.85 ± 0.06
  E_{cut} = 8.7 ± 2 TeV
- **Non zero signal at periastron**
- **Periodic signal (with orbit)**

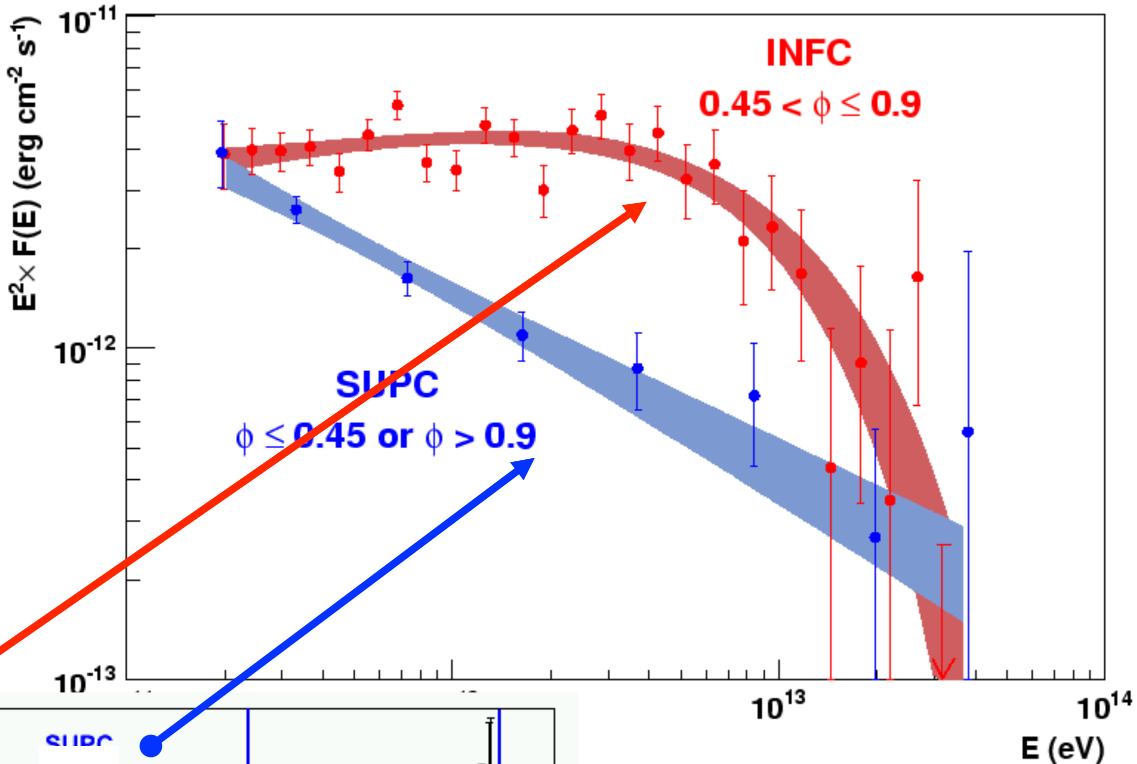

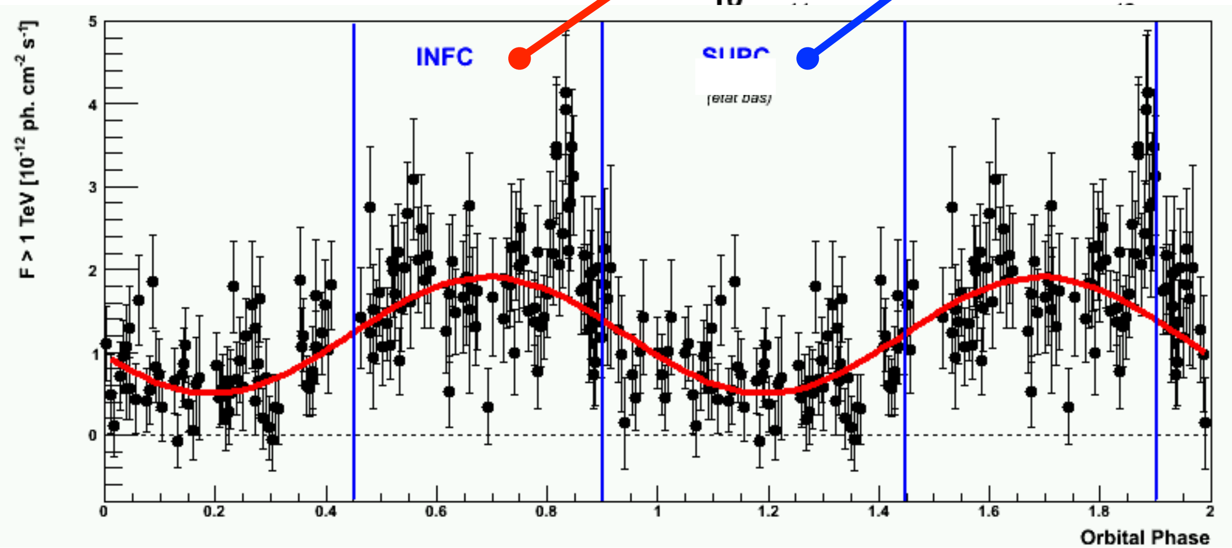

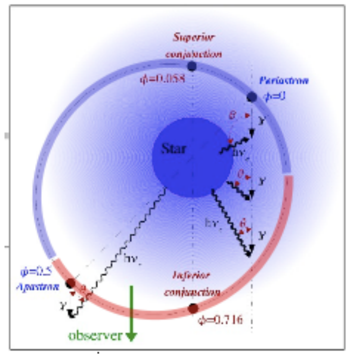

Gamma-ray binaries: LS 5039 GeV – TeV connection

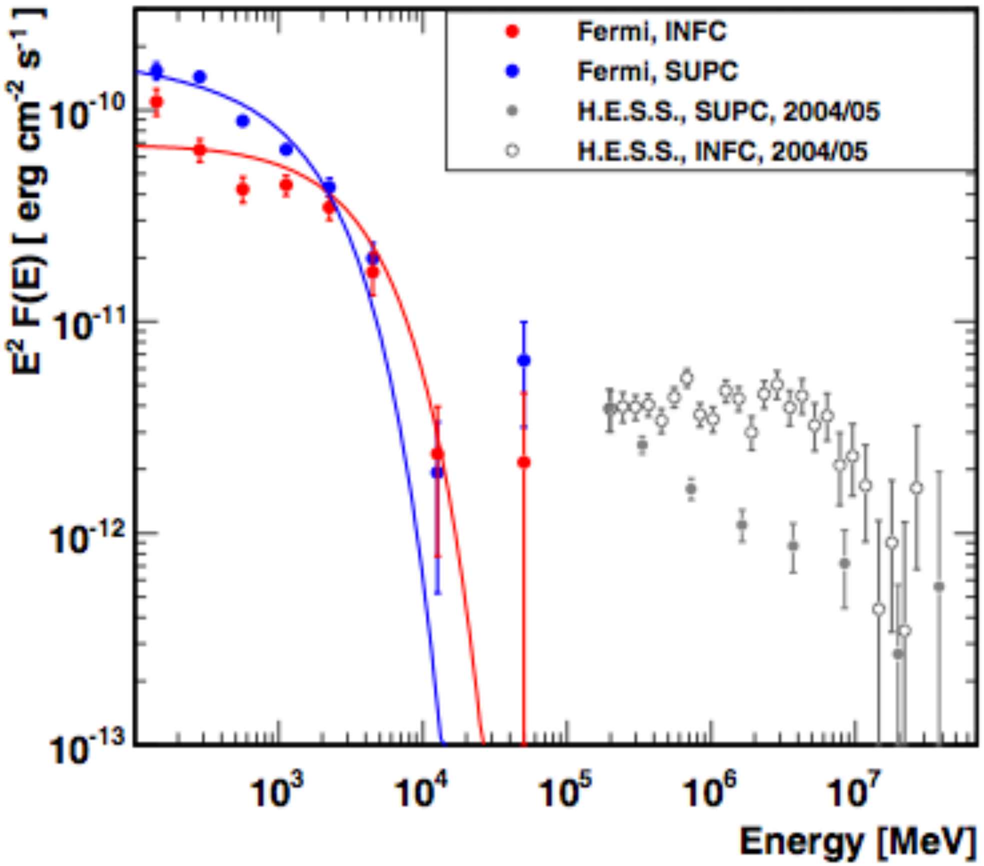

GeV and TeV stability along several years.

Power law with exponential cutoff at ~2 GeV

X-ray and hard X-ray stability also found (Takahashi et al. 2009)

Hadasch, DFT, et al. 2012

LS 5039: HESS II to explore possible pulsar contribution

PSR
- GeV-emission pulsed
- Cutoff is a balance btw acceleration/ curvature loss

Unpulsed radiation. Why?
- Not enough statistics
- Washed out in uncertain orbital parameters

Orbital variation?
- Curvature emission produced near pulsar
- No obvious reason for modulation

The GeV spectral distribution points to a natural pulsar interpretation of the emission, but the orbital variability argues against it.

A 2-components GeV flux hypothesis

GeV emission is formed by both a magnetospheric component, pulsed, steady along the orbit, plus an inter- or intra-wind shock component, unpulsed, modulated with the orbital motion.

TeV emission is only formed by the modulated signal, having the pulsed component died out at such energies.

LS 5039: HESS II to explore possible pulsar contribution

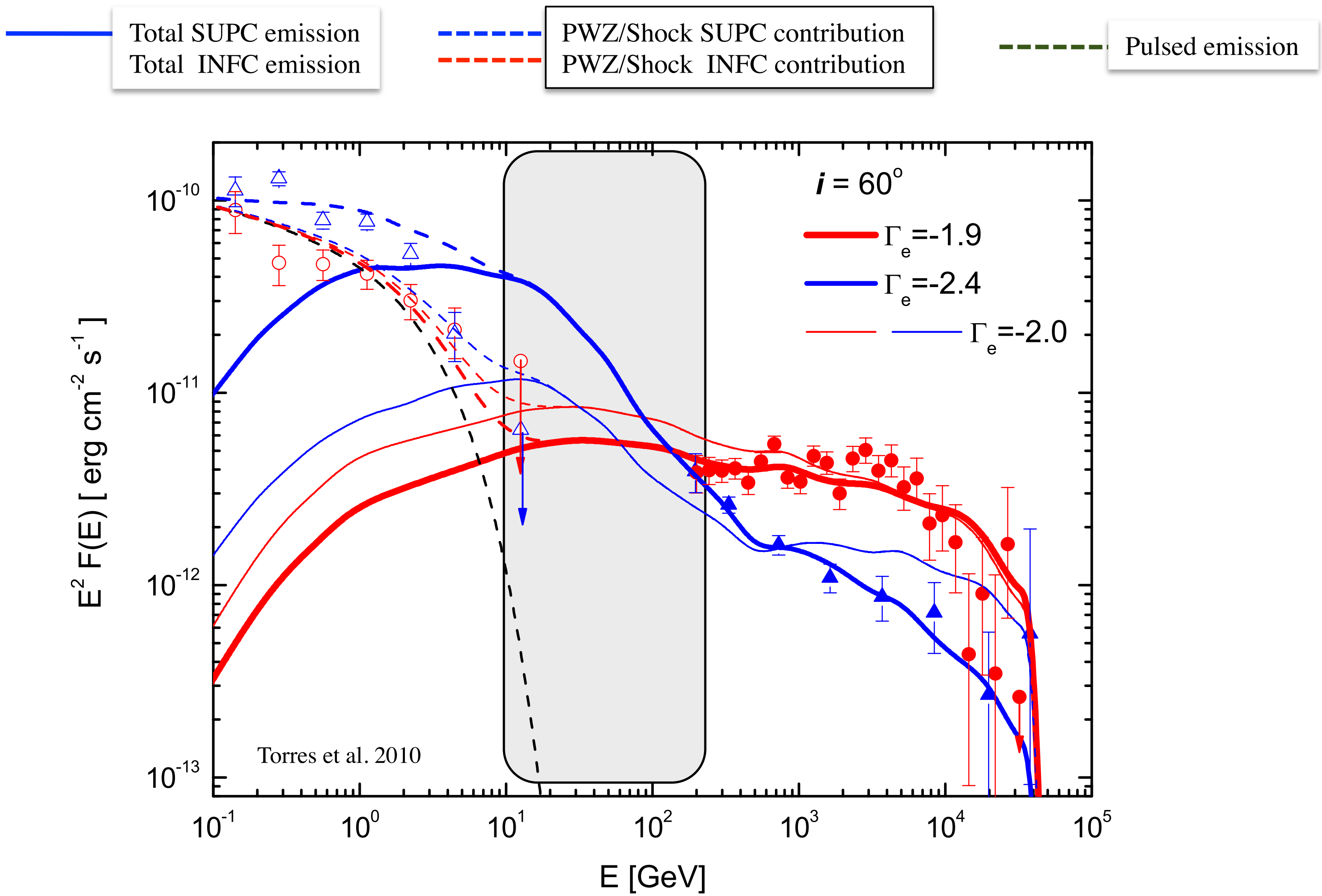

TeV lines fits from PWZ model by Sierpowska-Bartosik & DFT 2008, Pulsar model is a typical Fermi detection

HESS II to explore the sub-orbital structure of models

Predictions of spectra for particular phases in detailed PWZ and Shock models
Are not always well represented by power laws.

Internal structure of the emission useful for disentangling models.

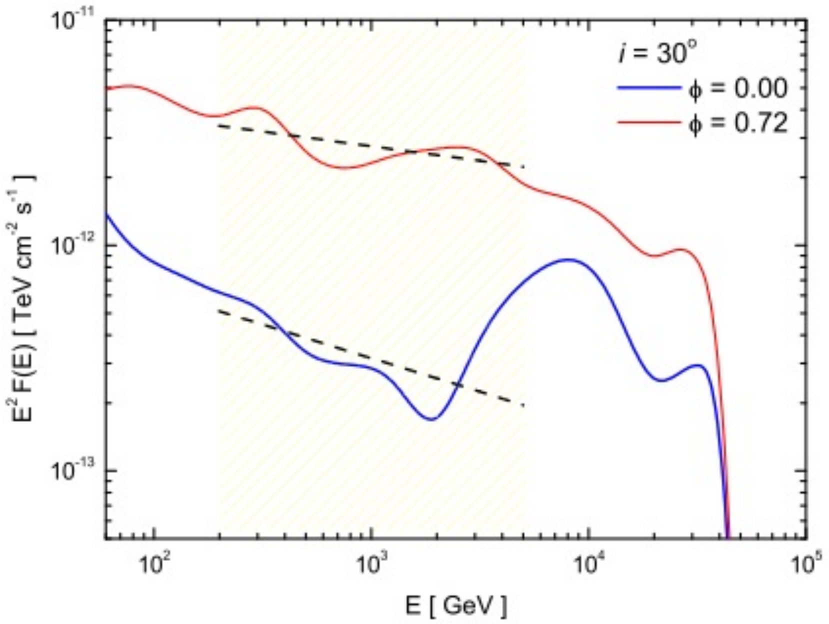

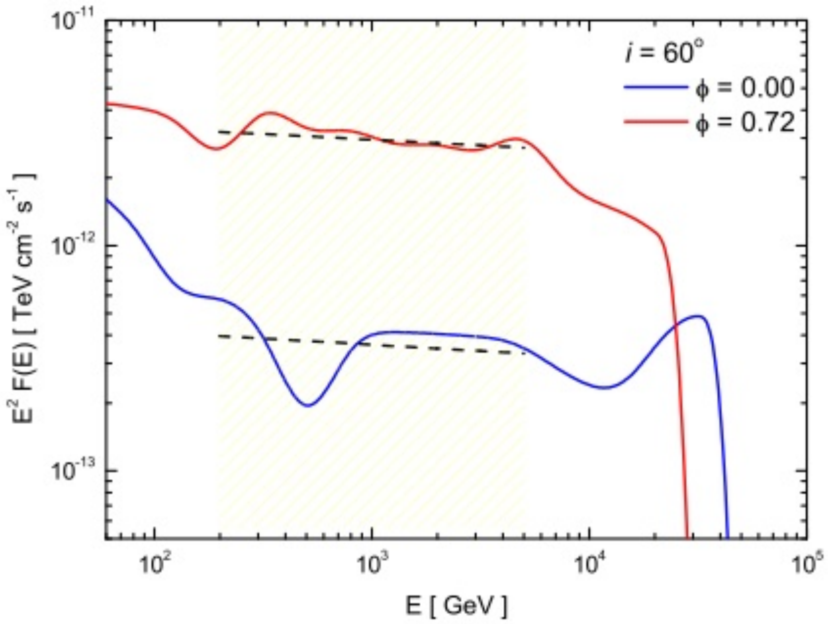

e.g., Sierpowska-Bartosik & DFT 2008

Can other binaries be revealed by long-term variability?

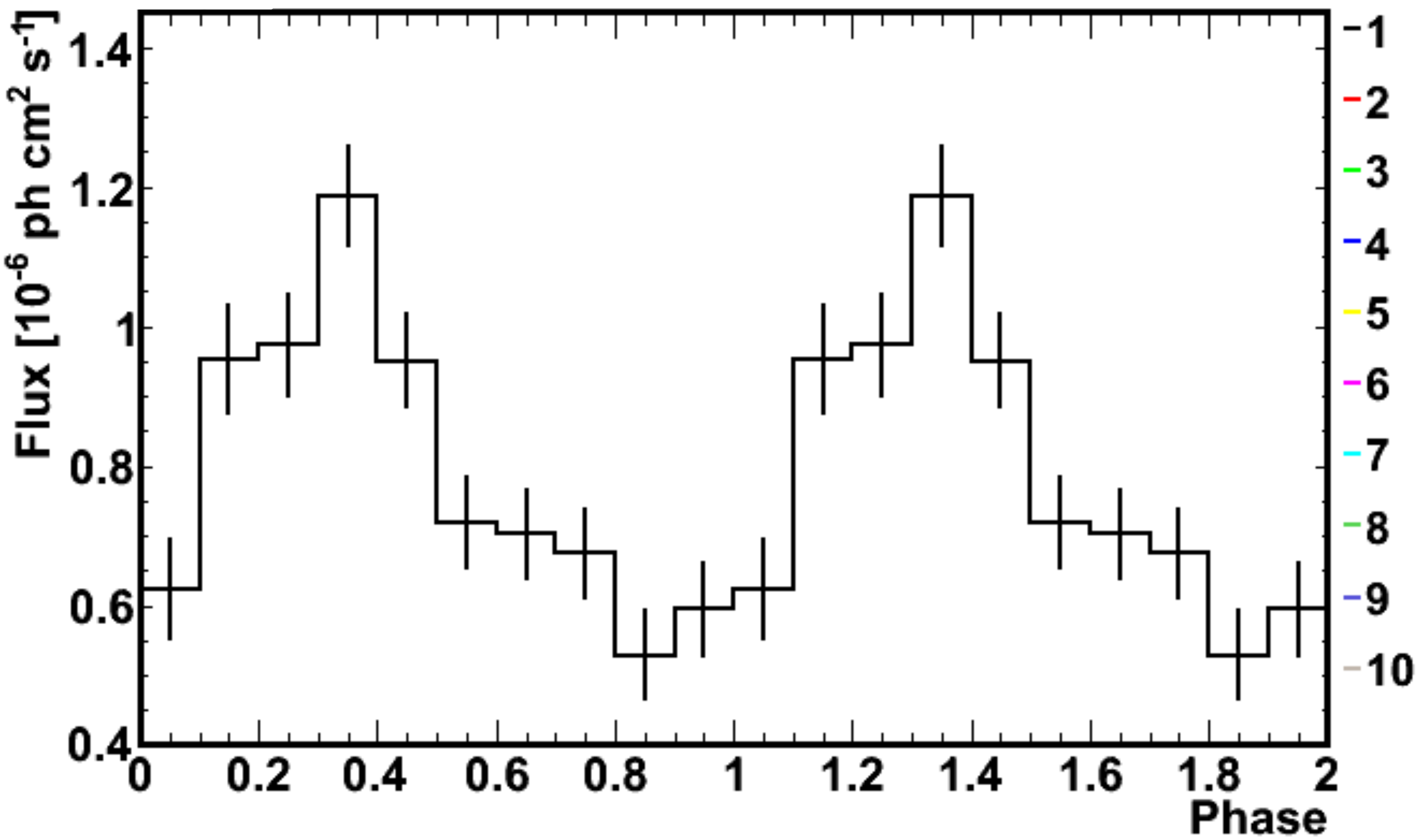

Orbital phase bins fluxes varying in Be-star super-orbital timescale

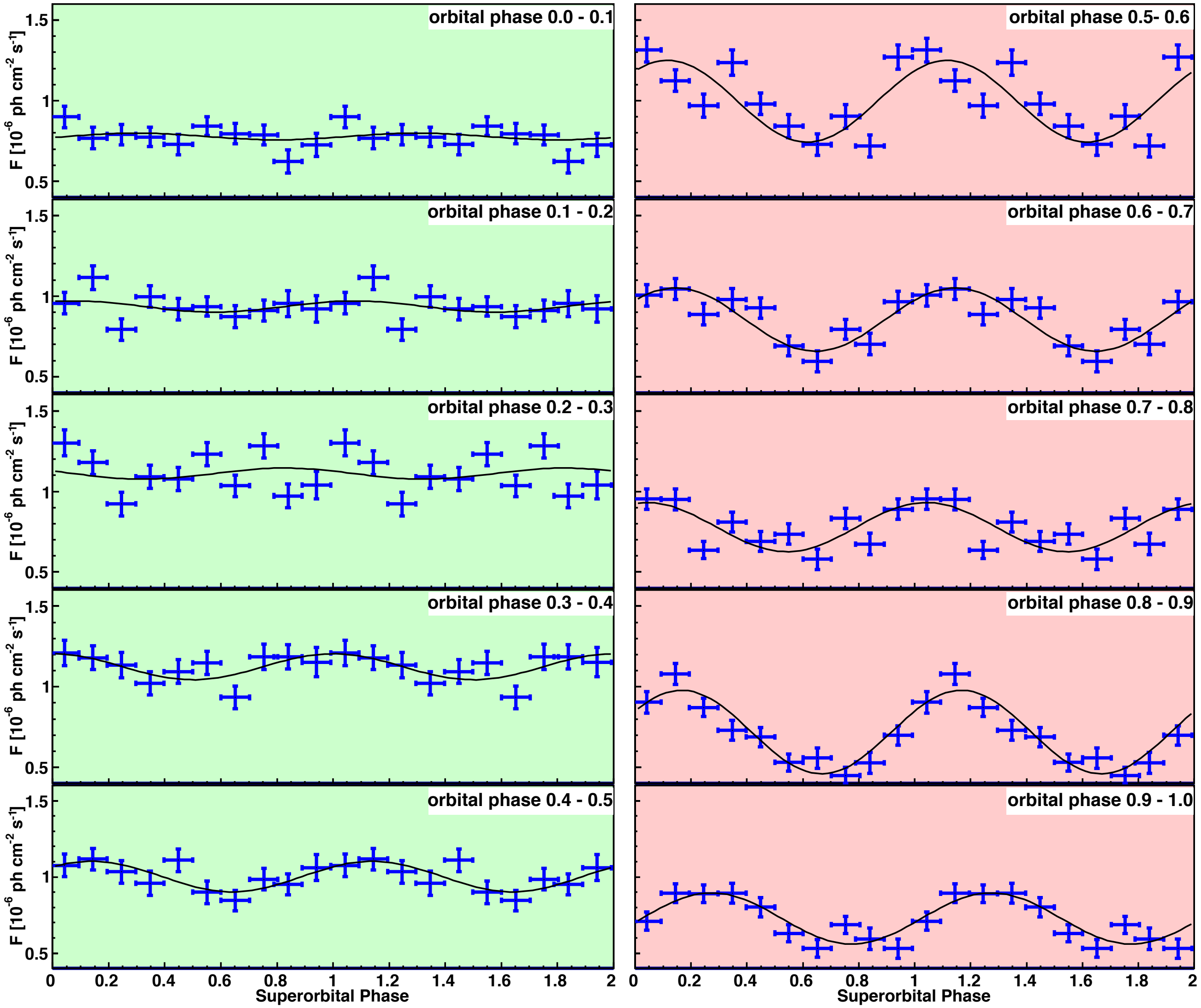

Each panel shows the GeV flux at a fixed orbital position, along a period of 4.5 years

Green and red background represent the region of periastron and apastron, respectively

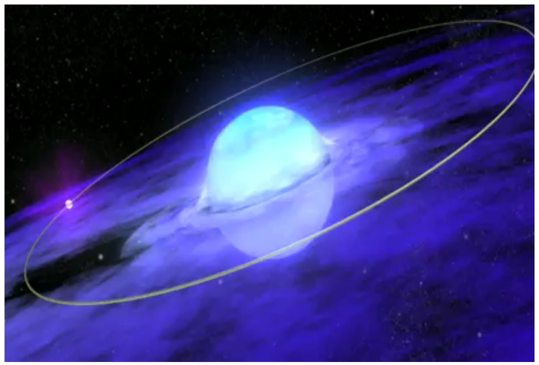

Credit: Walt Feimer, NASA/GSFC

Black lines represent a sine fit with fixed period of 1667 days.

Concluding remarks

Nice science prospects for Cerenkov Telescopes astrophysics before the CTA era.

- It is still likely that several discoveries are still to be made in several directions,
  - Pulsar tails
  - PWN
  - Variability phenomenology in binaries
- Surprises are also possible
  - Crab flares?
  - Fermi bubble connection with high energy CRs?
  - Magnetars and/or magnetar nebuale?
- In general, much more detailed Galactic physics studies (e.g., on energy dependent morphology, CR propagation, diffuse emission) will be possible with HESS II

Announcement of the Journal of High-Energy Astrophysics

Immediate open access the first year. Delayed open access similar to major journals thereafter.

No page charges. Free online color figures. Free printed color figures and language editors when needed.

Intended 1-month period from submission to first referee report.

Optional double-blind refereeing system.

Please give it a try!

Announcement of the Journal of High-Energy Astrophysics